



National Library  
of Canada

Bibliothèque nationale  
du Canada

Canadian Theses Service    Service des thèses canadiennes

Ottawa, Canada  
K1A 0N4

The author has granted an irrevocable non-exclusive licence allowing the National Library of Canada to reproduce, loan, distribute or sell copies of his/her thesis by any means and in any form or format, making this thesis available to interested persons.

The author retains ownership of the copyright in his/her thesis. Neither the thesis nor substantial extracts from it may be printed or otherwise reproduced without his/her permission.

L'auteur a accordé une licence irrévocable et non exclusive permettant à la Bibliothèque nationale du Canada de reproduire, prêter, distribuer ou vendre des copies de sa thèse de quelque manière et sous quelque forme que ce soit pour mettre des exemplaires de cette thèse à la disposition des personnes intéressées.

L'auteur conserve la propriété du droit d'auteur qui protège sa thèse. Ni la thèse ni des extraits substantiels de celle-ci ne doivent être imprimés ou autrement reproduits sans son autorisation.

ISBN 0-315-54877-0

Canada

THE UNIVERSITY OF MANITOBA

THREE DIMENSIONAL FINITE ELEMENT HEAT TRANSFER MODEL OF  
TEMPERATURE DISTRIBUTION IN GRAIN STORAGE BINS

by

KARUPPIAH ALAGUSUNDARAM

A THESIS

SUBMITTED TO THE FACULTY OF GRADUATE STUDIES  
IN PARTIAL FULFILLMENT OF THE REQUIREMENTS FOR THE DEGREE  
OF MASTER OF SCIENCE

DEPARTMENT OF AGRICULTURAL ENGINEERING  
UNIVERSITY OF MANITOBA  
WINNIPEG, MANITOBA

AUGUST 1989

**THREE DIMENSIONAL FINITE ELEMENT HEAT  
TRANSFER MODEL OF TEMPERATURE DISTRIBUTION  
IN GRAIN STORAGE BINS**

**BY**

**KARUPPIAH ALAGUSUNDARAM**

A thesis submitted to the Faculty of Graduate Studies of  
the University of Manitoba in partial fulfillment of the requirements  
of the degree of

**MASTER OF SCIENCE**

© **1989**

Permission has been granted to the LIBRARY OF THE UNIVER-  
SITY OF MANITOBA to lend or sell copies of this thesis, to  
the NATIONAL LIBRARY OF CANADA to microfilm this  
thesis and to lend or sell copies of the film, and UNIVERSITY  
MICROFILMS to publish an abstract of this thesis.

The author reserves other publication rights, and neither the  
thesis nor extensive extracts from it may be printed or other-  
wise reproduced without the author's written permission.

## ABSTRACT

A three-dimensional heat conduction problem in the Cartesian coordinate system was solved using the finite element method for predicting temperatures throughout grain storage bins. The model uses linear or quadratic hexahedron elements with 1, 2 or 3 point Gauss quadrature in each plane. The model can simulate the temperatures in bins of any shape filled with grains and at any geographical location. Input data required for the model include the three-dimensional grid data of linear or quadratic hexahedron elements, thermal properties of grain, bin wall material, soil, concrete and air, and the weather data for the geographical location of the bin. The weather data include the hourly values of ambient air temperature, solar radiation on a horizontal surface, and the wind velocity.

The model was validated against the measured temperatures at 16 locations in a 5.56-m-diameter bin containing rapeseed and at 20 locations in a 5.56-m-diameter bin containing barley, located near Winnipeg, Manitoba. The average absolute difference between the measured temperatures and the temperatures predicted by the model with linear elements was 2.7 K in the rapeseed bin and 2.4 K in the barley bin. These values for the temperatures predicted by the model with quadratic elements were 2.6 K and 2.1 K, respectively.

Temperatures predicted by the model in 3.0-m-tall and 4.0-m-tall rapeseed bulks of various diameter to height ratios were compared with the temperatures predicted by a two and three-dimensional finite difference models. The average absolute difference between the temperatures predicted by the 3D (three-dimensional) finite element model and the 2D (two-dimensional) finite difference model at half the

radius towards the south mid-way between the top and bottom layers, decreased with an increase in the diameter to height ratio of the grain bulk. Temperatures predicted by the 3D finite element and 3D finite difference models compared favorably with each other. Distinct differences were observed between the temperatures predicted by the 3D finite element model for the north and south sides of a bin.

## ACKNOWLEDGEMENTS

I sincerely thank Dr. D.S. Jayas for his invaluable guidance, constant encouragement and support during the past two years. Especially, I appreciate his willingness to share his knowledge, whenever I had problems during the course of this study.

I thank, Drs. N.D.G. White, W.E. Muir, and A.C. Trupp for serving on my thesis committee and reviewing the manuscript.

I wish to acknowledge the Natural Sciences and Engineering Research Council of Canada and the Manitoba Department of Agriculture for providing financial assistance.

I thank J. Putnam and B. Mogan for their help. Special thanks are due to Rameshbabu Manickam and Pankaj Shatadal for their friendly advises and encouragement.

Finally, I would like to thank my parents, brothers and sisters for their moral support, and my wife Kalyani and little daughter Meena for their patience and understanding, during the past two years.

## TABLE OF CONTENTS

ABSTRACT	(i)
ACKNOWLEDGEMENTS	(iii)
TABLE OF CONTENTS	(iv)
LIST OF FIGURES	(vi)
LIST OF TABLES	(vii)
LIST OF SYMBOLS	(viii)
1. INTRODUCTION	1
2. OBJECTIVES	4
3. LITERATURE REVIEW	5
3.1. Grain storage in Canada	5
3.2. Losses of Stored Food	5
3.3. Importance of Temperature in Grain Storage	6
3.4. Methods of Solving Heat Conduction Problems	8
3.5 Analytical Models	10
3.6 Finite Difference Models	11
4. MODEL DEVELOPMENT	15
4.1. Heat Conduction equation	15
4.2. Solution of Eq. (1) to (5) using variational approach	16
4.3. Time integration of Eq. (16)	21
4.4. Discretization of the Space Domain	22
4.5. Simulation of Grain Bin Temperatures	22
4.6. Convective Heat Transfer on the Circumference of the bin	23
4.7. Radiant Heat Transfer on the Boundary $S_2$	24
4.8. Temperature of the Nodes in the Bottom Layer of the Bulk	26

5. MODEL VALIDATION	28
5.1. Experimental Data for Model Validation	28
5.2. Simulation Procedure	28
5.3. Discussion on predicted temperatures	35
5.4. Comparison with 2D Finite Difference Model	43
5.5. Comparison with a 3D Finite Difference Model	46
6. CONCLUSIONS	51
7. SUGGESTIONS FOR FUTURE WORK	53
8. REFERENCES	54

#### APPENDICES

A. Interpolation functions in the natural coordinate system	58
B. Semi-auto grid generator for hexahedron element with model input data for a linear grid shown in Fig.5.3	63
C. Listing of the Three dimensional finite element heat transfer program	67
D. FE3DHT - 3D finite element heat transfer program	85
E. Fortran variables and the arrays used in FE3DHT	92
F. Input data for FE3DHT, listed in order of lines	99
G. Model input data for linear and quadratic elements	102
H. Measured and predicted temperatures	106



## LIST OF FIGURES

<u>Figure.</u>		<u>Page</u>
5.1	Thermocouple locations in rapeseed bin	29
5.2	Bottom layer of a 5.56-m-diameter bin discretized into 32 linear elements	30
5.3	Bottom layer of the 5.56-m-diameter bin discretized into 32 quadratic elements	31
5.4	A cylindrical bulk of 5.56-m-diameter and 2.7 m height discretized into 96 hexahedron elements	32
5.5	Temperatures predicted using linear finite elements and temperatures measured at 2m radius and 2m height in a 5.56-m-diameter bin filled with rapeseed to a depth of 2.7 m near Winnipeg, Canada	36
5.6	Temperatures predicted using linear finite elements and temperatures measured at 2m radius at 2.7 m height in a 5.56-m-diameter bin filled with barley to a depth of 3.2 m near Winnipeg, Canada	37
5.7	Plot of measured temperatures and temperatures predicted by the model with linear and quadratic elements at 2 m radius and 2 m height in a 5.56-m-diameter rapeseed bin	41
5.8	Average absolute difference between the temperatures predicted by the 3D finite element model and 2D finite difference model at half the radius towards the south mid-way between the top and bottom layers, for various d/h ratios	45
5.9	Average absolute difference of the temperatures predicted by the 3D finite element model, at half the radius towards the south and north in a bin filled with rapeseed, for a 12 month period beginning Jan 1, 1974. Initial temperature of the grain bulk was assumed to be 293 K	47
A.1	Location of local node numbers in linear (a) and quadratic (b) hexahedron elements	61
E.1	Face numbers for convection and radiation boundaries in an element	98
G.1	A rectangular domain discretized into two linear elements	102
G.2	A rectangular domain discretized into two quadratic elements	104

## LIST OF TABLES

<u>Table</u>	<u>Page</u>
4.1 Values of Fourier coefficients for soil temperature model	27
5.1 Properties of air, soil and concrete used in the simulation	34
5.2 Standard errors of estimate and the average absolute difference between the measured and the predicted temperatures in the rapeseed bin	38
5.3 Standard errors of estimate and the average absolute difference between the measured and the predicted temperatures in the barley bin	39
5.4 Temperatures (K) on the last day of the month at half the radius towards the south, predicted by 2D finite difference and 3D finite element models in a 3-m-tall rapeseed bulk located near Winnipeg with initial grain temperatures of 293 K on 1 January 1974	44
5.5 Temperatures (K) on the last day of the month at half the radius towards the south, predicted by 2D finite difference and 3D finite element models in a 4-m-tall rapeseed bulk located near Winnipeg with initial grain temperatures of 293 K on 1 January 1974	44
5.6 Temperatures (K) on the last day of the month at half the radius towards the south, predicted by 3D finite difference and 3D finite element models in a 3-m-tall rapeseed bulk located near Winnipeg with initial grain temperatures of 293 K on 1 January 1974	49
5.7 Temperatures (K) on the last day of the month at half the radius towards the south, predicted by 3D finite difference and 3D finite element models in a 4-m-tall rapeseed bulk located near Winnipeg with initial grain temperatures of 293 K on 1 January 1974	49
A.1 Natural coordinates of the nodes in the element shown in Fig. A.1	62
H.1 Measured and predicted temperatures (K) in a 5.56-m-diameter bin containing rapeseed to a depth of 2.7 m, located near Winnipeg.	106
H.2 Measured and predicted temperatures (K) in a 5.56-m-diameter bin containing barley to a depth of 3.2 m, located near Winnipeg.	110

## LIST OF SYMBOLS

$a_0, a_n$	Fourier coefficients ( $^{\circ}$ C)
$b_n$	Fourier coefficient ( $^{\circ}$ C)
[C]	capacitance matrix
d	diameter of the bin; m
D	day of the year; days
[D]	material property matrix
E	total number of elements in the domain
[F]	load vector
$F_{be}$	radiation shape factor for bin to earth
$F_{bs}$	radiation shape factor for bin to sky
(g)	vector of the derivatives of the field variable in x,y, and z coordinates
h	height of the grain bulk; m
$h_c$	convective heat transfer coefficient at the exterior wall surface; $W\ m^{-2}\ K^{-1}$
H	measured radiation on a horizontal surface; $W\ m^{-2}$
$H_b$	beam radiation on a horizontal surface; $W\ m^{-2}$
$H_d$	diffuse radiation on a horizontal surface; $W\ m^{-2}$
$H_v$	radiation on a vertical surface; $W\ m^{-2}$
$I_{sc}$	solar constant; $1353\ W\ m^{-2}$
[J]	the Jacobian matrix
$k_x$	thermal conductivity of the grain in x-coordinate; $W\ m^{-1}\ K^{-1}$
$k_y$	thermal conductivity of the grain in y-coordinate; $W\ m^{-1}\ K^{-1}$
$k_z$	thermal conductivity of the grain in z-coordinate; $W\ m^{-1}\ K^{-1}$
M	total number of nodal unknowns
[N]	the matrix of interpolation functions

$N_u$	Nusselt number
$\dot{q}$	Internal heat generation in an element; $W\ m^{-3}$
$q_d$	direct solar radiation; $W\ m^{-2}$
$q_e$	earth to bin radiation; $W\ m^{-2}$
$q_f$	diffuse solar radiation; $W\ m^{-2}$
$q_r$	net radiation; $W\ m^{-2}$
$q_o$	bin to surrounding radiation; $W\ m^{-2}$
$q_s$	sky to bin radiation; $W\ m^{-2}$
$R_b$	ratio of cosine of angle of incidence and cosine of zenith angle (Duffie and Beckman 1974)
$R_e$	Reynolds number
$s$	angle between the horizontal and the plane
$S_1$	surface on which the temperature is prescribed
$S_2$	surface in the radiation boundary
$S_3$	surface in the convection boundary
$\dot{T}$	Derivative of temperature in time domain
$\{T\}$	vector of the nodal temperatures
$T_\infty$	outside ambient temperature; K
$T_s^{(e)}$	average surface temperature of the element $e$ on the surface $S$ in the radiation boundary
$\alpha$	long wave absorptivity of the bin wall material
$\epsilon$	emissivity of bin wall material
$\iota$	direction cosines
$\nu$	ground reflectance (0.7 for snow cover and 0.2 for no snow)
$\Delta$	finite increment
$\sigma$	Stefan-Boltzman constant, $5.67 \times 10^{-8}$ ; $W\ m^{-2}\ K^{-4}$
$\mu$	viscosity of air; $N\ s\ m^{-2}$

$\rho$	density of air; $\text{kg m}^{-3}$
$\phi$	latitude
$\delta$	declination
$\omega_s$	hour angle
$\theta_t$	angle of incidence of beam radiation
$\theta_z$	zenith angle
$\gamma$	surface azimuth angle

## 1. INTRODUCTION

Canada produced an average of 51.5 Mt of grains and oilseeds annually during the years from 1978 to 1987 (Anon 1988). These products are stored and handled in bulk both on farms and during transportation. A common storage structure on the Canadian Prairies is the free-standing, corrugated galvanized steel, cylindrical bin of 60 m<sup>3</sup> capacity. Protecting the stored grain in these granaries from spoilage is an essential part of grain production. Temperature of grain in storage is an important factor that determines the keeping quality and control measures used to protect grain from insects, mites and damaging microflora (Oxley 1948, Muir 1980, Longstaff and Banks 1987)

Rates of respiration and multiplication of insects, mites and fungi and respiration of the grain itself are largely dependent on grain temperature (Oxley 1948). The development of the insects and mites that attack the stored grain occur at well defined temperature ranges of about 15 to 38 °C for the former and 5 to 40 °C for the latter, and have narrow optimum ranges near 30 °C (Sinha and Watters 1985). The growth and reproduction of the rusty grain beetle, Cryptolestes ferrugineus (Stephens), the predominant insect pest of stored grain in western Canada, is optimal at a temperature of about 31 °C and the development of the grain mite (Acarus siro L.) is optimal at a temperature of about 20 °C (Loschiavo 1984). A knowledge of temperature distribution in stored grain not only helps in identifying active deterioration, but also gives an indication of the potential for deterioration.

Temperature changes in the stored grain are caused by both internal and external sources of heat (Converse et al. 1973). Internal sources are heat of respiration of grain, microorganisms, insects and mites. External sources include the changes in the ambient air temperature and solar radiation which vary with the geographical location of the storage structure. The transfer of heat is also influenced by the local wind velocity.

Empirical temperature data can be collected at various points in grain storage bins of different sizes over a period of time. However this is an inefficient method, requiring a lot of time, cost and labour. On the other hand mathematical models, based on physical principles can potentially predict with accuracy the temperature distribution in a grain storage bin. Further, using the mathematical models, the effect of bin size, bin wall material, location, etc., on the temperature distribution can be studied.

Many attempts were made to develop mathematical models to predict the temperature distribution in grain storage bins (Muir 1970, Converse et al. 1973, Yaciuk et al. 1975, Lo et al. 1980, Muir et al. 1980, Longstaff and Banks 1987, White 1988). All these models use one or two-dimensions in space to describe the heat conduction. Assumptions restrict the use of these models to accurately predict the temperature distribution in grain storage bins. Further, when an actively spoiling pocket of warm grain (a "hotspot") occurs in the grain, the temperature of the grain mass surrounding the hotspot is raised in all three directions. Only a three-dimensional-model would precisely predict the effect of the hotspot in the surrounding grain mass.

This study was undertaken to solve the three dimensional heat conduction problem using the finite element method, for predicting the temperature distribution in stored grain under a wide range of conditions.



## 2. OBJECTIVES

The objectives of this study were:

1. to solve a three-dimensional heat conduction problem in the Cartesian coordinate system, using the finite element method, to formulate a predictive model of grain temperatures in bins.
2. to validate the model against the measured data available in the literature.
3. to compare the temperatures predicted by the finite element model with the temperatures predicted by a two-dimensional finite difference model and a three-dimensional finite difference model.

### 3. LITERATURE REVIEW

#### 3.1 Grain Storage in Canada

As already noted Canada produced an average of 51.5 Mt of grains and oilseeds annually during the years from 1978 to 1987 (Anon 1988). Eighty percent (41.1 Mt) of this was produced in Western Canada. Most of the grain harvested in Canada goes into farm storage before it is moved for sale or use. The total amount of grains and oilseeds carried over in storage in Canada from one crop year to the next, averaged over a 10 year period from 1978 to 1987 was 19.02 Mt (Anon 1988). Most of the farms in Canada must have on-farm storage capacity of about 1.5 to 2.0 times their average annual production because of large carryovers or large harvests, and these systems must maintain the grain quality for 2 years or more (Muir 1980).

#### 3.2 Losses of Stored Food

Losses to stored products may be of quantity or quality and may occur separately or together (Hall 1970). The quantity loss results from evaporation of moisture from the food grain, from nutrients such as carbohydrates being metabolized by microflora into water and carbon-di-oxide and the product being eaten by insects and rodents. The quality loss can be of reduction in grade due to sprouting, molding and rotting, decrease in germinative power and nutritive value (Oxley 1948) or the simple presence of contaminants such as insects. Several biological and non-biological variables interact to cause damage to the stored product. Three main abiotic factors affecting the rate of deterioration are temperature, gaseous composition of intergranular air and the grain moisture content (Oxley 1948, Muir 1980).

### 3.3 Importance of Temperature in Grain Storage

Temperature and moisture content of the grain are the determining factors in the development of organisms that affect the stored grain. Muir et al. (1987) stated that under Canadian conditions a small pocket of high moisture content grain may spoil in a large grain bulk. Moisture migration resulting from temperature differentials in the grain mass can result in localized high moisture levels. Other causes can be the entrance of snow or rain through the granary structure. Sinha and Wallace (1977) measured the temperatures at various locations in 46 t of rapeseed stored at a moisture content of 8.5 to 9% from August 1973 to December 1977. They reported that the centre temperature in this bin was higher in mid-winter than in mid-summer. Differences between the centre temperature of the grain bulk and the outside ambient air temperature cause convection currents in the grain accompanied by a movement of moisture from high temperature to low temperature areas.

Epperly et al. (1987) studied the effect of cooling on the population of insects that attack stored wheat. Reducing the temperature of the grain mass below 283 K during early fall produced an unfavorable environment for multiplication and activity of stored-grain insects. Allowing grain to remain cool during spring and summer months minimizes insect problems (Cuperus et al. 1986). When an aeration system was used to control temperature, the bins did not require chemical methods to control the stored grain insects. Also, if grain temperatures can be lowered to  $-5^{\circ}\text{C}$  for 6 weeks or  $-10^{\circ}\text{C}$  for 4 weeks, insects will be killed (Loschiavo 1984).

Certain temperature ranges in the grain storage bin influence in the outbreak of insects, mites and fungi, and temperature also affect the toxicity of chemicals applied to control these biological organisms. For example, application of the insecticide pirimphos methyl at 305 K and deltamethrin at 294 K is most effective in controlling Sitophilus oryzae (L.) (Longstaff and Desmarchelier 1983). Tyler and Binns (1982) studied the effect of eight organophosphorus insecticides at 283, 290.5 and 298 K on insecticide susceptible strains of adult Tribolium castaneum (Herbst) , Oryzaephilus surinamensis (L.) , and Sitophilus granarius (L.). The insects were exposed to a range of deposits from 10 to 5000 mg per square metre. Based on the knockdown and mortality, the effectiveness of all the insecticides was greater at 298.0 K than at 290.5 K and was distinctly lower at 283.0 K. Their results demonstrated that dosages should be regarded as temperature-specific and consideration must be given to the usual decline in effectiveness with temperature. Residues of insecticides also degrade much more slowly at cool (below 253 K) than at warm (above 293 K) temperatures (Abdel-Kader et al. 1980). Other insecticides such as pyrethroid permethrin are more toxic to insects at low (15 °C) than at high temperatures (32°C) (Harris and Kinoshita 1977). Also fumigants such as the phosphine gas become less effective with declining temperatures and are not recommended for use below 278 K (Anon 1989).

The knowledge of temperature distribution in stored grain will help in identifying active deterioration and in deciding on effective control measures to protect the grain. Collecting the temperature data using experimental procedures (Sinha and Wallace 1977,

Jiang et al. 1988), over a period of time can indicate the temperature distribution in a stored-grain mass. However, temperature data collected in a bin containing a particular grain can only be used for that grain, at the given location, and generalizations can not be made. Mathematical models, by solving one, two or three dimensional heat conduction problems, can be developed for predicting the temperature distribution in bins containing any type of grain and at any location.

### 3.4 Methods of Solving Heat Conduction Problems

Trupp (1964) discussed various methods of solving heat conduction problems, including analytical methods, numerical methods, analogous methods and experimental methods. Analytical methods of solving heat conduction problems consist of straight solutions of the partial differential equation of heat conduction. Any heat conduction problem can be solved analytically. But, in practice, even if the problem can be successfully formulated, the solution may be indeterminate due to the intricate mathematics involved. Also, problems involving anisotropic materials are usually difficult to solve analytically.

Numerical methods can be used to obtain an approximate solution when an analytical solution can not be obtained. The finite difference method is useful for solving heat transfer and fluid mechanics problems. In the finite difference approach of solving heat conduction problems, the geometry is subdivided into a number of regions. The thermal relations for each region are represented by its central point, called a node. Temperature is computed for each node in the domain, rather than at any point as done in the analytical method.

The method is rather cumbersome when the regions have curved or irregular boundaries and it is difficult to write general computer programs for the method (Segerlind 1984).

The finite element method has been successfully applied to solve several engineering problems such as heat conduction, fluid dynamics, seepage flow, electric and magnetic fields, and vibration analysis (Zinkiewich and Parekh 1970, Rao 1982, Neiber 1983, Shufen and Jofreit 1987, Parsons et al. 1987). The fundamental difference between the finite difference and the finite element method is that the finite difference method provides a pointwise approximation of the governing differential equation whereas the finite element method provides a piecewise approximation.

Segerlind (1976) has summarised the advantages of the finite element method as follows:

- (1) the material properties in adjacent elements do not have to be the same;
- (2) irregularly shaped boundaries can be approximated using elements with straight sides or matched exactly using elements with curved boundaries;
- (3) the size of the elements can be varied, which allows the element grid to be expanded or refined as the need exists;
- (4) mixed boundary conditions can be easily handled; and
- (5) a general computer program for a particular subject matter area can be written.

The availability of adequate computer memory and the relative high computational costs are the limiting factors for solving a problem

using the finite element method. Many researchers have solved the heat conduction problem using the analytical or numerical methods to predict the temperature distribution in grain storage bins.

### 3.5 Analytical Models

Converse et al. (1973) developed an analytical solution describing the heat transfer in cylindrical grain storage bins. They investigated the effect of changes in the external air temperature on the temperature of wheat stored in a concrete upright bin. Internal heat generation from respiration of the grains, microorganisms and insects was considered negligible. They concluded that the lag between the ambient temperature and the changes in the grain temperature increased almost linearly with the distance from the exposed wall and that the diurnal variation in temperature had little effect on the wheat temperature.

Manbeck and Britton (1988) developed a model to predict the surface temperature of a thin-walled metal grain bin on clear days. Energy input to the wall included the product of the incident direct normal radiation, the shortwave absorptivity of the outer wall surface and the cosine of the angle of solar incidence. Energy loss from the wall included the convection and radiation losses to the outside air, and the heat conduction losses to the grain mass. The model predicted both mean and local bin wall temperatures within 2 to 5 °C of observed values for 5 test days. The predicted mean bin wall temperature declines were from 4 to 8 °C h<sup>-1</sup> of the observed values on calm days and to less than 1 °C h<sup>-1</sup> of the observed temperatures on windy days.

### 3.6 Finite Difference Models

Lo et al. (1975) did a quantitative analysis of the influence of weather on grain temperatures and moisture contents. They used the finite difference method to solve the one dimensional heat conduction equation in the radial direction, for predicting the temperature distribution in grain storage bins. The day-by-day variation of the ambient air temperature was considered as the only source that would affect the grain temperature. Their results were in good agreement with several reports in the literature. Their analysis showed that the grain located at or near the wall and at the top was most susceptible to heat damage.

Yaciuk et al. (1975) developed a mathematical model of heat transfer in grain bin and solved it using the finite difference method. The main variables that can be studied using their model are: thermal properties of the grain, initial temperature of the grain, ambient air temperature, radiation, wind velocity, diameter of the bin and the type of bin wall material. Heat transfer by conduction in the vertical direction and by natural convection within the bin were assumed to be negligible. The prediction equations do not take into account the variable heating of the bin wall due to solar radiation and the heat generated by insects, mites and fungi. Also the heat flow was assumed to be entirely radial and the problem was treated as one-dimensional.

Muir et al. (1980) converted the one-dimensional finite difference model of Yaciuk et al. (1975) to simulate the conductive heat transfer in both the vertical and radial directions in free-standing cylindrical bins of stored grain. Temperature throughout the



bin was assumed to be symmetrical about the vertical axis and heat generation within the grain mass was assumed to be negligible. They concluded that the inclusion of convection currents in the grain bulk did not result in more accurate predictions of temperature.

Metzger and Muir (1983) extended the two dimensional finite difference model of Muir et al. (1980) to include forced convective heat transfer in the vertical direction in cylindrical granaries. Input to the model included the initial grain conditions, air flow rate, weather conditions and fan parameters. Predicted temperatures closely followed the measured temperatures at two locations in a 4.3 m diameter bin.

Longstaff and Banks (1987) developed a finite difference simulation model to predict the mean and variation of temperature in the region within 40 cm of the upper surface of a grain bulk, based on the measured temperatures below 40 cm and at the surface. They considered the heat transfer in the vertical plane only, and assumed the thermal properties of the grain to be constant in time and space.

White (1988) reported that grain temperature changes were primarily due to seasonal changes in ambient conditions which were transferred through the grain bulk by conduction. He presented a simulation model to describe temperature changes observed during summer and autumn in three grain bulks in horizontal storage bins in the sub tropical regions of Australia. In his model, the temperature of the surface layer was set at the mean monthly maximum at the middle of each month, with linear change from the middle of one month to the next. Temperatures at the bottom surface were assumed to reach temperature

equilibrium with the floor and soil under the floor of the storage. He used one dimensional finite difference equations describing the heat transfer by conduction. Predicted temperatures closely followed the observed values.

All these models are either one or two dimensional. Assumptions and the dimensionality restrict the use of these models to predict the temperature distribution of grain storage bulks with irregular boundaries. Further, when a hotspot occurs in a grain storage bin, the temperature of the grain mass surrounding the hotspot is raised in all three directions. Only a three dimensional model can precisely predict the effect of the hotspot on the surrounding grain mass.

Alagusundaram et al. (1988) solved a three dimensional heat transfer problem using the finite difference method to predict the temperature distribution in cylindrical grain storage bins. Their model can predict the temperatures using the input data of initial grain temperature, ambient air temperature, solar radiation, wind velocity and thermal properties of grain, bin structure, and the soil. They assumed the internal heat generation in the bulk to be negligible and that the thermal properties of the grain are constant throughout the grain mass. Predicted temperatures were in good agreement with the measured temperatures at 2 m from the centre at a height of 2 m above the floor in a 5.56-m-diameter bin containing rapeseed to a depth of 2.7 m.

All previous researchers have solved the heat conduction problem either analytically or by using the finite difference method,

to predict the temperature distribution in a stored grain mass. Due to the various advantages and the versatility of the finite element method over the analytical or the finite difference method, the finite element method was used for solving the three dimensional transient heat conduction problem to predict the temperature distribution in grain storage bins of any shape and at any location provided the weather data are available for the location. Development of the solution for the heat transfer in grain bins is given in the next chapter.

#### 4. MODEL DEVELOPMENT

##### 4.1 Heat conduction equation

The partial differential equation governing the transient heat conduction in an anisotropic solid body in the Cartesian coordinate system is given by (Kreith 1973, Bathe 1982, Rao 1982, Allaire 1985):

$$\frac{\partial}{\partial x}(k_x \frac{\partial T}{\partial x}) + \frac{\partial}{\partial y}(k_y \frac{\partial T}{\partial y}) + \frac{\partial}{\partial z}(k_z \frac{\partial T}{\partial z}) + \dot{q} = \rho c \frac{\partial T}{\partial \tau} \quad \dots\dots(1)$$

subject to the boundary conditions,

$$T(x,y,z,\tau) = T_0 \quad \text{for } \tau > 0 \text{ on } S_1 \quad \dots\dots(2)$$

$$K_x \frac{\partial T}{\partial x} \iota_x + K_y \frac{\partial T}{\partial y} \iota_y + K_z \frac{\partial T}{\partial z} \iota_z + q_r = 0 \quad \text{for } \tau > 0 \text{ on } S_2 \quad \dots\dots(3)$$

$$K_x \frac{\partial T}{\partial x} \iota_x + K_y \frac{\partial T}{\partial y} \iota_y + K_z \frac{\partial T}{\partial z} \iota_z + h_c(T-T_\infty) = 0 \quad \text{for } \tau > 0 \text{ on } S_3 \quad \dots\dots(4)$$

$$\text{and the initial condition, } T(x,y,z,\tau=0) = T_1 \quad \dots\dots(5)$$

Where:  $c$  = specific heat of the material ( $J \text{ kg}^{-1} \text{ K}^{-1}$ )

$h_c$  = convective heat transfer coefficient on the boundary  $S_3$  ( $W \text{ m}^{-2} \text{ K}^{-1}$ )

$k_x$ ,  $k_y$  and  $k_z$  = thermal conductivities of the material in x, y, and z coordinate directions, respectively ( $W \text{ m}^{-1} \text{ K}^{-1}$ )

$\iota_x$ ,  $\iota_y$  and  $\iota_z$  = direction cosines

$q_r$  = heat flux on the boundary  $S_2$  ( $W \text{ m}^{-2}$ )

$\dot{q}$  = internal heat generation ( $W \text{ m}^{-3}$ )

$T$  = temperature at time  $\tau > 0$  (K)

$T_\infty$  = surrounding temperature (K)

$T_0$  = specified temperature on boundary  $S_1$  (K)

$T_i$  = initial temperature of the material at time  $\tau = 0$

(K)

$\rho$  = density of the material ( $\text{kg m}^{-3}$ )

#### 4.2 Solution of Eq. (1) to (5) using Variational Approach

To solve Eq. 1 along with the associated boundary conditions two approaches (variational and weighted residuals) can be used in the finite element method. Details of these methods are given in Segerlind (1976, 1984), respectively. Both approaches arrive at the same final algebraic equations. To use variational approach, a functional is required, whereas the weighted residual method is more general and can be used with any partial differential equation. Because of the availability of a functional for Eq.1, it was decided to use the variational approach. The functional  $I$  for the three dimensional heat transfer problem described by Eqs.(1) to (5) is given as (Rao 1982):

$$I = \frac{1}{2} \int_V [K_x \left(\frac{\partial T}{\partial x}\right)^2 + K_y \left(\frac{\partial T}{\partial y}\right)^2 + K_z \left(\frac{\partial T}{\partial z}\right)^2 - 2(\dot{q} - \rho c \frac{\partial T}{\partial \tau}) T] dV + \int_{S_2} q_r T dS_2 + \frac{1}{2} \int_{S_3} h_c (T - T_\infty)^2 dS_3 \quad \dots\dots(6)$$

Defining two matrices  $(g)$  and  $[D]$  as:

$$(g)^T = \left( \frac{\partial T}{\partial x} \quad \frac{\partial T}{\partial y} \quad \frac{\partial T}{\partial z} \right)$$

$$\text{and} \quad [D] = \begin{bmatrix} K_x & 0 & 0 \\ 0 & K_y & 0 \\ 0 & 0 & K_z \end{bmatrix}$$

the functional,  $I$ , in Eq. (6) can be written as:

$$I = \frac{1}{2} \int_V [(g)^T [D] (g) - 2(\dot{q} - \rho c \frac{\partial T}{\partial \tau}) T] dV + \int_{S_2} q_r T dS_2 +$$

$$\frac{1}{2} \int_{S_3} h_c (T - T_\infty)^2 dS_3 \quad \dots\dots(7)$$

The functional,  $I$ , is to be minimized with respect to the nodal values  $\{T\}$ , subject to the satisfaction of the boundary condition of Eq. (2) and the initial condition of Eq. (5). To do this, a suitable form of variation of the field variable,  $T$ , in each finite element is assumed as follows:

$$T^{(e)}(x,y,z,r) = [N^{(e)}(x,y,z)] \{T^{(e)}\} \quad \dots\dots(8)$$

where  $[N^{(e)}(x,y,z)]$ , the matrix of the interpolation functions (Appendix A), is given by:

$$[N^{(e)}(x,y,z)] = [N_1(x,y,z) \quad N_2(x,y,z) \quad \dots\dots N_p(x,y,z)]$$

and  $\{T^{(e)}\}$ , the vector of nodal temperatures is given by:

$$\{T^{(e)}\} = \begin{bmatrix} T_1 \\ T_2 \\ \vdots \\ T_p \end{bmatrix}$$

for an element with  $p$  number of nodes.

Since the functions of temperatures are defined only over the individual elements, the functional  $I$  (Eq.7) can be expressed as the sum of  $E$  elemental quantities  $I^{(e)}$  as:

$$I = \sum_{e=1}^E I^{(e)} \quad \dots\dots(9)$$

where:

$$I(e) = \frac{1}{2} \int_{V(e)} [(g^{(e)})^T [D] (g^{(e)})] - [2(\dot{q}^{(e)} - \rho^{(e)} c^{(e)} \frac{\partial T^{(e)}}{\partial \tau})] T^{(e)} dV \\ + \int_{S_2(e)} q_r^{(e)} T^{(e)} dS_2 + \int_{S_3(e)} \frac{1}{2} h_c (T^{(e)} - T_\infty)^2 dS_3 \quad \dots\dots(10)$$

For the minimization of the functional, I, the necessary condition is:

$$\frac{\partial I}{\partial T_i} = \sum_{e=1}^E \frac{\partial I^{(e)}}{\partial T_i} = 0, \quad i = 1, 2, 3, \dots, M \quad \dots\dots(11)$$

where M is the total number of unknown nodal temperatures.

By differentiating Eq. (8)  $(g^{(e)})$  can be written as:

$$\begin{bmatrix} \frac{\partial T}{\partial x} \\ \frac{\partial T}{\partial y} \\ \frac{\partial T}{\partial z} \end{bmatrix} = \begin{bmatrix} \frac{\partial N_1}{\partial x} & \frac{\partial N_2}{\partial x} & \dots\dots\dots & \frac{\partial N_p}{\partial x} \\ \frac{\partial N_1}{\partial y} & \frac{\partial N_2}{\partial y} & \dots\dots\dots & \frac{\partial N_p}{\partial y} \\ \frac{\partial N_1}{\partial z} & \frac{\partial N_2}{\partial z} & \dots\dots\dots & \frac{\partial N_p}{\partial z} \end{bmatrix} \begin{bmatrix} T_1 \\ T_2 \\ \cdot \\ \cdot \\ T_p \end{bmatrix} \\ = [B^{(e)}] (T) \quad \dots\dots(12)$$

Substituting Eq. (8) and (12) in (10), the result is,

$$I(e) = \frac{1}{2} \int_{V(e)} (T)^T [B^{(e)}] T [D^{(e)}] [B^{(e)}] (T) dV + \\ \int_{V(e)} [\rho^{(e)} c^{(e)} (N^{(e)})^T (T) (N^{(e)}) \frac{\partial (T)}{\partial \tau} - (N^{(e)}) (T) \dot{q}] dV + \\ \int_{S_2(e)} q_r [N^{(e)}] (T) dS_2 + \frac{1}{2} \int_{S_3(e)} h_c^{(e)} (T)^T [N^{(e)}] T [N^{(e)}] (T) dS_3 - \\ \int_{S_3(e)} h_c^{(e)} T_\infty [N^{(e)}] (T) dS_3 - \frac{1}{2} \int_{S_3(e)} h_c^{(e)} T_\infty^2 dS_3 \quad \dots\dots(13)$$

Carrying out the differentiation of Eq. (13) term by term,

$$\frac{\partial}{\partial T_1} \int_{V(e)} \{T\}^T [B(e)]^T [D(e)] [B(e)] \{T\} dV = \int_{V(e)} [B(e)]^T [D(e)] [B(e)] \{T\} dV$$

$$\frac{\partial}{\partial T_1} \int_{V(e)} \rho^{(e)} c^{(e)} [N(e)] \{T\} [N(e)] \frac{\partial \{T\}}{\partial \tau} - [N(e)] \{T\} \dot{q} dV$$

$$= \int_{V(e)} \rho^{(e)} c^{(e)} [N(e)]^T [N(e)] \frac{\partial \{T\}}{\partial \tau} - [N(e)]^T \dot{q} dV$$

$$\frac{\partial}{\partial T_1} \int_{S_2(e)} q_r^{(e)} [N(e)] \{T\} dS_2 = \int_{S_2(e)} q_r^{(e)} [N(e)]^T dS_2$$

$$\frac{\partial}{\partial T_1} \frac{1}{2} \int_{S_3(e)} h_c^{(e)} \{T\} [N(e)]^T [N(e)] \{T\} dS_3$$

$$= \int_{S_3(e)} h_c^{(e)} [N(e)]^T [N(e)] \{T\} dS_3$$

$$\frac{\partial}{\partial T_1} \int_{S_3(e)} h_c^{(e)} T_\infty [N(e)] \{T\} dS_3 = \int_{S_3(e)} h_c^{(e)} T_\infty [N(e)]^T dS_3$$

$$\frac{\partial}{\partial T_1} \frac{1}{2} \int_{S_3(e)} h_c^{(e)} T_\infty^2 dS_3 = 0$$

and adding them all gives:

$$\frac{\partial I^{(e)}}{\partial T_1} = \int_{V(e)} [B(e)]^T [D(e)] [B(e)] \{T\} dV + \int_{V(e)} [\rho^{(e)} c^{(e)} [N(e)]^T [N(e)] \frac{\partial \{T\}}{\partial \tau}$$

$$- [N(e)]^T \dot{q} dV + \int_{S_2(e)} q_r^{(e)} [N(e)]^T dS_2$$

$$+ \int_{S_3(e)} h_c^{(e)} [N(e)]^T [N(e)] \{T\} dS_3 - \int_{S_3(e)} h_c^{(e)} T_\infty [N(e)]^T dS_3 +$$

.....(14)



Equating  $\frac{\partial I^{(e)}}{\partial T_i}$  to 0, Eq. (14) can be written in a condensed form as follows

$$[C^{(e)}] \frac{\partial \{T\}}{\partial \tau} + [K^{(e)}] \{T\} = \{F^{(e)}\} \quad \dots (15)$$

where,

$$[C^{(e)}] = \int_{V^{(e)}} \rho^{(e)} c^{(e)} [N^{(e)}]^T [N^{(e)}] dV$$

$$[K^{(e)}] = \int_{V^{(e)}} [B^{(e)}]^T [D^{(e)}] [B^{(e)}] dV + \int_{S_3^{(e)}} h_c^{(e)} [N^{(e)}]^T [N^{(e)}] dS_3$$

$$\begin{aligned} \{F^{(e)}\} = & \int_{V^{(e)}} [N^{(e)}]^T \dot{q} dV - \int_{S_2^{(e)}} q_r^{(e)} [N^{(e)}]^T dS_2 + \\ & \int_{S_3^{(e)}} h_c^{(e)} T_\infty [N^{(e)}]^T dS_3 \end{aligned}$$

$[C^{(e)}]$  = element capacitance matrix

$\{F^{(e)}\}$  = element load vector

$[K^{(e)}]$  = element conductance matrix

The surface integral over  $S_2$ , or  $S_3$ , do not appear in Eq. (15) if node  $i$  does not lie on the corresponding boundary. Eq. (15) is for an element in the domain. Adding the capacitance,  $[C^{(e)}]$ , and conductance,  $[K^{(e)}]$  matrices and the element load vector,  $\{F^{(e)}\}$ , of individual elements, over all the elements in the grid will yield the following equation,

$$[C] \frac{\partial \{T\}}{\partial \tau} + [K] \{T\} = \{F\} \quad \dots (16)$$

$[C]$  = global capacitance matrix

$\{F\}$  = global load vector

$[K]$  = global conductance matrix

#### 4.3 Time Integration of Eq. (16)

To solve Eq. (16) in the time domain a  $\theta$  family of approximation, which approximate a weighted average of the time derivative, is introduced as follows:

$$\theta \dot{(T)}_{n+1} + (1-\theta) \dot{(T)}_n = \frac{(T)_{n+1} - (T)_n}{\Delta\tau} ; \quad 1 < \theta < 1 \dots (17)$$

A number of different schemes can be obtained by choosing the value of  $\theta$  as follows (Wood and Lewis 1975),

- $\theta = 0$  forward difference scheme
- $\theta = 0.5$  Crank-Nicholson scheme
- $\theta = 0.667$  Galerkin method
- $\theta = 1$  backward difference scheme

The finite difference recurrence relationship is stable for any value of  $\theta$  between 0.5 and 1.0.

Assuming  $\dot{(T)}_{n+1} = \dot{(T)}_n = \dot{(T)}$ , which means the slopes at times  $\tau_{n+1}$  and  $\tau_n$  are equal, and rearranging the terms in Eq. (17), gives the following equation :

$$\dot{(T)} = \frac{(T)_{n+1} - (T)_n}{\Delta\tau} \frac{1}{[\theta + (1-\theta)]}$$

Substituting the value of  $\dot{(T)}$  in Eq. (16) yields:

$$[C] (T)_{n+1} = [C] (T)_n + \Delta\tau [\theta + (1-\theta)] [(F) - [K](T)]$$

Accounting for the time change in the boundary condition vector  $\{F\}$  the above equation can be rewritten as follows:

$$[C] \{T\}_{n+1} = [C] \{T\}_n + \theta \Delta \tau [(F)_{n+1} - [K] \{T\}_{n+1}] + (1-\theta) \Delta \tau [(F)_n - [K] \{T\}_n] \quad \dots (18)$$

Rearranging (18) to obtain  $\{T\}_{n+1}$  in terms of  $\{T\}_n$  and dividing by  $\Delta \tau$ , the resulting equation is:

$$\left[ \frac{[C]}{\Delta \tau} + \theta [K] \right] \{T\}_{n+1} = \left[ \frac{[C]}{\Delta \tau} - (1-\theta) [K] \right] \{T\}_n + \left[ \theta (F)_{n+1} + (1-\theta) (F)_n \right] \quad \dots (19)$$

Eq. (19) is solved to obtain the temperatures at time  $\tau + \Delta \tau$  by using the temperatures at time  $\tau$ .

#### 4.4 Discretization of the Space Domain

One of the major steps involved in solving a problem using the finite element method is discretization of the domain. Visualizing a three dimensional grid is very difficult and becomes almost impossible when higher order elements are used. The amount of work and time required to enter three-dimensional grid data and subsequent checking for errors are phenomenal. No automatic grid generators were available. A program that would generate three dimensional linear and quadratic hexahedron grid data was written. The input data required for this program are the grid data of a two dimensional plane in the bottom layer of the domain. This program can discretize any three dimensional body, provided the body has straight edges in the third dimension. Listing of this program, SAGG, and sample input data are given in Appendix B.

#### 4.5 Simulation of Grain Bin Temperatures

The finite element heat transfer model was coded in FORTRAN

to predict the temperature distribution in stored grain (Appendix C). Description of the program and subroutines are given in Appendix D. All the variables used in the program are defined in Appendix E. The program can handle linear and quadratic elements with 1, 2 or 3 point Gauss quadrature in each plane. Any number of faces of an element can have convective or radiative heat transfer across the boundary. The maximum number of nodes in the continuum is dependent only on the availability of computer memory.

Input data required for the program are: the node and element data, the boundary condition codes (set equal to 1 for the nodes lying in the bottom layer of the grain bulk), thermal properties of grain, soil, air, initial temperatures of all the nodes in the domain, and the weather data for the location. The weather data include the hourly values of the ambient air temperature, solar radiation on a horizontal surface and the local wind velocity. The complete list of input data required for the program with the format are given in Appendix F. Sample input data for a linear and a quadratic element are shown in Appendix G. The convection and the radiation boundary conditions along the circumference of the bin and the prescribed nodal temperatures in the bottom layer of the grain bulk were calculated using the procedures described below.

#### 4.6 Convective Heat Transfer on the Circumference of the Bin

Eq. (20) given by Longstaff and Fennigan (1983), was used to calculate the convective heat transfer coefficient,  $h_c$ , around the circumference of a bin.

$$N_u = 0.227 R_e^{0.633} \quad \dots\dots(20)$$

$$N_u = \text{Nusselt number} = \frac{h_c d}{k} \quad \dots\dots(21)$$

$$R_e = \text{Reynolds number} = \frac{\rho v d}{\mu} \quad \dots\dots(22)$$

Where :  $d$  = diameter of the bin (m)

$h_c$  = convective heat transfer coefficient ( $\text{W m}^{-2}$ )

$k$  = thermal conductivity of air ( $\text{W m}^{-1} \text{K}^{-1}$ )

$v$  = local wind velocity ( $\text{m s}^{-1}$ )

$\mu$  = viscosity of air ( $\text{N s m}^{-2}$ )

$\rho$  = density of air ( $\text{kg m}^{-3}$ )

Using the thermal properties of air and the local wind velocity,  $h_c$  at the end of each hour was calculated and averaged over NHOURL (Appendix D), specified by the user.

#### 4.7 Radiant Heat Transfer on the Boundary $S_2$

The net radiant heat flow,  $q_r$ , in equation (16) is calculated using the following relationship (Duffie and Beckman 1974):

$$q_r = q_e + q_s + q_f + q_d - q_o \quad \dots\dots(23)$$

where,

$$q_e = \sigma \alpha F_{be} T_{\infty}^4 \quad \dots\dots(24)$$

$$q_s = \sigma \alpha F_{bs} T_s^4 \quad \dots\dots(25)$$

$$q_o = \sigma \epsilon [T_s^{(e)}]^4 \quad \dots\dots(26)$$

Where:

$q_d$  = direct solar radiation ( $\text{W m}^{-2}$ )

$q_e$  = earth to bin radiation ( $\text{W m}^{-2}$ )

$q_f$  = diffuse solar radiation ( $\text{W m}^{-2}$ )

$q_o$  = bin to surrounding radiation ( $\text{W m}^{-2}$ )

$q_s$  = sky to bin radiation ( $\text{W m}^{-2}$ )

Based on the study of Muir et al. (1980), the values for the longwave absorptivity and emissivity of the bin wall material were set equal to 0.28, and the two shape functions  $F_{be}$  and  $F_{bs}$  were set equal to 0.5. The estimated sky temperature of 210 K was used. For calculating the solar radiation components,  $q_f$  and  $q_d$ , on the face of an element lying in the radiation boundary  $S_2$ , the radiation on a vertical surface ( $H_v$ ) at the end of each hour was calculated using the measured values of radiation on a horizontal surface ( $H$ ), and Eq. (27)

$$H_v = (2R_b H - 2R_b H_b + H_d + \nu H)/4 \quad \dots\dots(27)$$

Where;

$$R_b = \frac{\cos \theta_T}{\cos \theta_z} \quad \dots\dots(28)$$

$H_b$  = beam radiation on a horizontal surface ( $W m^{-2}$ )

$H_d$  = diffuse radiation on a horizontal surface ( $W m^{-2}$ )

$\nu$  = ground reflectance

$\theta_T$  = angle of incidence of beam radiation (radian)

$\theta_z$  = zenith angle (radian)

The angles  $\theta_T$  and  $\theta_z$  were calculated using Eqns. (29) and (30) (Duffie and Beckman 1974):

$$\begin{aligned} \cos \theta_T = & \sin \delta \sin \theta \cos s - \sin \delta \cos \theta \sin s \cos \gamma + \\ & \cos \delta \cos \theta \cos s \cos \omega_z + \cos \delta \sin \theta \sin s \cos \omega \cos \gamma \\ & \cos \delta \sin s \sin \omega \sin \gamma \end{aligned} \quad \dots\dots(29)$$

$$\cos \theta_z = \sin \delta \sin \theta + \cos \delta \cos \theta \cos \omega \quad \dots\dots(30)$$

where,  $s$  = angle the plane makes with the horizontal

$\gamma$  = the surface azimuth angle, that is the deviation of the normal to the surface from the local meridian, the zero

point being due south, east positive and west negative

$\omega$  = hour angle, solar noon being zero and each hour equaling

15° with mornings positive and afternoons negative

The diffuse ( $H_d$ ) and beam ( $H_b$ ) radiation components and  $R_b$  were estimated using the procedure given below.

$H_d$  was determined by calculating the non-dimensional parameter  $K$ , which is the ratio of  $H_d$  to  $H$ . The non-dimensional parameter,  $K$ , was calculated using the relationship between  $KT$ , which is the ratio of  $H$  to the extra terrestrial radiation,  $H_0$ , and  $K$  (Ruth and Chant 1976). Then the value of  $H_b$  was calculated by subtracting the diffuse component from  $H$ .  $H_0$  was calculated using Eq. (31) (Duffie and Beckman 1974):

$$H_0 = \frac{24}{\pi} I_{sc} \left[ \left[ 1 + 0.033 \cos\left(\frac{360n}{365}\right) \right] \left[ \cos \phi \cos \delta \sin \omega_s + \frac{2 \omega_s}{360} \sin \phi \sin \delta \right] \right] \quad \dots (31)$$

where:

$n$  = day of the year beginning at January 1

$I_{sc}$  = solar constant ( $1353 \text{ W m}^{-2}$ )

$\phi$  = latitude

$\omega_s$  = sunrise hour angle ( $-\cos^{-1}(-\tan \phi \tan \delta)$ )

$\delta$  = declination =  $23.45 \left(360 \frac{284+n}{365}\right)$

$H_v$  and the shortwave absorptivity of the bin wall material were multiplied to get the value of  $(q_f + q_d)$ .

#### 4.8 Temperature of the Nodes in the Bottom Layer of the Bulk

The Fourier series (Eq. 33) given by Singh (1977) was used to calculate the soil temperature at a depth  $z$ . Soil temperature profile in the horizontal direction under a bin was approximated to the soil

temperature profile in the vertical direction (Muir et al. 1980). So  $z$  is the distance of the corresponding node from the circumference.

$$T(z,D) = a_0 + \sum e^{[\sqrt{-(n\pi/365\alpha)} \cdot z]} \cdot \left[ a_n \cos\left[\frac{2n\pi}{365} \cdot D - \frac{/(n\pi)}{365\alpha} \cdot z\right] + b_n \sin\left[\frac{2n\pi}{365} \cdot D - \frac{/(n\pi)}{365\alpha} \cdot z\right] \right] \quad \dots\dots(33)$$

The series was truncated after six terms (Singh 1977). The coefficients  $a_0$ ,  $a_1$ s and  $b_1$ s given by Singh (1977) were used (Table 4.1).

TABLE 4.1 Values of Fourier coefficients for the soil temperature model (Singh 1977)

Parameters	Values (°C)	Parameters	Values (°C)
$a_0$	4.894		
$a_1$	-10.919	$b_1$	-5.129
$a_2$	1.157	$b_2$	0.574
$a_3$	-0.091	$b_3$	0.119
$a_4$	0.031	$b_4$	-0.365
$a_5$	0.519	$b_5$	0.332
$a_6$	0.027	$b_6$	0.068

A one-dimensional finite difference equation in the vertical plane was used to calculate the temperature of the node,  $i$ , in the bottom layer of the bulk. The finite difference solution uses the thermal properties of soil, concrete, and grain, calculated soil temperature (Eq. 33), and the temperature of the node above node  $i$  to calculate the temperature of node  $i$ .



#### 4. MODEL VALIDATION

##### Experimental Data for Model Validation

Temperature data collected in two 5.56-m-diameter galvanized steel bins filled with rapeseed (canola) and barley respectively and used to validate the two-dimensional finite difference model of Muir et al. (1980) were also used to validate the three-dimensional finite element model. The 5.56-m-diameter rapeseed bin was filled to a depth of 2.7 m. Temperatures were recorded at four levels: near the floor, 1 m and 2 m from the floor and near the surface of the grain bulk, over a three year period from 17 May 1974 to 11 Jan 1978. At each level thermocouples were located at the centre, at 1 m and 2 m radii and near the bin wall (Fig.5.1). The other bin contained barley to a depth of 3.2 m. The temperatures were recorded from 13 Aug 1974 to 28 Nov 1975. Location of thermocouples in this bin were the same as those of the rapeseed bin, except that the temperatures were recorded at 5 levels: near the floor, 1 m, 2 m and 2.7 m from the floor and at the surface of the grain bulk.

##### Simulation Procedure

Temperatures of the rapeseed and barley bins were simulated using the model with linear and quadratic elements with 2 X 2 X 2 quadrature. Figs. 5.2 and 5.3 show the bottom layer of the 5.56-m-diameter grain bulk discretized into 32 linear and quadratic elements, respectively. The node and element data of these grids were inputted to the program SAGG (Appendix B) to generate complete three dimensional element data for the program FE3DHT (Appendix C). Fig 5.4 shows the rapeseed bulk (5.56 m diameter and 2.7 m depth) discretized into 96

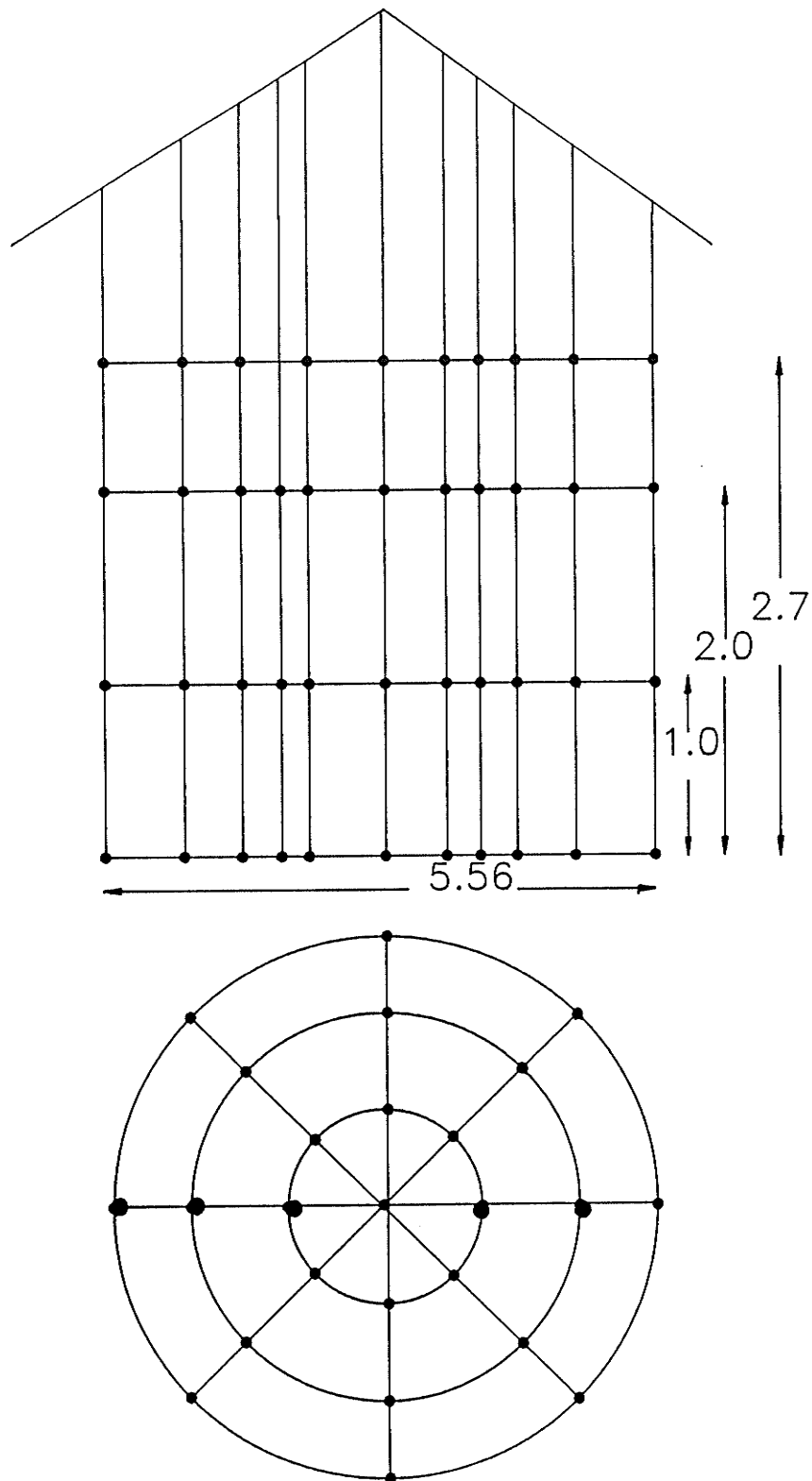


Fig 5.1: Thermocouple locations in rapeseed bin.  
(Source Muir et al. 1980).

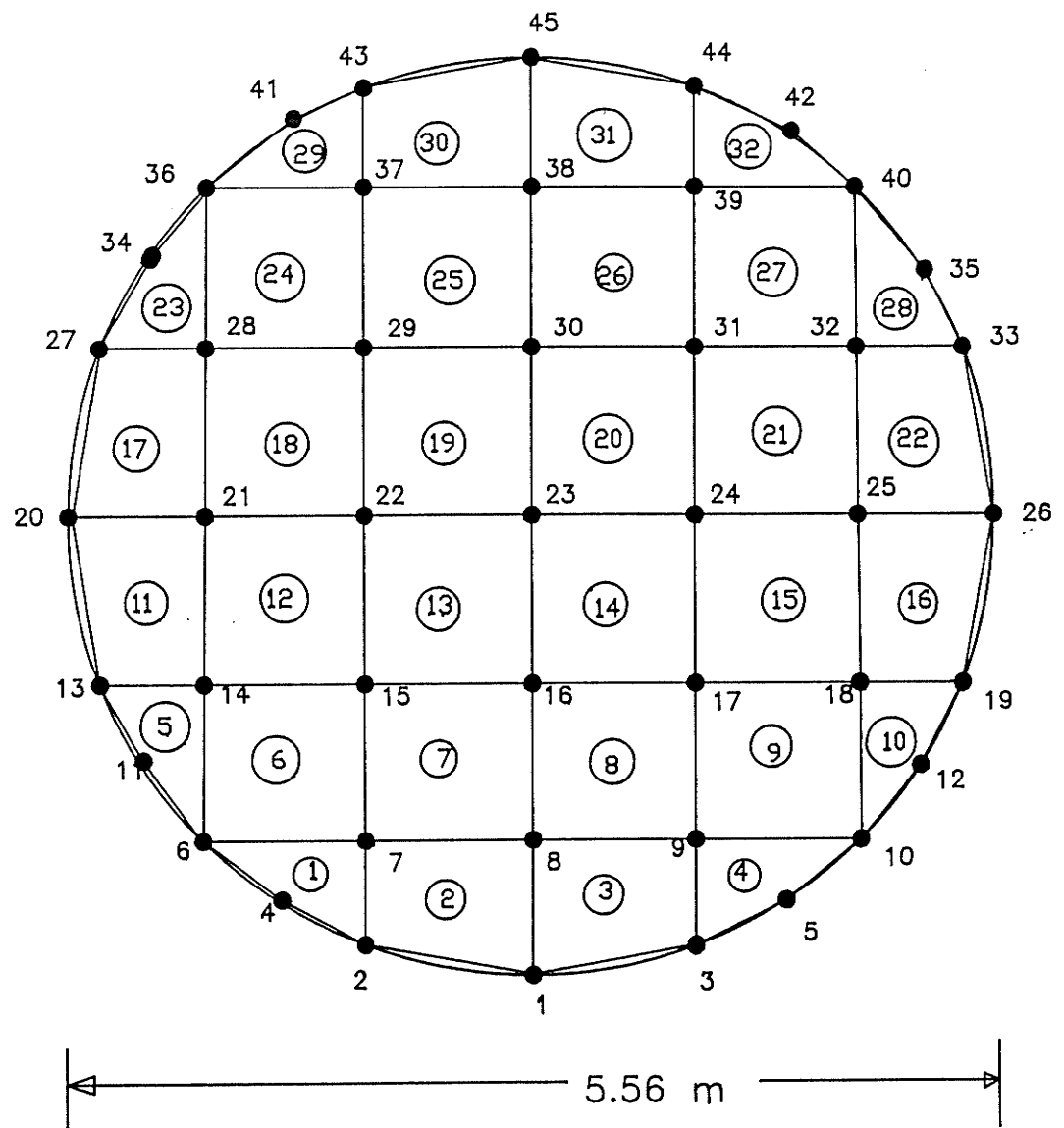


Fig 5.2: Bottom layer of a 5.56-m-diameter bin discretized into 32 linear elements.

(Numbers circumscribed by circles are element numbers, others are node numbers)

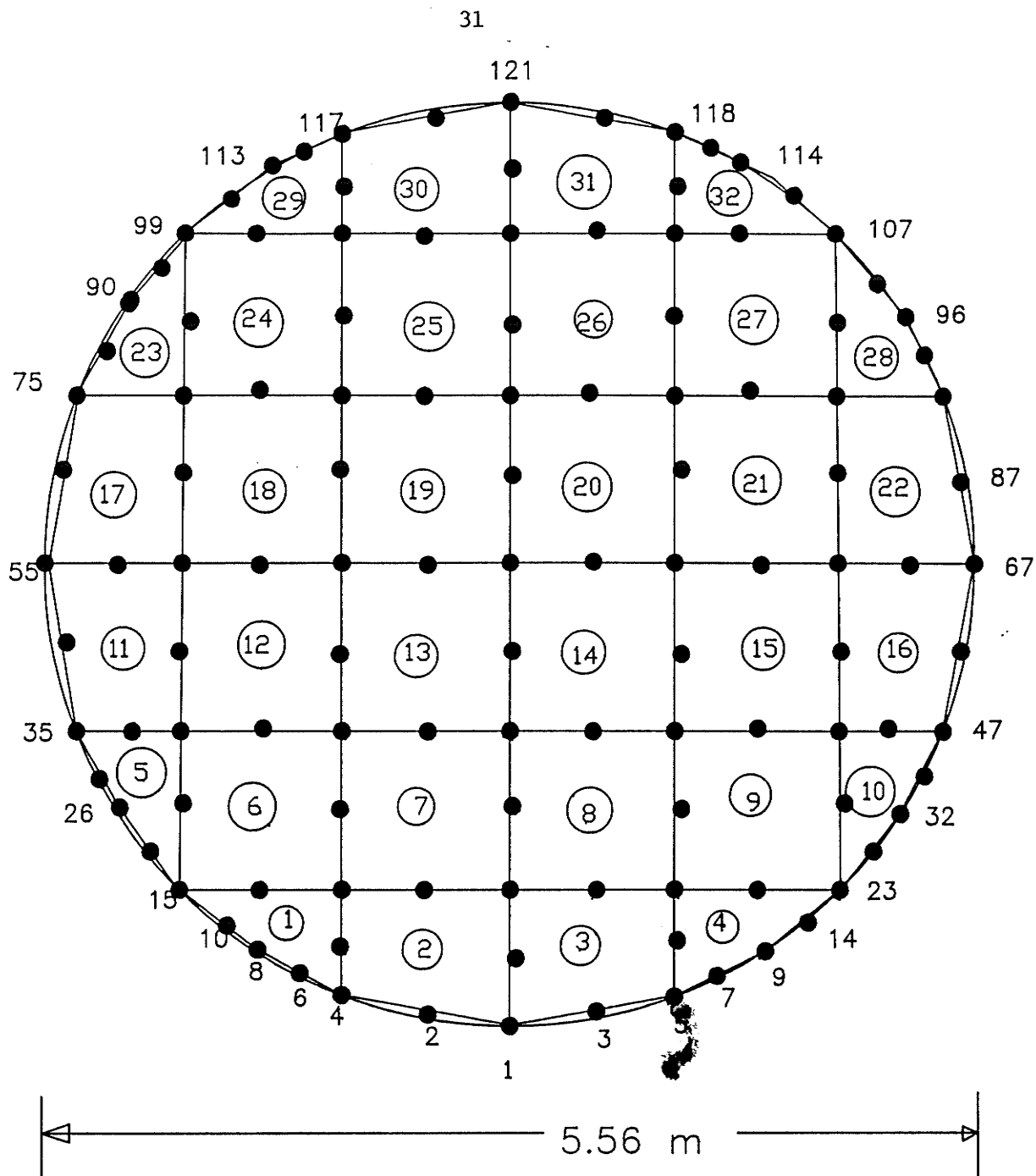


Fig 5.3: Bottom layer of a 5.56-m-diameter bin discretized into 32 quadratic elements.

(Numbers circumscribed by circles are element numbers, others are node numbers)

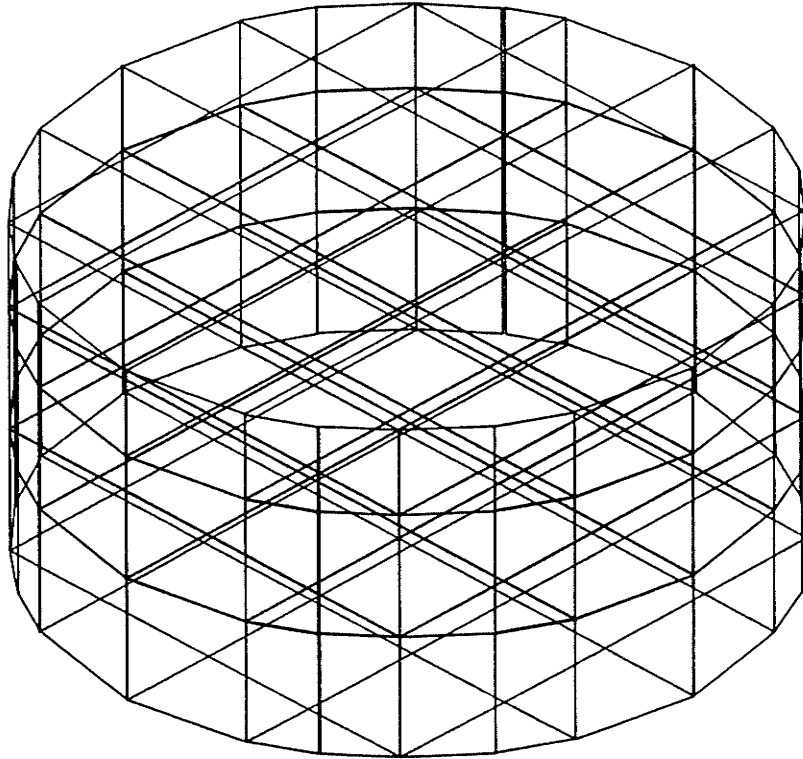


Fig 5.4: A cylindrical bulk of 5.56-m-diameter and 2.7 m height discretized into 96 hexahedron elements.

hexahedron elements. The total number of nodes in this grid were 180 for linear elements and 619 for quadratic elements.

The memory available in the University of Manitoba main frame computer (AMDAHL 5870) was not sufficient to use the grid shown in Fig 5.3. for quadratic elements. Hence the grain bulk was cut along the north-south diameter and one half of the bulk was discretized into quadratic elements. Temperatures of the nodes lying in the bottom layer of the bulks were prescribed by the temperatures calculated using a one dimensional finite difference equation. The finite difference equation uses the temperature of the node lying above the corresponding node and the soil temperature calculated using the model of Singh (1977), to calculate the temperature of the bottom node.

The hourly weather data for Winnipeg were used (20 km from the site). Thermal and physical properties of rapeseed used were as follows: specific heat,  $1700 \text{ J kg}^{-1} \text{ K}^{-1}$ ; thermal conductivity,  $0.12 \text{ W m}^{-1} \text{ K}^{-1}$ ; and bulk density,  $700 \text{ kg m}^{-3}$  (Moysey et al. 1977, Jayas et al. 1989). The thermal and physical properties of barley were assumed to be: specific heat,  $1560 \text{ J kg}^{-1} \text{ K}^{-1}$ , thermal conductivity,  $0.15 \text{ W m}^{-1} \text{ K}^{-1}$ , and bulk density,  $670 \text{ kg m}^{-3}$  (Muir et al. 1980). The longwave and shortwave emissivities, 0.28 and 0.89, respectively, for dirty galvanized iron, given by Kreith (1973), were used. The temperature of the air above the grain surface was set at 5 K above the ambient air temperature, and the convective heat transfer coefficient above the grain surface was assumed to be  $1 \text{ W m}^{-2} \text{ K}^{-1}$  (Muir et al. 1980). Various other values used in the simulation and their sources are listed in Table 5.1.

Table 5.1: Properties of air, soil and concrete used in the simulation.

Property	Value	Unit
<u>Air</u> *		
Thermal conductivity	0.02593	$\text{W m}^{-1} \text{K}^{-1}$
Density	1.205	$\text{kg m}^{-3}$
Viscosity	$18.14 \times 10^{-6}$	$\text{N s m}^{-2}$
<u>Soil</u> *		
Thermal conductivity	0.865	$\text{W m}^{-1} \text{K}^{-1}$
Density	1600	$\text{kg m}^{-3}$
Specific heat	865	$\text{J kg}^{-1} \text{K}^{-1}$
<u>Concrete</u> #		
Thermal conductivity	1.279	$\text{W m}^{-1} \text{K}^{-1}$
Density	2300	$\text{kg m}^{-3}$
Specific heat	1130	$\text{J kg}^{-1} \text{K}^{-1}$

\* Source, ASHRAE (1982)

# Source, Incropera and Dewitt (1985)

### Discussion on predicted temperatures

The temperatures measured at equal radii were averaged and reported as one value, thus giving 16 locations in the rapeseed bin and 20 locations in the barley bin. The temperatures predicted by the model at equal radii were also averaged and the results were printed. Thus, the measured and predicted temperatures were compared at 16 locations in the rapeseed bin and at 20 locations in the barley bin. The measured temperatures at various locations in the rapeseed and barley bins and the temperatures predicted by the model with linear and quadratic elements are shown in Appendix H.

Fig. 5.5 shows the measured temperatures and the temperatures predicted by the model with linear elements at 2.0 m radius from the centre at a height of 2.0 m from the floor, in the rapeseed bulk. The measured temperatures and the temperatures predicted by the model with linear elements at 2.0 m radius from the centre at a height of 2.7 m from the floor, in the barley bin are shown in Fig. 5.6. As could be seen from these figures the predicted temperatures closely followed the measured values. The same pattern was observed at all other locations compared for both the bins.

To estimate the accuracy of prediction with the measured values, the standard error of estimate and the average of the absolute difference were calculated at all the locations compared in the bins. These values for the rapeseed bin are tabulated in Table 5.2 and for the barley bin in Table 5.3. To determine the accuracy of prediction, linear regression lines were fit between the measured temperatures and the temperatures predicted by the model with linear and quadratic elements at every location compared for in both the bins. The intercept



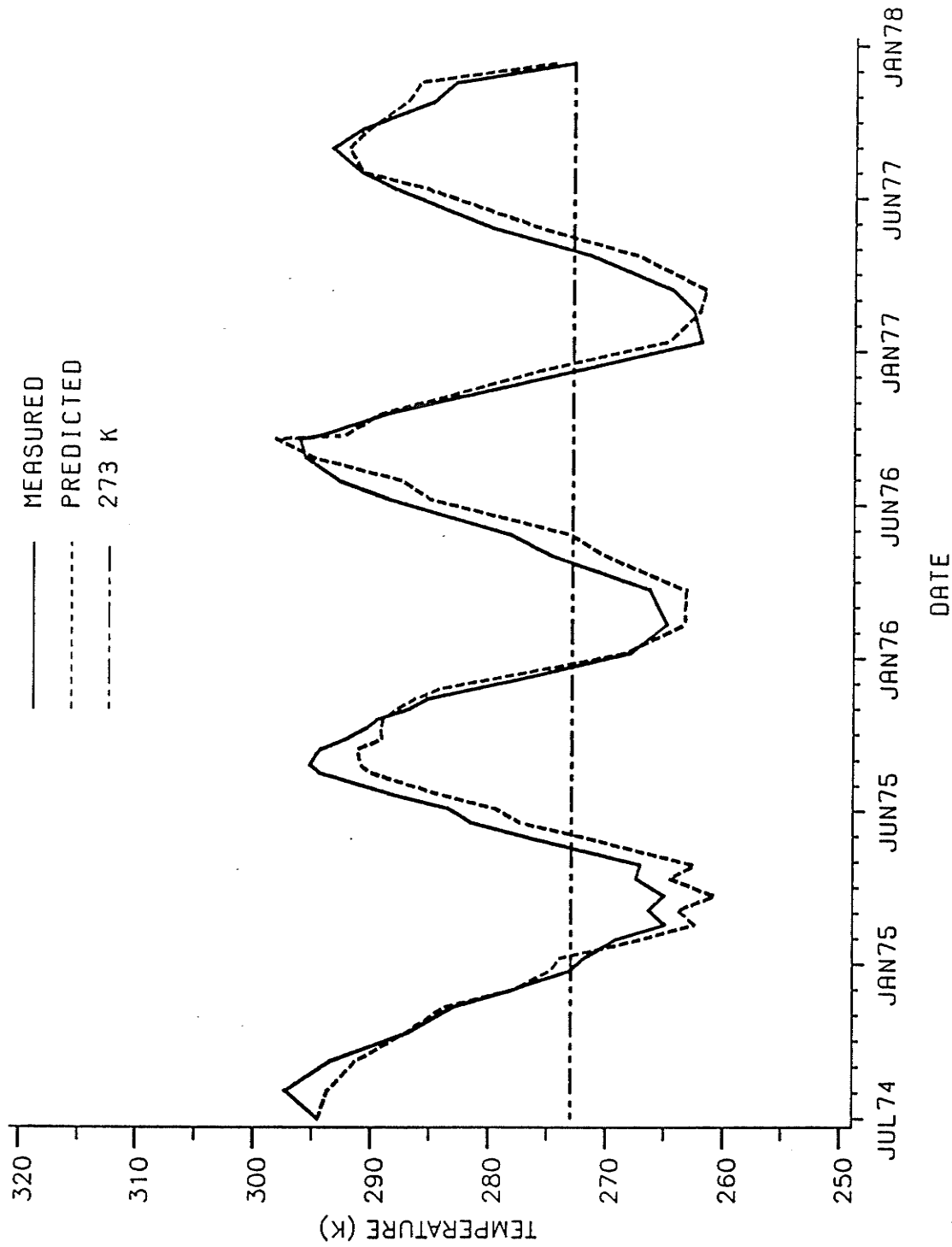


Fig 5.5: Temperatures predicted using linear finite elements and temperatures measured at 2 m radius and 2 m height in a 5.56-m-diameter bin filled with rapeseed to a depth of 2.7 m located near Winnipeg, Canada.

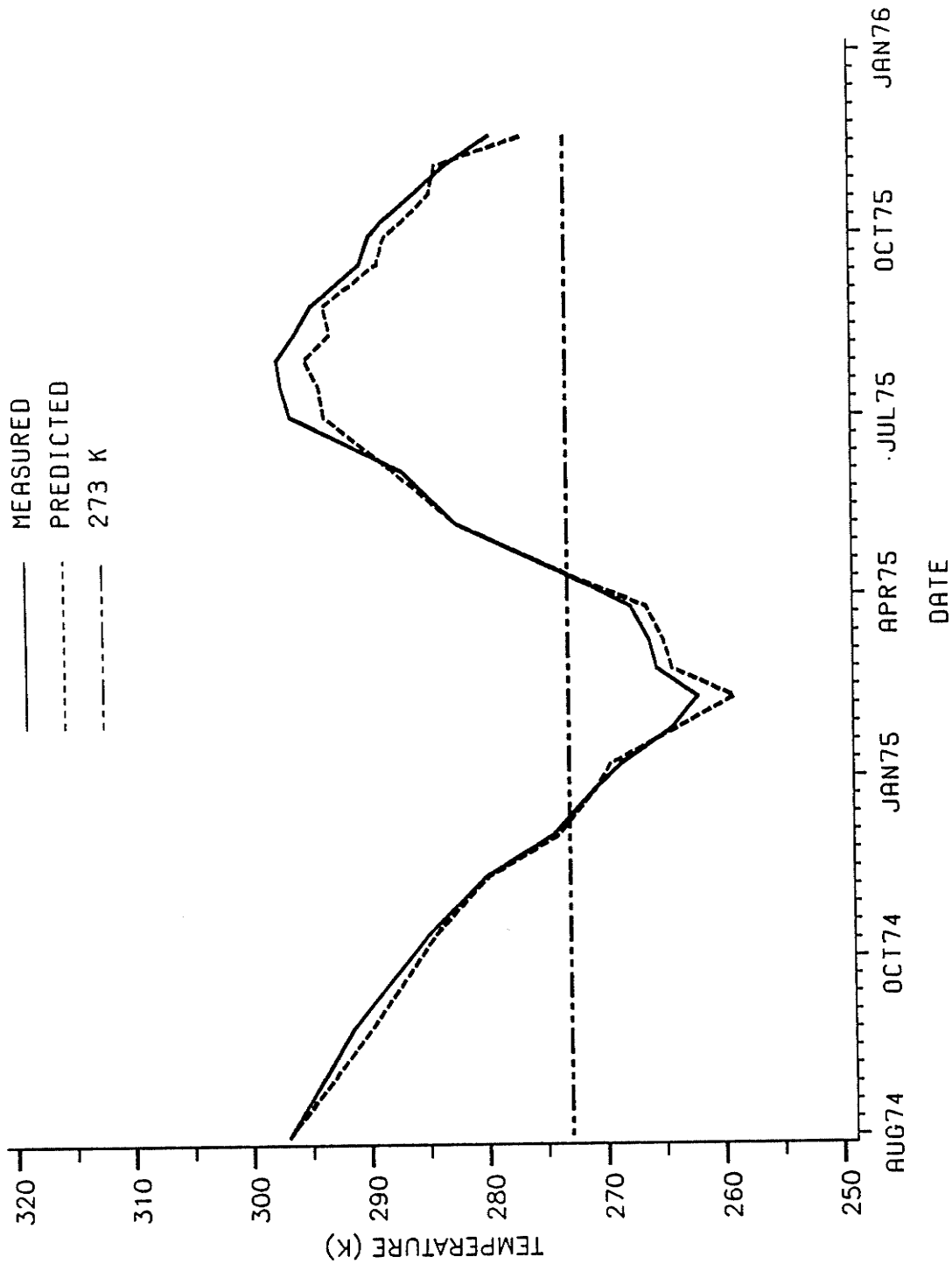


Fig 5.6: Temperatures predicted using linear finite elements and temperatures measured at 2 m radius and 2.7 m height in a 5.56-m-diameter bin filled with barley to a depth of 3.2 m located near Winnipeg, Canada

Table 5.2. Standard error of estimate and the average of the absolute difference between the measured and the predicted temperatures in the rapeseed bin.

Height from the floor (m)	Radius							
	Centre		1.0 m		2.0 m		Wall	
	S.E.	AAD	S.E.	AAD	S.E.	AAD	S.E.	AAD
<u>Linear element</u>								
2.7	4.9	3.7	3.1	2.5	3.3	2.7	3.5	2.7
2.0	3.6	2.9	3.0	2.5	2.9	2.5	3.5	2.7
1.0	3.0	2.7	3.0	2.6	3.0	2.6	3.2	2.5
0.0	2.2	1.9	2.3	1.9	2.8	2.4	5.1	4.3
<u>Quadratic element</u>								
2.7	3.9	3.0	3.9	3.1	4.5	3.5	5.3	4.3
2.0	3.1	2.4	2.5	2.0	3.0	2.5	4.2	3.4
1.0	2.3	1.9	1.6	1.3	3.3	2.5	4.1	3.3
0.0	1.5	1.3	1.5	1.2	2.8	2.2	5.0	3.9

Note : AAD - Average absolute difference  
 S.E. - Standard error =  $\sqrt{((Pt-Mt)^2/n)}$

where: Pt - predicted temperature  
 Mt - measured temperature

Table 5.3. Standard error of estimate and the average of the absolute difference between the measured and predicted temperatures in the barley bin

Height from the floor (m)	Radius							
	Centre		1 m		2 m		Wall	
	S.E.	AAD	S.E.	AAD	S.E.	AAD	S.E.	AAD
<u>Linear element</u>								
3.2	2.7	2.1	4.4	3.5	3.2	2.5	4.0	3.1
2.7	3.9	2.9	2.9	2.2	1.7	1.3	2.9	2.2
2.0	3.9	3.0	3.8	2.9	2.9	2.4	2.7	1.9
1.0	3.0	2.6	2.9	2.5	3.4	2.9	2.8	2.1
0.0	1.8	1.6	1.8	1.6	2.1	1.8	3.8	3.0
<u>Quadratic element</u>								
3.2	3.1	2.5	2.4	1.9	2.9	2.2	3.7	2.8
2.7	3.0	2.4	2.2	1.8	2.2	1.9	3.4	2.8
2.0	2.0	1.7	1.9	1.5	1.8	1.5	3.5	2.8
1.0	3.3	2.8	2.6	2.1	3.2	2.4	3.6	2.8
0.0	1.4	0.9	1.5	1.2	1.8	1.5	3.8	3.2

Note : AAD - Average absolute difference  
 S.E. - Standard error =  $\sqrt{((Pt-Mt)^2/n)}$

where: Pt - predicted temperature  
 Mt - measured temperature

was forced to zero. The slopes of these lines were close to 1.0 (0.989 to 1.004), with  $R^2$  values not lower than 0.999. One such plot with 95% confidence limits for the data points for the location at 2.0 m radius at a height of 2.0 m from the floor in the rapeseed bin is shown in Fig. 5.7.

The model with linear elements predicted the temperatures with an average standard error of estimate of 3.3 K in the rapeseed bin and with an average standard error of estimate of 3.1 K in the barley bin. The average of the absolute difference between the measured temperatures and the temperatures predicted by the model with linear elements were 2.7 K in the rapeseed bin and 2.4 K in the barley bin. The average standard errors of estimate of the temperatures predicted by the model with quadratic elements were the same as those using linear elements in the rapeseed bin (3.2 K), and 0.4 K closer to the measured temperatures in the barley bin (2.7 K). The average absolute difference between the temperatures measured and predicted by the model with quadratic elements were 2.6 K in the rapeseed bin and 2.1 K in the barley bin.

These errors of estimate are acceptable for analyzing stored product ecosystems because the measured grain temperatures could also have been influenced by several other factors including internal heat generation due to insect and microorganism respiration, and variations in thermal properties of the grain due to moisture content and foreign material. Moisture content of the grain at different dates and locations in the bulk, internal heat generation, and foreign material content were not available. The thermal properties of grain in space and time were assumed constant, and internal heat generation was

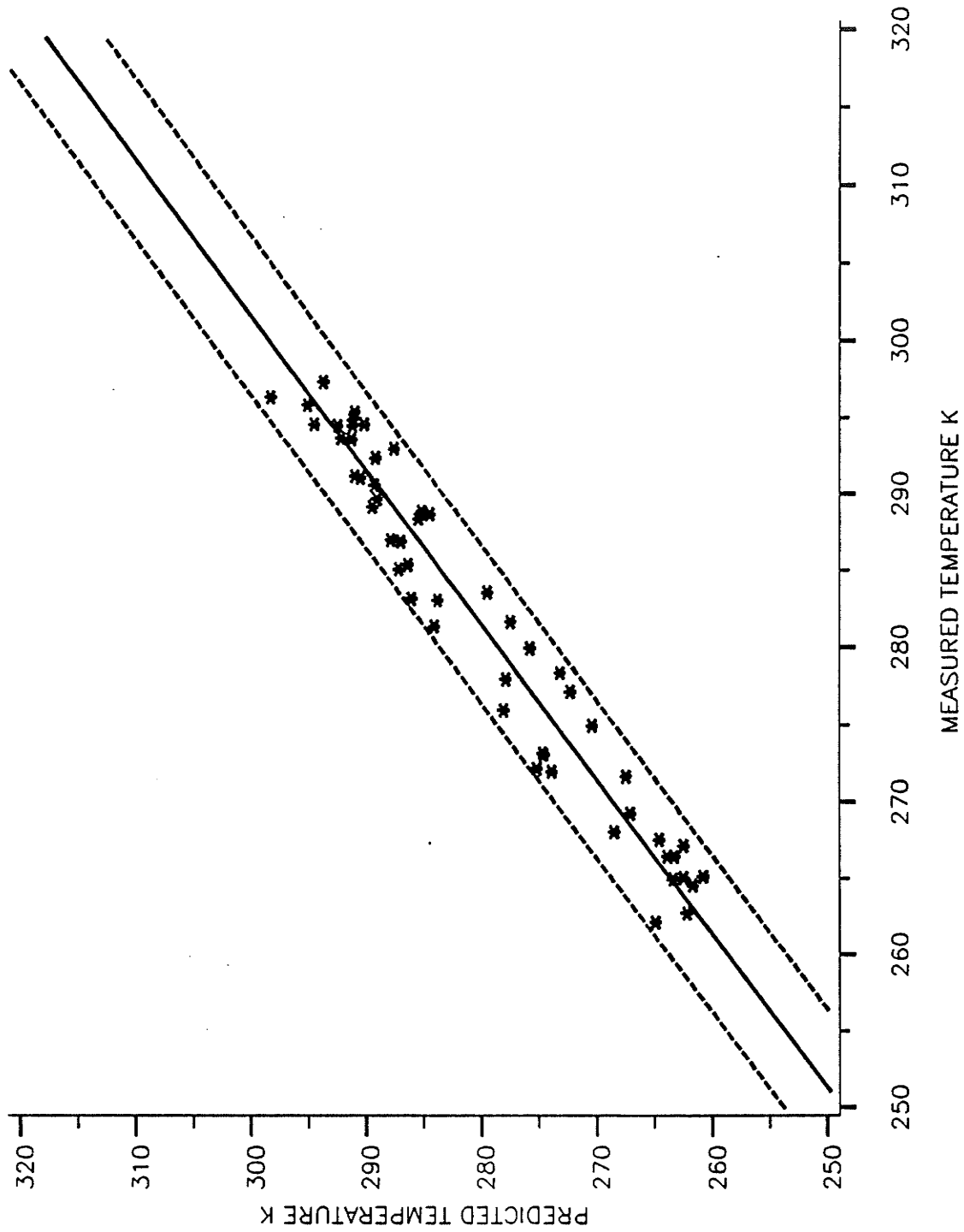


Fig 5.7: Measured temperatures and temperatures predicted by the model with linear elements at 2-m-radius and 2-m-height in the rapeseed bin. Dashed lines show the 95% confidence limits for the data points.

assumed to be zero. The accuracy of prediction might be improved by taking these factors into consideration although extreme variations from predicted values could be used to indicate active grain spoilage in the future.

The average standard errors of estimate of the predicted temperatures compared to the measured temperatures at points lying along the circumference of the bin and the top surface were larger (4.1 K in the rapeseed bin and 3.3 K in the barley bin, using the model with the linear elements) than those of points within the bulk (2.6 K in the rapeseed bin and 2.7 K in the barley bin). The temperatures near the bin wall and the surface of the bulk are influenced by the diurnal variation of the ambient temperature and solar radiation. The time of recording the temperature data in a day will affect the temperatures at these points, rather than at a point inside the bulk. Since, the time of temperature measurement and the time when the simulated temperatures were outputted might not be exactly the same, the standard errors of estimate at points close to the bin wall and the top surface of the bulk were larger in both the bins.

Computer time required for execution of the model with 96 linear elements (180 nodes) was  $7.8 \text{ s day}^{-1}$  of simulation and for execution of the model with 48 quadratic elements (346 nodes) it was  $24.9 \text{ s day}^{-1}$ . Considering the reduced computer time and similar accuracy of prediction, linear elements were preferable for predicting grain temperatures.

### Comparison with 2D finite difference model

The temperatures of 3.0-m and 4.0-m tall rapeseed bulks were simulated using the 2D finite difference model (Muir et al. 1980) and the 3D finite element model for a 12 month period starting from January 1, 1974. The diameter of the 3.0 m grain bulk was varied from 1 to 12 m and that of the 4.0 m bulk was varied from 2 to 16 m. This gave a maximum diameter to height ratio ( $d/h$ ) of 4.0 for both the grain bulks. Initial grain temperature was assumed to be 293 K throughout the bulk. Since the 2D model uses the calculated radiation values on the southern 55% of the bin wall (Muir et al. 1980), the temperatures predicted by the 2D finite difference model at half the radius mid-way between the top and bottom surfaces and the temperatures predicted by the 3D finite element model at half the radius towards the south, at this height, were compared. These values for the 3.0-m-tall grain bulk for different  $d/h$  ratios are given in Table 5.4 and for the 4.0 m tall bulk in Table 5.5. Average absolute difference of the temperatures predicted by the two models decreased with an increase in the  $d/h$  ratio, except for the  $d/h$  ratio of 2.0 in the 4.0-m-tall bulk (Fig. 5.8). In the 3.0-m-tall bulk the average absolute difference between the temperatures predicted by the two models decreased from 4.4 K for  $d/h$  ratio of 0.33 to 1.8 K for  $d/h$  ratio of 4.0.

Eventhough both the models predicted almost the same temperatures for various  $d/h$  ratios, only the 3D model can predict the effect of hotspot in the surrounding grain mass, temperature distribution in non-cylindrical and hopper bottom bins, and in grain bulks that are not levelled on top. Also the effect of variable heating



Table 5.4: Temperatures (K), on the last day of the month at half the radius towards the south, predicted by 2D finite difference and 3D finite element models in a 3-m-tall rapeseed bulk at Winnipeg with initial grain temperature of 293 K on 1 January 1974.

		Diameter to height ratio									
		0.33		0.66		1.0		2.0		4.0	
MONTH	AT	2DFD	3DFE	2DFD	3DFE	2DFD	3DFE	2DFD	3DFE	2DFD	3DFE
Jan	246	256	263	265	267	278	280	289	292	291	292
Feb	268	264	263	263	269	268	274	281	284	287	288
Mar	273	267	267	265	265	267	269	277	279	283	286
Apr	277	282	287	278	279	273	276	275	275	280	283
May	286	289	294	284	284	280	279	277	274	280	280
Jun	290	298	303	294	294	288	288	280	276	280	279
Jul	291	296	302	298	301	294	297	285	281	284	280
Aug	285	299	301	293	297	293	296	287	285	284	281
Sep	277	292	295	296	291	295	295	288	289	285	282
Oct	282	281	283	284	290	287	294	287	288	284	282
Nov	261	267	275	274	276	280	282	285	288	284	283
Dec	263	268	274	268	272	273	277	281	283	282	282
AAD =		4.4		3.8		2.8		2.3		1.8	

Note : Explanation for the abbreviations are given in the foot note of Table 5.5

Table 5.5: Temperatures (K), on the last day of the month at half the radius towards the south, predicted by 2D finite difference and 3D finite element models in a 4-m-tall rapeseed bulk at Winnipeg with initial grain temperature of 293 K on 1 January 1974.

		Diameter to height ratio									
		0.5		1.0		2.0		3.0		4.0	
MONTH	AT	2DFD	3DFE	2DFD	3DFE	2DFD	3DFE	2DFD	3DFE	2DFD	3DFE
Jan	246	265	268	283	289	292	293	293	294	293	293
Feb	268	263	269	275	280	288	289	291	291	291	292
Mar	273	267	264	272	275	284	283	288	289	288	290
Apr	276	277	278	273	273	281	279	285	285	286	288
May	286	284	283	277	274	280	276	283	283	284	286
Jun	290	294	293	283	279	280	275	283	281	283	285
Jul	291	298	301	289	288	282	276	283	280	283	284
Aug	285	293	298	291	293	284	278	284	280	284	283
Sep	277	296	293	292	295	286	280	285	281	284	283
Oct	282	284	292	289	292	287	281	285	281	285	283
Nov	261	274	278	284	289	286	282	285	282	283	283
Dec	263	268	272	278	282	284	280	284	281	283	283
AAD =		3.5		3.3		3.7		2.1		1.2	

Note : 2DFD - Predicted by two dimensional finite difference model  
 3DFE - Predicted by three dimensional finite element model  
 AT - Ambient temperature  
 AAD - Average absolute difference between values predicted by the two models

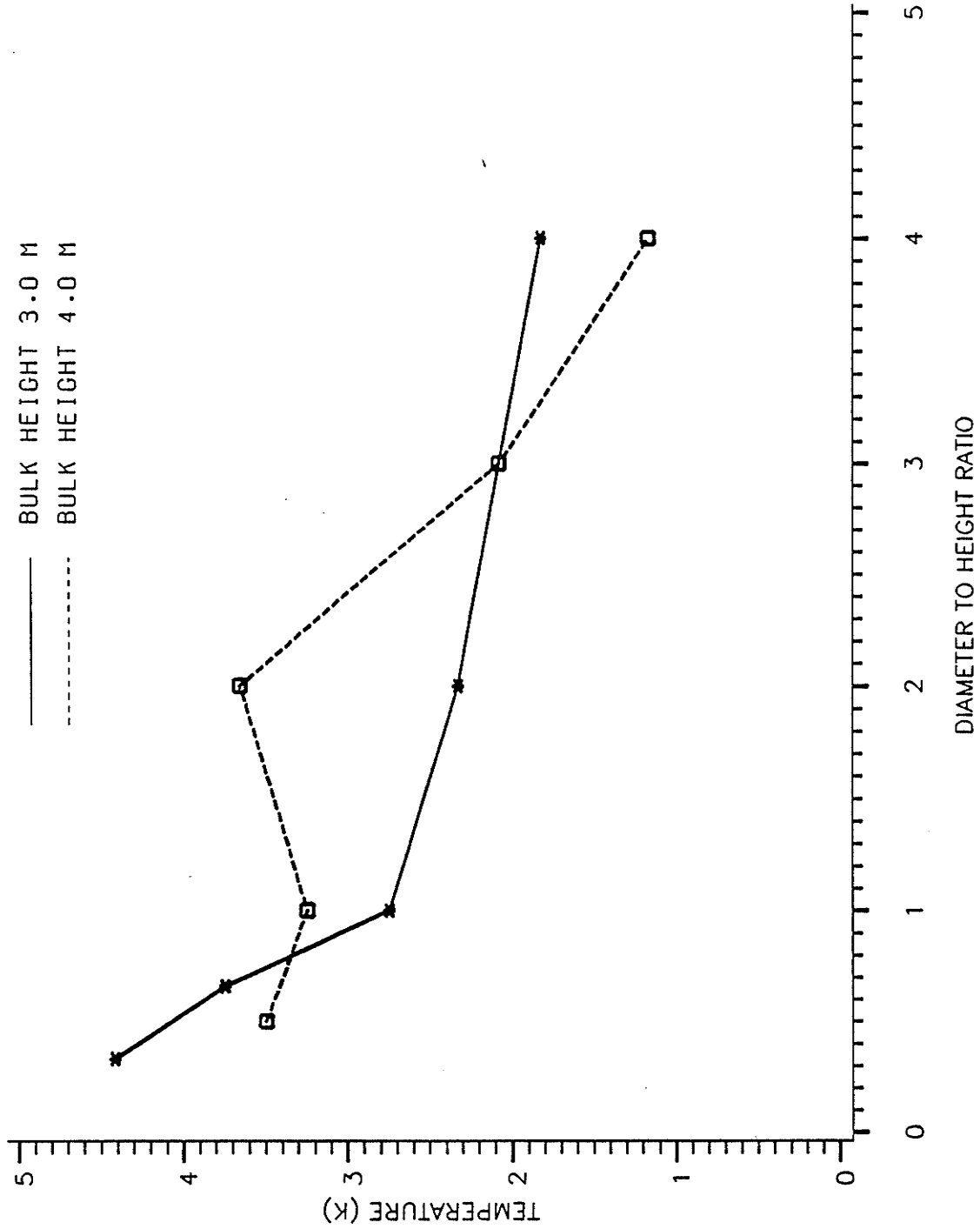


Fig 5.8: Average absolute difference between the temperatures predicted by the 3D finite element model and 2D finite difference model at half the radius towards the south mid-way between the top and bottom layers, for various  $d/h$  ratios.

of the bin wall due to solar radiation on the grain temperatures can be studied only by using a 3D model.

To study the effect of variable heating of the bin wall due to solar radiation on the grain temperatures, the average of the absolute difference of the temperatures predicted by the 3D finite element model at half the radius towards the south and north and midway between the top and bottom layers were compared. Fig. 5.9 shows the average absolute difference of the predicted temperatures at these points for different  $d/h$  ratios. The temperatures of this point on the south radius were higher than the corresponding point on the north radius by 15 K for a 3.0-m-tall bulk with  $d/h$  ratio of 0.33 and by 5 K for  $d/h$  ratio of 4.0. The difference in temperatures between these points in 3.0-m-tall bulk were more than in 4.0-m-tall grain bulk. The effect of the top and bottom surface temperatures at a point mid-way between these surfaces will be more when the height of the bulk is less.

The 2D model does not incorporate the differential heating of the bulk towards the north and the south sides of the bin. As predicted by the 3D finite element model and expected in actual bins there is a distinct difference between the temperatures towards the north and south sides of the bin. Therefore, for more precise estimates of the temperatures at all locations in the bins a 3D model is a better alternative than a 2D model.

#### Comparison with a 3D Finite Difference Model

The temperatures predicted by the 3D finite element model and 3D finite difference model (Alagusundaram et al. 1988) were compared in two stages.

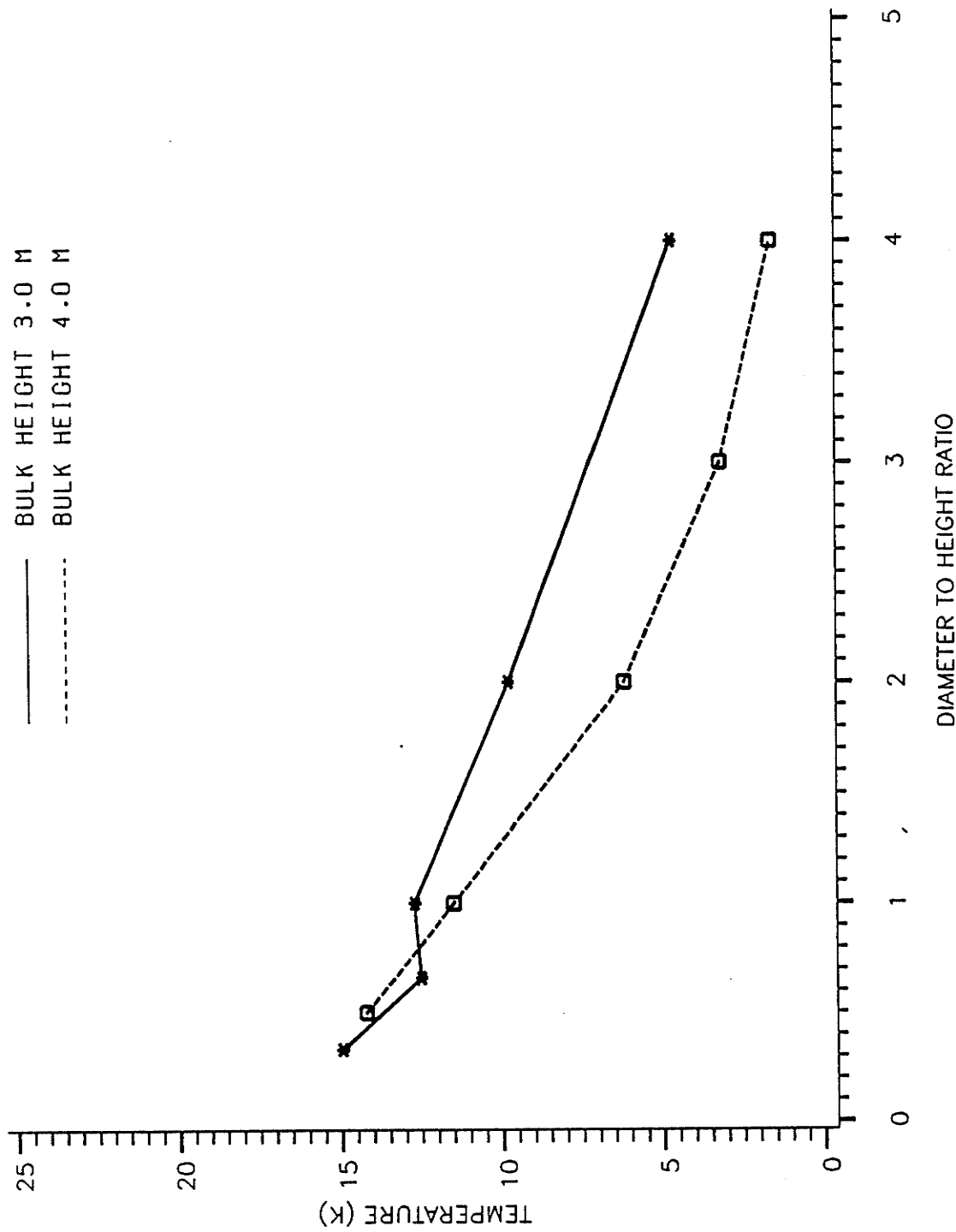


Fig 5.9: Average absolute difference of the temperatures predicted by the 3D finite element model, at half the radius towards the south and north, in a bin filled with rapeseed, for a 12 month period beginning 1 Jan, 1974. Initial temperature of the bulk was assumed to be 293 K.

1. The temperatures of the 5.56-m-diameter rapeseed bulk were predicted using the 3D finite difference model. In this model 250 temperature nodes (5 vertical, 5 radial and 10 circumferential) were used. The thermal properties of the rapeseed, bin wall, soil, concrete and air used were the same as the values used for the simulation using the 3D finite element model. The temperatures predicted by the two models were comparable. The 3D finite difference model predicted temperatures of the rapeseed bulk with an average standard error of estimate of 3.0 K and an average of absolute difference of 2.4. These values for the temperatures predicted by the 3D finite element model were 3.3 K and 2.7 K, respectively.

2. Temperatures in 3.0-m and 4.0-m-tall rapeseed bulks were predicted using both 3D models. The diameter of the 3.0-m-tall grain bulk was varied from 1 to 12 m and that of the 4.0-m bulk from 2 to 16 m. The initial grain temperature was assumed at 293 K and the temperatures were predicted for a 12 month period from January 1, 1974. Table 5.6 and Table 5.7 show the temperatures predicted by the two models at half the radius towards the south, for various d/h ratios in 3.0-m-tall and 4.0-m-tall rapeseed bulks, respectively. The average absolute difference between the temperatures predicted by the two models were from 3.0 to 7.5 K. The difference in the predicted temperatures between the two models may be due to the inherent properties of the two methods and to the differences in calculation of the solar radiation component. In the 3D finite difference model the solar radiation values on the bin wall were calculated at 10 sectors of 36 degrees each (inherent in the program), whereas in the finite

Table 5.6: Temperatures (K), on the last day of the month at half the radius towards the south, predicted by 3D finite difference and 3D finite element models in a 3-m-tall rapeseed bulk at Winnipeg with initial grain temperature of 293 K on 1 January 1974.

Diameter to height ratio											
		0.33		0.66		1.0		2.0		4.0	
MONTH	AT	3DFD	3DFE	3DFD	3DFE	3DFD	3DFE	3DFD	3DFE	3DFD	3DFE
Jan	246	261	263	274	267	281	280	291	292	293	292
Feb	268	271	263	273	269	276	274	288	284	291	288
Mar	273	274	267	273	265	274	269	285	279	289	286
Apr	277	282	287	279	279	277	276	283	275	287	283
May	286	290	294	283	284	279	279	282	274	286	280
Jun	290	295	303	290	294	285	288	283	276	285	279
Jul	291	296	302	295	301	291	297	285	281	285	280
Aug	285	290	301	293	297	292	296	287	285	285	281
Sep	277	284	295	290	291	291	295	288	289	286	282
Oct	282	284	283	286	290	288	294	288	288	286	282
Nov	261	271	275	274	276	282	282	286	288	286	283
Dec	263	271	274	273	272	276	277	284	283	285	282
AAD		5.9		3.3		3.0		3.3		3.9	

Note : Explanation for the abbreviations are given in the foot note of Table 5.7

Table 5.7: Temperatures (K), on the last day of the month at half the radius towards the south, predicted by 3D finite difference and 3D finite element models in a 4-m-tall rapeseed bulk at Winnipeg with initial grain temperature of 293 K on 1 January 1974.

Diameter to height ratio											
		0.5		1.0		2.0		3.0		4.0	
MONTH	AT	3DFD	3DFE	3DFD	3DFE	3DFD	3DFE	3DFD	3DFE	3DFD	3DFE
Jan	246	274	268	288	289	292	293	293	294	293	293
Feb	268	272	269	284	280	291	289	292	291	292	292
Mar	273	272	264	282	275	289	283	291	289	292	290
Apr	277	279	278	282	273	288	279	290	285	291	288
May	286	282	283	282	274	287	276	289	283	290	286
Jun	290	289	293	285	279	287	275	288	281	289	285
Jul	291	295	301	288	288	287	276	288	280	288	284
Aug	285	293	298	290	293	287	278	288	280	288	283
Sep	277	289	293	290	295	288	280	288	281	288	283
Oct	282	287	292	289	292	288	281	288	281	288	283
Nov	261	278	278	286	289	288	282	288	282	287	283
Dec	263	273	272	282	282	286	280	287	281	287	283
AAD		3.7		4.0		7.6		5.2		3.3	

Note : 3DFE - Predicted by three dimensional finite element model  
 3DFD - Predicted by three dimensional finite difference model  
 AT - Ambient temperature  
 AAD - Average absolute difference between values predicted by the two models

element model, the solar radiation values on the bin wall were calculated at 24 points along the circumference (Fig.5.2)

Although both models predicted the temperatures with the same degree of accuracy, the finite element model would be a better choice in the following circumstances:

- (i) for predicting the temperatures of grain bins of different geometrical shapes because the finite element model is written for Cartesian coordinate system.
- (iii) for including effects of variable thermal properties of the grain bulk due to moisture differentials and foreign materials.
- (iv) in places where the surface of the grain bulk is conically shaped, rather than flattened.

## 6. CONCLUSIONS

Based on the results of this study the following conclusions were drawn:

1. The temperatures predicted by the three dimensional finite element model with linear and quadratic elements were in close agreement with the measured temperatures in a 5.56-m-diameter bin containing rapeseed and a 5.56-m-diameter bin containing barley, located near Winnipeg.
2. The model with quadratic elements did not improve the accuracy of prediction, but it took more computer time for execution of the program than with linear elements. Hence, the model with linear elements can be used for predicting stored grain temperatures.
3. The average absolute difference between the temperatures predicted by the 3D finite element model and a 2D finite difference model at half the radius towards the south, mid-way between the top and bottom surfaces, decreased with an increase in the  $d/h$  ratio of the grain bulk.
4. The temperatures predicted by the 3D finite element model compare favorably with the temperatures predicted by a 3D finite difference model.
5. The 3D finite element model is preferable to the 3D finite difference model because the 3D finite difference model is unique for a cylindrical grain storage bin with a flat top surface, whereas the 3D finite element model can be used to predict the grain temperatures in grain bins of any shape.



6. There were distinct differences between the temperatures predicted for the north and south sides of a bin by both 3D models.
7. This model can be used for predicting the temperature distribution in other stored commodities like flour, dried feed, hay etc. if the forced or free convective heat transfer inside the bulk is negligible compared to the conductive heat transfer.

## 7. SUGGESTIONS FOR FUTURE WORK

1. In the present model the temperature of the air above the grain surface was assumed to be 5 K above the ambient air temperature and the convective heat transfer coefficient was assumed to be  $1 \text{ W m}^{-2} \text{ K}^{-1}$ . Heat transfer to the roof and through the head space should be calculated by calculating radiative and convective heat transfer in this area.
2. Due to the limitations of the computer memory, finer meshes could not be tried. The accuracy of prediction can be checked by running the program with finer meshes using a more powerful computer with larger memory.
3. The model can be coupled to a mass transfer model for predicting moisture migration in the stored grain and to study the effect of these non-biological factors on the growth and reproduction of biological organisms affecting the stored grain.

## 8. REFERENCES

- Abdel-Kader, M.H.K., G.R.B. Webster, S.R. Loschiavo and F.L. Watters. 1980. Low temperature degradation of malathion in stored wheat. J. Econ. Entomol. 73: 654-656.
- Alagusundaram, K., D.S. Jayas, W.E. Muir and N.D.G. White. 1988. Three dimensional heat transfer model of temperature distribution in grain storage bins. ASAE paper No. NCR 88-602. Am. Soc. Agric. Eng., St. Joseph, Michigan.
- Allaire, P.E. 1985. Basics of the Finite Element Method. Solid Mechanics, Heat transfer, and Fluid mechanics. W.M.C. Brown Publishers, Dubuque, Iowa. 691 pp.
- Anonymous. 1988. Canadian Grains Industry Statistical Handbook - 1988. Canada Grains Council, Winnipeg, Manitoba. 278 pp
- Anonymous. 1989. Stored-grain pests. Supplement to the official grain inspectors manual. Inspection Division, Canadian Grain Commission, Winnipeg, Manitoba. 43 pp.
- ASHRAE. 1982. Hand Book of Applications. Am. Soc. for Heat., Refrig. and Air cond. Eng., Atlanta, GA.
- Bathe, K.J. 1982. Finite Element Procedures in Engineering Analysis. Prentice-Hall Inc. Englewood Cliffs, New Jersey 07632. 735 pp.
- Converse, H.H., A.H. Graves and D.S. Chung. 1973. Transient heat transfer within wheat stored in cylindrical bins. Trans. ASAE (Am. Soc. Agric. Eng.), 16:129-133.
- Cuperus, G.W., C.K. Pickett, P.D. Bloome and J.T. Pitts. 1986. Insect populations in aerated and unaerated stored wheat in Oklahoma. J. Kansas Entomol. Soc. 59: 620-627.
- Duffie, J.A. and W.A. Beckman. 1974. Solar Energy Thermal Process. John Wiley and Sons, New York, 386 pp.
- Epperly, D.R., R.T. Noyes., C.W. Cuperus and B.L. Clary. 1987. Control of stored grain insects by grain temperature management. ASAE Paper No. 87-6035. Am. Soc. Agric. Eng., St. Joseph, MI.
- Jayas, D.S., S. Sokhansanj and N.D.G. White. 1989. Bulk density and porosity of two Canola species. Trans. ASAE (Am. Soc. Agric. Eng.) 32: 291-294.
- Hall, D.W. 1970. Handling and Storage of Food Grains in Tropical and sub Tropical Areas. Food and Agriculture Organizations of the United Nations, Rome. 350 pp.

- Harris, C.R. and G.B. Kinoshita. 1977. Influence of post-treatment temperature on the toxicity of pyrethroid insecticides. *J. Econ. Entomol.* 70: 215-218.
- Incropera, F.P. and D.P. Dewitt. 1985. *Fundamentals of Heat and Mass transfer*, Second edition. John Wiley & Sons, New York. 801 pp.
- Jiang, S, J.C. Jofreit and B.Smith. 1988. Temperature observations in a bottom-unloading silo. *Can. Agric. Eng.* 30:249-255.
- Kreith, F. 1973. *Principles of Heat Transfer*, 3rd edition. Intext Educational Publishers, New York. 656 pp.
- Lo, K.M., C.S.Chen., J.T. Clayton. and D.D. Adrian. 1975. Simulation of temperature and moisture changes in wheat storage due to weather variability. *J. Agric. Eng. Res.* 20:47-53.
- Longstaff, R.A. and H.J. Banks. 1987. Simulation of temperature fluctuations near the surface of grain bulks. *J. Stored Prod. Res.* 23:21-30.
- Longstaff, B.C. and J.M. Desmarchelier. 1983. The effects of the temperature-toxicity relationships of certain pesticides upon the population growth of Sitophilus oryzae (L.) (Coleoptera Curculionidae) *J. Stored Prod. Res.* 19: 25-29.
- Longstaff, R.A. and J.J. Fennigan. 1983. A wind tunnel model study of forced convective heat transfer from horizontal grain storage due to weather variability. *J. Stored Prod. Res.* 19:81-87.
- Loschiavo, S.R. (ed). 1984. *Insects, mites and molds in farm-stored grain in the prairie provinces*. Agric. Can. Pub. 1595/E. 31pp.
- Manbeck, H.B. and M.G. Britton. 1988. Prediction of bin wall declines. *Trans ASAE (Am. Soc. Agric. Eng.)* 31: 1767-1773.
- Metzger, J.F., and W.E. Muir. 1983. Computer model of two dimensional conduction and forced convection in stored grain. *Can. Agric. Eng.* 25:119-125.
- Moysey, E.B., J.T. Shaw and W.P. Lampman. 1977. The effect of temperature and moisture on the thermal properties of rapeseed. *Trans. ASAE (Am. Soc. Agric. Eng.)* 20:768-771.
- Muir, W.E. 1970. Temperatures in grain bins. *Can. Agric. Eng.* 12:21-24.
- Muir, W.E. 1980. Grain drying and storage in Canada. *J. Soc. Agric. Struc., Japan.* 10(2): 91-105.
- Muir, W.E., B.M. Fraser and R.N. Sinha. 1980. Simulation model of two dimensional heat transfer in controlled atmosphere grain bins.

- In: J. Shejbal (ed), Controlled Atmosphere Storage of Grains, Elsevier Sci. Pub. Co., Amsterdam. pp. 385-397.
- Muir, W.E., D.S. Jayas, M.G. Britton, R.N. Sinha and N.D.G. White. 1987. Interdisciplinary grain storage research at the University of Manitoba. ASAE Paper No. 87-6544. Am. Soc. Agric. Eng., St. Joseph, MI.
- Neiber, L.J. 1983. Graduate instruction in finite element analysis applications in agricultural engineering. ASAE Paper No. 83-5536. Am. Soc. Agric. Eng., St. Joseph, MI.
- Oxley, T.A. 1948. The Scientific Principles of Grain Storage. The Northern Publishing Co. Ltd., Liverpool. 103 pp.
- Parsons, J.E., R.W. Skaggs and C.W. Doty. 1987. Application of three dimensional water management model. Trans. ASAE (Am. Soc. Agric. Eng.) 30: 960-968.
- Rao, S.S. 1982. The Finite Element Method in Engineering. Pergamon press, New York. 625 pp.
- Ruth, D.W. and R.E. Chant. 1976. The relationship of diffuse radiation to total radiation in Canada. Sol. Energy 18:153-154.
- Segerlind, L.J. 1976. Applied Finite Element Analysis. 1st edition. John Wiley and Sons, New York, 422 pp.
- Segerlind, L.J. 1984. Applied Finite Element Analysis. 2nd edition. John Wiley and Sons, New York, 427 pp.
- Shufen, J. and J.C. Jofreit. 1987. Finite element prediction of silage temperatures in tower silos. Trans. ASAE (Am. Soc. Agric. Eng.) 30: 1744-1750.
- Singh, R.K. 1977. Computer simulation of energy recovery through anaerobic digestion of livestock manure. Unpublished Masters Thesis, University of Manitoba, Winnipeg.
- Sinha, R.N., and H.A.H. Wallace. 1977. Storage stability of farm-stored rapeseed and barley. Can. J. Plant Sci. 57: 351-365.
- Sinha, R.N. and F.L. Watters. 1985. Insects, Pests of Flour Mills, Grain Elevators, and Feed Mills and Their Control. Agric. Can. Pub. 1776. 290 pp.
- Trupp, A.C. 1964. Methods of solving heat conduction problems with particular reference to frozen dams. Unpublished Masters Thesis. Dept. of Mechanical Engineering. University of Manitoba, Winnipeg.

- Tyler, P.S. and T.J. Binns. 1982. The influence of temperature on the susceptible and resistant strains of Tribolium castaneum, Oryzaephilus surinamensis, and Sitophilus granarius. J. Stored Prod. Res. 18:13-19.
- White, G.G. 1988. Temperature changes in bulk stored wheat in sub-tropical Australia. J. Stored Prod. Res. 24: 5-11.
- Wood, E.L. and R.W. Lewis. 1975. A comparison of time marching schemes for the transient heat conduction equation. Int. J. Num. Methods In Eng. 9: 679-689.
- Yaciuk, G., W.E. Muir and R.N. Sinha. 1975. A simulation model of temperatures in stored grain. J. Agric. Eng. Res. 20:245-258.
- Zinkiewich, O.C. and C.J. Parekh. 1970. Transient field problems: Two dimensional and three dimensional analysis by Isoparametric finite elements. Int. J. Num. Methods. 2:61-71.

**Appendix A.**  
**Interpolation functions in natural coordinate system**  
(source Rao 1982)

The location of nodes and the local node numbers in a hexahedron element are shown in Figure A-1. The origin of the natural coordinate system is taken at the interface of the lines joining the mid-points of the opposite faces of the hexahedron, and the sides are defined by,

$$r = \pm 1, \quad s = \pm 1, \quad \text{and}, \quad t = \pm 1.$$

The relationship between the natural and Cartesian coordinates for an element with P number of nodes is given by:

$$x = \sum_{i=1}^P N_i x_i$$

$$y = \sum_{i=1}^P N_i y_i$$

and, 
$$z = \sum_{i=1}^P N_i z_i$$

This relationship in matrix form can be written as:

$$\begin{bmatrix} x \\ y \\ z \end{bmatrix} = \begin{bmatrix} N_1 & N_2 & \dots & N_P & 0 & 0 & 0 & 0 & 0 \\ 0 & 0 & 0 & N_1 & N_2 & \dots & N_P & 0 & 0 \\ 0 & 0 & 0 & 0 & 0 & 0 & N_1 & N_2 & \dots & N_P \end{bmatrix} \begin{bmatrix} x_1 \\ x_2 \\ \vdots \\ x_P \\ y_1 \\ y_2 \\ \vdots \\ y_P \\ z_1 \\ z_2 \\ \vdots \\ z_P \end{bmatrix}$$

For a linear element,

$$N_i = \frac{1}{8} (1+rr_i)(1+ss_i)(1+tt_i) ; \quad i = 1, 2, \dots, 8$$

and for a quadratic element,

$$N_i = \frac{1}{8} (1+rr_i)(1+ss_i)(1+tt_i)(rr_i+ss_i+tt_i-2) ; \quad \text{for } i = 1, 2, \dots, 8$$

$$N_i = \frac{1}{8} (1-r^2)(1+ss_i)(1+tt_i) ; \quad \text{for } i = 9, 11, 19, 17$$

$$N_i = \frac{1}{8} (1+rr_i)(1-s^2)(1+tt_i) ; \quad \text{for } i = 10, 12, 18, 20$$

$$N_i = \frac{1}{8} (1+rr_i)(1+ss_i)(1-t^2) ; \quad \text{for } i = 13, 14, 15, 16$$

The values of  $r_i$ ,  $s_i$  and  $t_i$ , the natural coordinates of node  $i$ , are given in table A-1 and  $(x_i, y_i, z_i)$  are the Cartesian coordinates of node  $i$ .

If  $T$  is a function of  $r, s$ , and  $t$ , its derivatives can be numerically found as follows,

$$\begin{bmatrix} \frac{\partial T}{\partial x} \\ \frac{\partial T}{\partial y} \\ \frac{\partial T}{\partial z} \end{bmatrix} = [J]^{-1} \begin{bmatrix} \frac{\partial T}{\partial r} \\ \frac{\partial T}{\partial s} \\ \frac{\partial T}{\partial t} \end{bmatrix}$$

Where  $[J]$ , the Jacobian matrix, is given by:

$$[J] = \begin{bmatrix} \frac{\partial x}{\partial r} & \frac{\partial y}{\partial r} & \frac{\partial z}{\partial r} \\ \frac{\partial x}{\partial s} & \frac{\partial y}{\partial s} & \frac{\partial z}{\partial s} \\ \frac{\partial x}{\partial t} & \frac{\partial y}{\partial t} & \frac{\partial z}{\partial t} \end{bmatrix} = \begin{bmatrix} \sum_{i=1}^P \frac{\partial N_i}{\partial r} x_i & \sum_{i=1}^P \frac{\partial N_i}{\partial r} y_i & \sum_{i=1}^P \frac{\partial N_i}{\partial r} z_i \\ \sum_{i=1}^P \frac{\partial N_i}{\partial s} x_i & \sum_{i=1}^P \frac{\partial N_i}{\partial s} y_i & \sum_{i=1}^P \frac{\partial N_i}{\partial s} z_i \\ \sum_{i=1}^P \frac{\partial N_i}{\partial t} x_i & \sum_{i=1}^P \frac{\partial N_i}{\partial t} y_i & \sum_{i=1}^P \frac{\partial N_i}{\partial t} z_i \end{bmatrix}$$

By differentiating the relationship for  $N_i$  on page A1, for a linear element:

$$\frac{\partial N_i}{\partial r} = \frac{1}{8} r_i (1+ss_i)(1+tt_i)$$

$$\frac{\partial N_i}{\partial s} = \frac{1}{8} s_i (1+rr_i)(1+tt_i)$$



$$\frac{\partial N_i}{\partial t} = \frac{1}{8} t_i (1+rr_i)(1+ss_i)$$

for  $i = 1, 2, \dots, 8$

and for a quadratic element,

$$\frac{\partial N_i}{\partial r} = \frac{1}{8} r_i (1+ss_i)(1+tt_i)(2rr_i+ss_i+tt_i-1)$$

$$\frac{\partial N_i}{\partial s} = \frac{1}{8} s_i (1+rr_i)(1+tt_i)(rr_i+2ss_i+tt_i-1)$$

$$\frac{\partial N_i}{\partial t} = \frac{1}{8} t_i (1+rr_i)(1+ss_i)(rr_i+ss_i+2tt_i-1)$$

for  $i = 1, 2, \dots, 8$

$$\frac{\partial N_i}{\partial r} = -\frac{1}{2} r (1+ss_i)(1+tt_i)$$

$$\frac{\partial N_i}{\partial s} = \frac{1}{4} s_i (1-r^2)(1+tt_i)$$

$$\frac{\partial N_i}{\partial t} = \frac{1}{4} t_i (1-r^2)(1+tt_i)$$

for  $i = 9, 11, 17, 19$

$$\frac{\partial N_i}{\partial r} = \frac{1}{4} r_i (1-s^2)(1+tt_i)$$

$$\frac{\partial N_i}{\partial s} = -\frac{1}{2} s (1+rr_i)(1+tt_i)$$

$$\frac{\partial N_i}{\partial t} = \frac{1}{4} t_i (1-s^2)(1+rr_i)$$

for  $i = 10, 12, 18, 20$

$$\frac{\partial N_i}{\partial r} = \frac{1}{4} r_i (1-t^2)(1+ss_i)$$

$$\frac{\partial N_i}{\partial s} = \frac{1}{4} s_i (1-t^2)(1+rr_i)$$

$$\frac{\partial N_i}{\partial t} = -\frac{1}{2} t (1+rr_i)(1+ss_i)$$

for  $i = 13, 14, 15, 16$

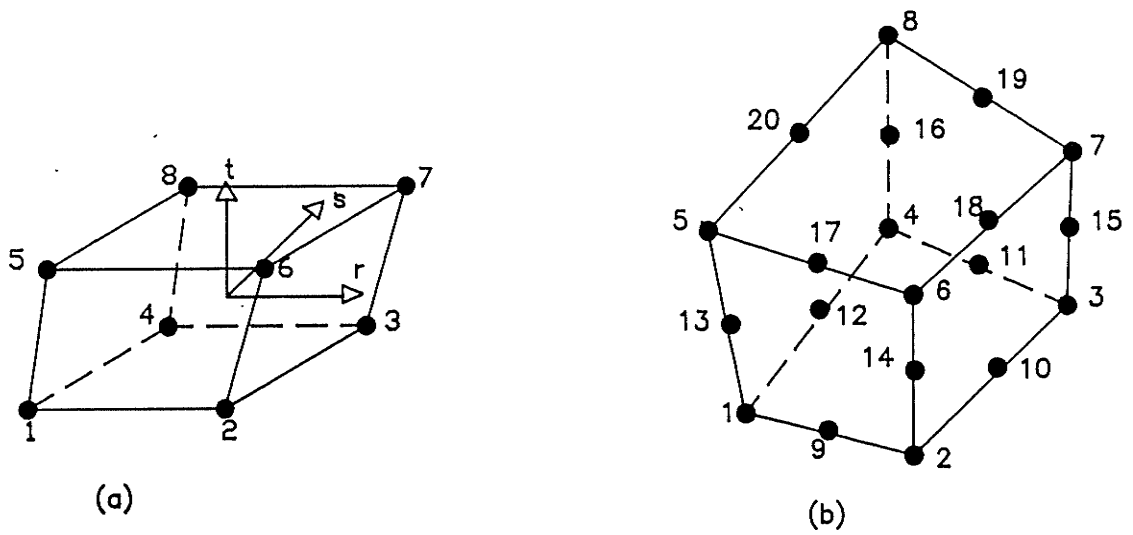


Fig A.1: Location of local node numbers in linear (a) and quadratic (b) hexahedron elements

Table A-1 : Natural coordinates of the nodes in the element shown in figure A-1.

Node number	$r_i$	$s_i$	$t_i$
1	-1	-1	-1
2	1	-1	-1
3	1	1	-1
4	-1	1	-1
5	-1	-1	1
6	1	-1	1
7	1	1	1
8	-1	1	1
9	0	-1	-1
10	1	0	-1
11	0	1	-1
12	-1	0	-1
13	-1	-1	0
14	1	-1	0
15	1	1	0
16	-1	1	0
17	0	-1	1
18	1	0	1
19	0	1	1
20	-1	0	1

# APPENDIX - B

SEMI-AUTO GRID GENERATOR FOR HEXAHEDRAN ELEMENT  
WITH MODEL INPUT DATA FOR A LINEAR GRID SHOWN IN FIG.5.3

```

      IMPLICIT REAL (A-H,O-Z)
      DIMENSION CONOD(3,2000),IELM(20,2000),NABCN(2000),NCNN(4,2000)
      $Z(100)
      READ(5,999)EMTYPE
999  FORMAT(I5)
      IF(EMTYPE.EQ.1)GO TO 998
      GO TO 997
998  MM=0
      NELMAT = 0
      MMN = 1
      NELL = 8
      Q = 0.0
      DO 10 J = 1,5000
      DO 20 I = 1,3
20   CONOD(I,J)=0.0
      DO 30 I = 1,8
30   IELM(I,J)=0
10  CONTINUE
      READ(5,40)NNO,NELM,NLAY,THETA,RAD
      THETA=(2.0*3.141593*THETA)/360.0
40  FORMAT(3I5,2F10.5)
      NNLAY = NLAY-1
      READ(5,51)(Z(I),I=1,NLAY)
51  FORMAT(5F10.5)
      DO 50 J=1,NNO
      READ(5,60)M,(CONOD(I,M),I=1,2)
50  CONTINUE
60  FORMAT(I5,2F10.5)
      DO 70 J=1,NELM
      READ(5,80)M,(IELM(I,M),I=1,4)
80  FORMAT(5I5)
      DO 90 M=1,NELM
      DO 100 I = 5,8
      IELM(I,M)=IELM(I-4,M)+NNO
      K = IELM(I,M)-NNO
      KK = IELM(I,M)
      CONOD(1,KK)=CONOD(1,K)
      CONOD(2,KK)=CONOD(2,K)
      CONOD(3,KK)=CONOD(3,K)+Z(1)
100 CONTINUE
90  CONTINUE
      M=NELM
      DO 130 II=2,NLAY
      DO 150 III=1,NELM
      M=M+1
      DO 120 I = 5,8
      IELM(I-4,M)=IELM(I,M-NELM)
120  IELM(I,M)=IELM(I-4,M)+NNO
      DO 140 I = 5,8
      K = IELM(I,M)-NNO
      KK = IELM(I,M)
      MN=KK
      IF(MN.GT.MM)MM=MN
      MM=MM
      CONOD(1,KK)=CONOD(1,K)
      CONOD(2,KK)=CONOD(2,K)
      CONOD(3,KK)=CONOD(3,K)+Z(II)
140 CONTINUE
150 CONTINUE
130 CONTINUE
      MTNO = MM-NNO+1
      DO 700 II = MTNO,MM
      DIST = SQRT((CONOD(1,II)-RAD)**2+(CONOD(2,II)-RAD)**2)
      DIST = ABS(RAD-DIST)
      Z(NLAY) = DIST*TAN(THETA)
      CONOD(3,II) = CONOD(3,II)+Z(NLAY)
700 CONTINUE
      DO 180 J = 1,MM
180  WRITE(03,190)J,(CONOD(I,J),I=1,3)

```

```

190 FORMAT(I5,5X,3F10.5)
DO 160 J = 1,M
160 WRITE(03,170)J,NELMAT,MMN,NELL,(IELM(I,J),I=1,8),Q
170 FORMAT(I5,11I5,F10.5)
GO TO 996
997 MM = 0
    NELMAT = 1
    NELL = 20
    Q = 0
    DO 10 J=1,2000
    DO 20 I=1,3
20    CONOD(I,J)=0.0
    DO 30 I = 1,20
30    IELM(I,J)=0.0
    DO 31 I=1,4
31    NCNN(I,J)=0
10    NABCN(I)=0
    DO 11 I = 1,10
11    Z(I) = 0.0
    READ(5,40)NNO,NELM,NCNO,NLAY,THETA,RAD
    THETA=(2.0*3.141593*THETA)/360.0
40    FORMAT(4I5,2F10.5)
   >NNLAY = NLAY-1
    READ(5,41)(Z(I),I=1,NLAY)
41    FORMAT(5F10.5)
    DO 50 J = 1,NNO
    READ(5,60)M,(CONOD(I,M),I=1,2)
50    CONTINUE
60    FORMAT(I5,2F10.5)
    DO 70 J = 1,NELM
70    READ(5,80)M,(IELM(I,M),I=1,4),(IELM(I,M),I=9,12)
    DO 71 J = 1,NELM
71    READ(5,300)M,(NCNN(I,M),I=1,4)
300    FORMAT(5I5)
80    FORMAT(9I5)
    DO 310 I = 1,NCNO
    NABCN(I)=NNO+I
310    CONTINUE
    DO 90 M=1,NELM
    DO 100 I = 5,8
        IELM(I,M)=IELM(I-4,M)+NNO+NCNO
        K = IELM(I,M)-NNO-NCNO
        KK = IELM(I,M)
        CONOD(1,KK)=CONOD(1,K)
        CONOD(2,KK)=CONOD(2,K)
        CONOD(3,KK)=CONOD(3,K)+Z(1)
100    CONTINUE
    DO 200 I = 13,16
        K = NCNN(I-12,M)
        IELM(I,M)=NABCN(K)
        K = IELM(I-12,M)
        KK = IELM(I,M)
        CONOD(1,KK)=CONOD(1,K)
        CONOD(2,KK)=CONOD(2,K)
        CONOD(3,KK)=CONOD(3,K)+Z(1)/2.0
200    CONTINUE
    DO 210 I = 17,20
        IELM(I,M)=IELM(I-8,M)+NNO+NCNO
        K = IELM(I,M)-NNO-NCNO
        KK = IELM(I,M)
        CONOD(1,KK)=CONOD(1,K)
        CONOD(2,KK)=CONOD(2,K)
        CONOD(3,KK)=CONOD(3,K)+Z(1)
210    CONTINUE
90    CONTINUE
    M = NELM
    DO 130 II=2,NLAY
    DO 150 III = 1,NELM
    M = M+1
    DO 120 I = 5,8
        IELM(I-4,M)=IELM(I,M-NELM)
120    IELM(I,M)=IELM(I-4,M)+NNO+NCNO
    DO 320 I = 13,16
        IELM(I-4,M)=IELM(I+4,M-NELM)
        IELM(I+4,M)=IELM(I-4,M)+NNO+NCNO
320    IELM(I,M)=IELM(I,M-NELM)+NNO+NCNO

```

```

DO 330 I = 13,16
K = IELM(I,M)-NNO-NCNO
KK = IELM(I,M)
CONOD(1,KK)=CONOD(1,K)
CONOD(2,KK)=CONOD(2,K)
CONOD(3,KK)=CONOD(3,K)+(Z(II)/2.0)+(Z(II-1)/2.0)
MN=KK
IF(MN.GT.MM)MM=MN
MM=MM
330 CONTINUE
I = 4
460 I = I+1
K = IELM(I,M)-NNO-NCNO
KK = IELM(I,M)
CONOD(1,KK)=CONOD(1,K)
CONOD(2,KK)=CONOD(2,K)
CONOD(3,KK)=CONOD(3,K)+Z(II)
MN=KK
IF(MN.GT.MM)MM=MN
MM=MM
IF(I.EQ.8)GO TO 450
GO TO 451
450 IF(I.EQ.8)I=16
IF(I.EQ.20)GO TO 452
451 IF(I.EQ.20)GO TO 452
GO TO 460
452 CONTINUE
150 CONTINUE
130 CONTINUE
MTNO = MM-NNO+1
DO 700 II = MTNO,MM
DIST = SQRT((CONOD(1,II)-RAD)**2+(CONOD(2,II)-RAD)**2)
DIST = ABS(RAD-DIST)
Z(NLAY)=DIST*TAN(THETA)
CONOD(3,II)=CONOD(3,II)+Z(NLAY)
700 CONTINUE
DO 180 J = 1,MM
180 WRITE(03,190)J,(CONOD(I,J),I=1,3)
190 FORMAT(15,5X,3F10.5)
DO 160 J = 1,M
WRITE(03,170)J,NELMAT,NELL,(IELM(I,J),I=1,8)
160 WRITE(03,171)(IELM(I,J),I=9,20),Q
170 FORMAT(15,5X,10I5)
171 FORMAT(12I5,F10.5)
996 STOP
END

```

\$ENTRY

1				
45	32	3	0.0	3.885
	0.900	0.900	0.900	
1	2.78		0.0	
2	1.8		0.15	
3	3.8		0.15	
4	1.35		0.40	
5	4.3		0.40	
6	0.8		0.80	
7	1.8		0.80	
8	2.78		0.80	
9	3.8		0.80	
10	4.8		0.80	
11	0.45		1.30	
12	5.2		1.30	
13	0.2		1.80	
14	0.8		1.80	
15	1.8		1.80	
16	2.78		1.80	
17	3.8		1.80	
18	4.8		1.80	
19	5.4		1.80	
20	0.0		2.78	
21	0.8		2.78	
22	1.8		2.78	
23	2.78		2.78	
24	3.8		2.78	
25	4.8		2.78	
26	5.56		2.78	

27	0.2	3.80
28	0.8	3.80
29	1.8	3.80
30	2.78	3.80
31	3.8	3.80
32	4.8	3.80
33	5.45	3.80
34	0.4	4.30
35	5.2	4.30
36	0.8	4.80
37	1.8	4.80
38	2.78	4.80
39	3.8	4.80
40	4.8	4.80
41	1.3	5.20
42	4.3	5.20
43	1.8	5.45
44	3.8	5.45
45	2.78	5.560
1	4	2
2	2	1
3	1	3
4	3	5
5	11	6
6	6	7
7	7	8
8	8	9
9	9	10
10	10	12
11	13	14
12	14	15
13	15	16
14	16	17
15	17	18
16	18	19
17	20	21
18	21	22
19	22	23
20	23	24
21	24	25
22	25	26
23	27	28
24	28	29
25	29	30
26	30	31
27	31	32
28	32	33
29	36	37
30	37	38
31	38	39
32	39	40

/\*

# APPENDIX - C

## LISTING OF THE THREE DIMENSIONAL FINITE ELEMENT HEAT TRANSFER PROGRAM

```

IMPLICIT REAL*4 (A-H,O-Z)
CHARACTER*4 HEAD(15)
DIMENSION A(600001)
COMMON/BLK1/NUMNP,NUMEL,NDM,MNEL,NUMAT,NEQ,NTP,MBAND,NPROP
$,NBEL,NNEF,IELMT
COMMON/BLK2/MA,IELB,IELG,NST
COMMON/BLK5/IPHR,NSYR,NSMO,NSDAY,NCYR,NCMO,
$,NCDAY,ND,NHOUR,IHOUR,ICDAY,IPDAY,IPC,IDAY
COMMON/BLK6/TINF(24),DT,EMS,EMA
C
C READ AND WRITE CONTROL INFORMATION
C
READ(03,2)HEAD,NUMNP,NUMEL,NDM,MNEL,NUMAT,NTP,NPROP
$,NBEL,NNEF,IELMT
READ(03,4)NSYR,NSMO,NSDAY,NCYR,NCMO,NCDAY,NHOUR,IPHR,DT
2  FORMAT(15A4/10I5)
WRITE(6,3)HEAD,NUMNP,NUMEL,NDM,MNEL,NUMAT,NTP,NPROP,NBEL,
$,NNEF,NSYR,NSMO,NSDAY,NCYR,NCMO,NCDAY,NHOUR,DT,IPHR,IELMT
4  FORMAT(8I5,F10.5)
3  FORMAT('1',15A4//
$   ' NO OF NODES ..... = ',I4/
$   ' NO OF ELEMENTS ..... = ',I4/
$   ' NO OF DIMENSIONS ..... = ',I4/
$   ' MAX NO OF NODES/ELEMENT ..... = ',I4/
$   ' NO OF MATERIAL SETS ..... = ',I4/
$   ' NO OF NODES TEMP. SPECIFIED . = ',I4/
$   ' NO OF MATERIAL DATA ..... = ',I4/
$   ' NO OF BOUNDARY ELEMENTS..... = ',I4/
$   ' MAX NO OF NODES IN EACH FACE = ',I4//
$   ' STARTING DATE = ',I4,'-',I2,'-',I2//
$   ' FINISHING DATE = ',I4,'-',I2,'-',I2//
$   ' NO OF HOURS BEFORE RE-CALC = ',I4/
$   ' TIME STEP = ',F10.5//
$   ' NO OF HRS BEFORE PRINTING = ',I5//
$   ' ELEMENT TYPE = ',I4)
DT = DT*3600.0
CALL DAYCAL(NTDAY)
NST = MNEL
IPDAY = 0
IPC = 0
N1 = 1
N2 = N1 + NDM*NUMNP
N3 = N2 + NUMEL
N4 = N3 + NUMEL
N5 = N4 + MNEL*NUMEL
N6 = N5 + NPROP*NUMAT
N7 = N6 + NUMNP
N8 = N7 + NUMAT
N9 = N8 + MNEL*MNEL
N10 = N9 + MNEL*MNEL
N11 = N10 + NDM*MNEL
N12 = N11 + MNEL
N13 = N12 + MNEL
N17 = N13 + NUMEL
N18 = N17 + NUMEL
N19 = N18 + MNEL*6*NUMEL
N20 = N19 + MNEL*6*NUMEL
N21 = N20 + 24
N22 = N21 + 6*NUMEL
N23 = N22 + MNEL*MNEL
N24 = N23 + MNEL
N25 = N24 + MNEL
N27 = N25 + 6*NUMEL
N31 = N27 + 6*NUMEL
N32 = N31 + NUMEL
IDAY = 0
ICDAY = 0
CALL READ(A(N1),A(N2),A(N3),A(N4),A(N5),A(N6),A(N7),

```



```

$A(N10),A(N8),A(N12),A(N9),A(N13),A(N17),A(N18),A(N19)
$,A(N20),A(N21),A(N22),A(N23),A(N24),A(N25),A(N27),A(N31))
N14 = N32 + NUMNP
CALL INITM(A(N32),A(N6))
N15 = N14 + NUMNP*MBAND
N16 = N15 + NUMNP
N26 = N16 + NUMNP*MBAND
N28 = N26 + NUMNP
N29 = N28 + NUMNP
N30 = N29 + NUMNP
40 CALL BOUNDT(A(N1),A(N32),A(N20),A(N6),2)
II = IABS(24/NHOUR)
DO 10 IHOURL = 1,II
ICDAY = ICDAY+1
CALL BOUNDT(A(N1),A(N32),A(N20),A(N6),3)
CALL ASSEMB(A(N1),A(N2),A(N3),A(N4),A(N5),A(N8)
$,A(N10),A(N12),A(N14),A(N32),A(N6),A(N7),A(N9)
$,A(N13),A(N17),A(N18),A(N19),A(N20),A(N21),A(N22),A(N23),
$,A(N24),A(N16),A(N25),A(N26),A(N27),A(N31))
CALL TRANS(A(N16),A(N14),A(N32),A(N26),A(N28),NUMNP,
$MBAND,A(N4),A(N29),A(N6))
10 CONTINUE
IDAY = IDAY+1
IF(IDAY.EQ.NTDAY)GO TO 30
ICDAY = 0
GO TO 40
30 STOP
END
C
C*****
C
SUBROUTINE DAYCAL(NTDAY)
IMPLICIT REAL*4 (A-H,O-Z)
DIMENSION NDAY(12)
COMMON/BLK5/IPHR,NSYR,NSMO,NSDAY,NCYR,NCMO,
$NCDAY,ND,NHOUR,IHOURL,ICDAY,IPDAY,IPC,IDAY
DATA NDAY/31,28,31,30,31,30,31,31,30,31,30,31/
ND = 0
NTDAY = 0
NTE1 = 0
NTE2 = 0
NSYR1 = NSYR
IF(NSYR.EQ.NCYR)GO TO 90
120 NSYR1 = NSYR1+1
IF(NSYR1.LT.NCYR)NTDAY = NTDAY+365
IF(NSYR1.EQ.NCYR)GO TO 90
GO TO 120
90 IF(NSMO.EQ.1)GO TO 70
J = NSMO-1
DO 80 I = 1,J
ND = ND+NDAY(I)
80 NTE1 = NTE1+NDAY(I)
70 ND = ND+NSDAY
NTE1 = NTE1+NSDAY
IF(NSYR.NE.NCYR)NTE1=365-NTE1
IF(NCMO.EQ.1)GO TO 170
J = NCMO-1
DO 180 I = 1,J
180 NTE2 = NTE2+NDAY(I)
170 NTE2 = NTE2+NCDAY
IF(NSYR.NE.NCYR)GO TO 171
GO TO 172
171 NTDAY = NTDAY+NTE2+NTE1+1
GO TO 160
172 NTDAY = NTDAY+NTE2-NTE1+1
160 WRITE(6,161)NTDAY
161 FORMAT(' TOTAL NUMBER OF DAYS = ',I5)
RETURN
END
C
C*****
C
SUBROUTINE READ(X,NELMAT,NELND,NP,D,ID,MEL,XL,SL,RL,CL
$,NFCN,NFRAD,NNCON,NNRAD,HC,IFACE,HCL,SQRL,
$SHCL,ANG,IRFACE,Q)
IMPLICIT REAL*4(A-H,O-Z)

```

```

COMMON/BLK1/NUMNP,NUMEL,NDM,MNEL,NUMAT,NEQ,NTP,MBAND,NPROP
$,NBEL,NNEF,IELMT
DIMENSION X(NDM,1),NELMAT(1),NP(MNEL,1),XL(1),SL(1),CL(1),
$NB(1),D(NPROP,1),ID(1),MEL(1),RL(1),NELND(1),Q(1),
$NFCN(1),NFRAD(1),NNCON(MNEL,6,1),NNRAD(MNEL,6,1),HC(1)
$,IFACE(6,1),HCL(1),SQRL(1),SHCL(1),ANG(6,1),IRFACE(6,1)
C
C READ AND WRITE NODEL CO-ORDINATES
C
  WRITE(6,10)
10  FORMAT(///10H NODE DATA//
  $      5H NODE,11X,5H-1ORD,11X,5H2-ORD,11X,5H3-ORD)
  DO 20 J = 1,NUMNP
    READ(03,30)M,(X(I,M),I=1,NDM)
20  WRITE(6,40)M,(X(I,M),I=1,NDM)
30  FORMAT(15,5X,3E10.5)
40  FORMAT(15,3F16.5)
C
C READ AND WRITE ELEMENT DATA
C
  WRITE(6,50)
  DO 62 I=1,NUMEL
62  Q(I)=0.0
  DO 60 J = 1,NUMEL
    IF(IELMT.EQ.1)GO TO 301
    GO TO 302
301  READ(03,70)M,NELMAT(M),NEL,(NP(I,M),I=1,MNEL),Q(M)
    GO TO 303
302  READ(03,71)M,NELMAT(M),NEL,(NP(I,M),I=1,MNEL),Q(M)
303  NELND(M) = NEL
60  WRITE(6,80)M,NELMAT(M),NEL,(NP(I,M),I=1,MNEL)
80  FORMAT(13,14,14,1X,20(1X,13))
70  FORMAT(15,5X,10I5,E10.5)
71  FORMAT(15,5X,10I5/12I5,E10.5)
50  FORMAT(///1X,' ELEMENT DATA'//
  $50X,'NODE NUMBERS'/'ELMT MSET NEL',
  $2X,' 1   2   3   4   5   6   7   8   9  10  11  12  13  14'
  $,' 15  16  16  18  19  20'//)
C
C READ AND WRITE BOUNDARY CONDITIONS
C
  DO 90 J = 1,NUMNP
90  ID(J) = 0
  WRITE(6,120)
  IF(NTP.EQ.0)GO TO 121
  DO 130 J = 1,NTP
    READ(03,100)N,ID(N)
    WRITE(6,110)N,ID(N)
130  CONTINUE
110  FORMAT(15,18)
100  FORMAT(2I5)
120  FORMAT(//1X,' BOUNDARY CONDITION CODES'//
  $1X,'NODE',5X,'CODE')
C
C READ AND WRITE CONVECTION AND RADIATION B.C'S
C
121  DO 240 I = 1,MNEL
    DO 240 J = 1,6
    DO 240 K = 1,NUMEL
      NFCN(K) = 0
      NFRAD(K) = 0
      IFACE(J,K)=0
      IRFACE(J,K)=0
      NNCON(I,J,K) = 0
240  NNRAD(I,J,K) = 0
    WRITE(6,230)
    DO 200 II = 1,NBEL
      READ(03,221)M,NFCN(M),NFRAD(M)
      LL = NFCN(M)
      IF(LL.EQ.0)GO TO 202
      READ(03,222)(IFACE(J,M),J=1,LL)
      DO 885 J = 1,LL
        KK = IFACE(J,M)
885  CALL CONRAD(J,M,KK,NNCON)
202  LL = NFRAD(M)
    IF(LL.EQ.0)GO TO 200

```

```

      DO 204 J = 1,LL
      READ(03,223)IRFACE(J,M),ANG(J,M)
      KK = IRFACE(J,M)
204  CALL CONRAD(J,M,KK,NNRAD)
200  CONTINUE
      WRITE(6,340)
340  FORMAT(//1X,' ELEMENT NO.',5X,' CONVECTION FACES'//)
      DO 341 I = 1,NUMEL
      IF(NFCON(I).NE.0)GO TO 342
      GO TO 341
342  LL = NFCON(I)
      WRITE(6,231)I,(IFACE(J,I),J=1,LL)
341  CONTINUE
      WRITE(6,351)
351  FORMAT(//1X,' ELEMENT NO.',3X,' RADIATION FACE',2X,' ANGLE'//)
      DO 352 I = 1,NUMEL
      IF(NFRAD(I).NE.0)GO TO 353
      GO TO 352
353  LL = NFRAD(I)
      DO 355 II=1,LL
355  WRITE(6,232)I,IRFACE(II,I),ANG(II,I)
352  CONTINUE
221  FORMAT(3I5)
222  FORMAT(6I5)
223  FORMAT(I5,F10.5)
230  FORMAT(// ' CONVECTION AND RADIATION BOUNDARY CONDITIONS'//)
231  FORMAT(3X,I5,5X,6I5)
232  FORMAT(3X,I5,5X,I5,5X,F13.7)
C
C  READ AND WRITE MATERIAL DATA
C
      DO 11 I = 1,NPROP
      DO 11 J = 1,NUMAT
11  D(I,J) = 0.0
      DO 12 J = 1,NUMAT
      READ(03,13)MA,IELB
13  FORMAT(2I5)
      MEL(MA) = IELB
      WRITE(6,14)MA,IELB
14  FORMAT(/// ' MATERIAL SET NO      ',I5,9X,' ELEMENT LIB NO  ',
$15/)
      CALL ELMLIB(D(1,MA),NEL,XL,SL,RL,CL,HCL,SQRL,SHCL,
$NFCON,NFRAD,NNCON,NNRAD,HC,NFACE,1,IELB,Q)
12  CONTINUE
      CALL BANDW(MBAND,NELND,NP)
      CALL BOUNDT(X,T,HC,ID,1)
      RETURN
      END
C
C*****
C
      SUBROUTINE CONRAD(J,M,KK,NCON)
      IMPLICIT REAL*4 (A-H,O-Z)
      COMMON/BLK1/NUMNP,NUMEL,NDM,MNEL,NUMAT,NEQ,NTP,MBAND,NPROP
      $,NBEL,NNEF,IELMT
      DIMENSION NCON(MNEL,6,1)
      IF(KK.EQ.1)GO TO 12
      IF(KK.EQ.2)GO TO 11
      IF(KK.EQ.3)GO TO 13
      IF(KK.EQ.4)GO TO 14
      IF(KK.EQ.5)GO TO 15
      IF(KK.EQ.6)GO TO 16
      GO TO 301
11  L = 1
      DO 20 I = 1,4
      NCON(I,J,M)=L
20  L = L+1
      IF(IELMT.EQ.1)GO TO 301
      L = 9
      DO 21 I = 5,8
      NCON(I,J,M)=L
21  L = L+1
      GO TO 301
12  L = 5
      DO 22 I = 1,4
      NCON(I,J,M)=L

```

```

22  L = L+1
    IF(IELMT.EQ.1)GO TO 301
    L = 17
    DO 23 I = 5,8
      NCON(I,J,M)=L
23  L = L+1
    GO TO 301
13  NCON(1,J,M)=1
    NCON(2,J,M)=2
    NCON(3,J,M)=6
    NCON(4,J,M)=5
    IF(IELMT.EQ.1)GO TO 301
    NCON(5,J,M)=9
    NCON(6,J,M)=14
    NCON(7,J,M)=17
    NCON(8,J,M)=13
    GO TO 301
14  NCON(1,J,M)=2
    NCON(2,J,M)=3
    NCON(3,J,M)=7
    NCON(4,J,M)=6
    IF(IELMT.EQ.1)GO TO 301
    NCON(5,J,M)=10
    NCON(6,J,M)=15
    NCON(7,J,M)=18
    NCON(8,J,M)=14
    GO TO 301
15  NCON(1,J,M)=4
    NCON(2,J,M)=3
    NCON(3,J,M)=7
    NCON(4,J,M)=8
    IF(IELMT.EQ.1)GO TO 301
    NCON(5,J,M)=11
    NCON(6,J,M)=15
    NCON(7,J,M)=19
    NCON(8,J,M)=16
    GO TO 301
16  NCON(1,J,M)=1
    NCON(2,J,M)=4
    NCON(3,J,M)=8
    NCON(4,J,M)=5
    IF(IELMT.EQ.1)GO TO 301
    NCON(5,J,M)=12
    NCON(6,J,M)=16
    NCON(7,J,M)=20
    NCON(8,J,M)=13
301 RETURN
    END

```

C

C\*\*\*\*\*

C

```

      SUBROUTINE BOUNDT(X,T,HC,ID,IC)
      IMPLICIT REAL*4 (A-H,O-Z)
      REAL AN,BN,A0,DTT,TD,WIND
      COMMON/BLK1/NUMNP,NUMEL,NDM,MNEL,NUMAT,NEQ,NTP,MBAND,NPROP
      $,NBEL,NNEF,IELMT
      COMMON/BLK5/IPHR,NSYR,NSMO,NSDAY,NCYR,NCMO,
      $NCDAY,ND,NHOUR,IHOUR,ICDAY,IPDAY,IPC,IDAY
      COMMON/BLK6/TINF(24),DT,EMS,EMA
      DIMENSION T(1),ID(1),AN(6),BN(6),TD(24),TEMPZ(15)
      $,HC(1),WIND(24),NDAY(12),X(NDM,1)
      DATA AN/-10.919,1.157,-0.091,0.031,0.519,0.027/
      DATA BN/-5.129,0.574,0.119,-0.365,0.332,0.068/
      DATA NDAY/31,28,31,30,31,30,31,31,30,31,30,31/
      A0 = 4.894
      GO TO(1,2,3),IC
1  READ(03,20)DIA,AIRK,AIRRO,AIRVIS,SK,SROW,SCP,CK,
  $CROW,CCP,EMS,EMA,CT,NNIEL
20  FORMAT(5F10.5/5F10.5/3F10.5,I5)
    AIRVIS = AIRVIS/1000000.0
    WRITE(6,21)DIA,AIRK,AIRRO,AIRVIS,SK,SROW,SCP,CK,
  $CROW,CCP,EMS,EMA,CT,NNIEL
21  FORMAT(//
  $      ' DIAMETER OF THE BIN .....= ',F10.5/
  $      ' CONDUCTIVITY OF AIR.....= ',F10.5/
  $      ' DENSITY OF AIR .....= ',F10.5/

```

```

$      ' VISCOSITY OF AIR .....= ',F10.5/
$      ' CONDUCTIVITY OF SOIL .....= ',F10.5/
$      ' DENSITY OF SOIL .....= ',F10.5/
$      ' SPECIFIC HEAT OF SOIL .....= ',F10.5/
$      ' CONDUCTIVITY OF CONCRETE .....= ',F10.5/
$      ' DENSITY OF CONCRETE .....= ',F10.5/
$      ' SPECIFIC HEAT OF CONCRETE .....= ',F10.5/
$      ' SHORT WAVE EMISS OF BIN WALL ...= ',F10.5/
$      ' LONG WAVE EMISS OF BIN WALL ...= ',F10.5/
$      ' THICKNESS OF CONCRETE .....= ',F10.5/
$      ' NUMBER OF NODES IN EACH LAYER .= ',I5)
      RETURN
2      RADIUS = DIA/2.0
      ALFA = 24*3600*(SK/(SROW*SCP))
      DO 301 IJK = 1,NUMNP
      TZ=0.0
      IF(ID(IJK).EQ.1)GO TO 300
      GO TO 301
C 300 Z = X(1,IJK)
300 XC = DIA/2.0
      YC = DIA/2.0
      DIST = SQRT((X(1,IJK)-XC)**2+(X(2,IJK)-YC)**2)
      Z = RADIUS-DIST
      IF(Z.GT.RADIUS)Z=DIA-Z
      IF(Z.EQ.0.0.OR.Z.LT.0.0)Z=0.01
      DO 10 I = 1,6
      A10=SQRT(I*3.141593)
      A = A10/(365*ALFA)
      AA = SQRT(I*3.141593/(365*ALFA*Z))
      B = (2*I*3.141593/365)*ND-A*Z
10      TZ = TZ+ EXP(-AA)*(AN(I)*COS(B)+BN(I)*SIN(B))
      TZ = TZ+A0+273.0
C      T(IJK)=TZ
      J = IJK+NNIEL
      IF(J.GT.NUMNP)GO TO 301
      TEMPT = T(J)
      DTT = 0.5
      INN = NHOUR/DTT
      CC = ((0.25*CROW*CCP)/(CK*1800.0))
      DO 79 KK = 1,INN
      TNEW = (TZ+TEMPT+((CC-2)*T(IJK)))/CC
79      T(IJK) = TNEW
301 CONTINUE
      RETURN
3      IF(ICDAY.EQ.1)GO TO 50
      GO TO 60
50      IF(IDAY.EQ.0)GO TO 85
      GO TO 86
85      NSSD = NSDAY-1
      NSSMO = NSMO
      IF(NSSD.EQ.0)GO TO 185
      GO TO 88
185      NSSMO = NSMO-1
      NSSD=NDAY(NSSMO)
88      READ(16,99)IYR,IMO,IDD,IHR
      IF(IYR.EQ.NSYR.AND.IMO.EQ.NSSMO.AND.NSSD.EQ.IDD)GO TO 86
      GO TO 88
86      DO 331 I = 1,24
331      READ(16,599)IYR,IMO,IDD,IHR,TD(I)
99      FORMAT(I2,I2,I2,I2)
599      FORMAT(I2,I2,I2,I2,F6.1)
      IF(IDAY.EQ.0)GO TO 98
      GO TO 96
98      READ(18,199)IYR,IMO,IDD
199      FORMAT(I2,I2,I2)
      IF(IYR.EQ.NSYR.AND.IMO.EQ.NSSMO.AND.NSSD.EQ.IDD)GO TO 96
      GO TO 98
96      IF(IDAY.EQ.0)GO TO 198
      GO TO 196
198      READ(14,299)MSTNID,IYR,IMO,IDD
299      FORMAT(I8,I2,I2,I2)
      IF(IYR.EQ.NSYR.AND.IMO.EQ.NSSMO.AND.NSSD.EQ.IDD)GO TO 196
      GO TO 198
196      DO 200 I = 1,24
      READ(18,201)WIND(I)
      IF(WIND(I).EQ.0)WIND(I)=1.0

```

```

200 WIND(I) = WIND(I)*0.277778
201 FORMAT(23X,F3.0)
    K = 1
    IN = IABS(24/NHOUR)
    DO 70 II = 1,IN
    C = 0.0
    AW = 0.0
    KK = K+NHOUR-1
    DO 80 I = K, KK
    TD(I) = TD(I)+273
    AW = AW+WIND(I)
80  C = C+TD(I)
    TINF(II) = C/NHOUR
    WIND(II) = AW/NHOUR
    HC(II) = (0.227*AIRK/DIA)*((AIRRO*WIND(II)
    $*DIA/AIRVIS)**0.633)
70  K = K+NHOUR
    WRITE(6,71)(TINF(I),I=1,IN)
71  FORMAT(' TINF = ',8F10.3)
60  CONTINUE
    RETURN
    END
C
C*****
C
    SUBROUTINE INITEM(T,ID)
    IMPLICIT REAL*4 (A-H,O-Z)
    COMMON/BLK1/NUMNP,NUMEL,NDM,MNEL,NUMAT,NEQ,NTP,MBAND,NPROP
    $,NBEL,NNEF,IELMT
    DIMENSION T(1),ID(1),TL(1000)
    DO 10 I = 1,NUMNP
    T(I) = 0.0
10  CONTINUE
    WRITE(6,20)
20  FORMAT(// ' INITIAL NODAL TEMPERATURES' //)
    READ(03,50)(TL(I),I=1,NUMNP)
    WRITE(6,60)(TL(I),I=1,NUMNP)
    DO 80 II = 1,NUMNP
    T(II) = T(II) + TL(II)
80  CONTINUE
50  FORMAT(6E10.0)
60  FORMAT(6E12.3)
51  RETURN
    END
C
C*****
C
    SUBROUTINE BANDW(MB,NELND,NP)
    IMPLICIT REAL*4 (A-H,O-Z)
    COMMON/BLK1/NUMNP,NUMEL,NDM,MNEL,NUMAT,NEQ,NTP,MBAND,NPROP
    $,NBEL,NNEF,IELMT
    DIMENSION NELND(1),NP(MNEL,1)
    MB = 0
    DO 10 J = 1,NUMEL
    NEL = NELND(J)
    NLAR = NP(1,J)
    NSMA = NP(1,J)
    DO 20 I = 1,NEL
    IF(NSMA.GT.NP(I,J))NSMA=NP(I,J)
    IF(NLAR.LT.NP(I,J))NLAR=NP(I,J)
20  CONTINUE
    MM = NLAR-NSMA+1
    IF(MB.GT.MM)GO TO 10
    MB = MM
    MEL = J
10  CONTINUE
    WRITE(6,30)MB,MEL
30  FORMAT(// ' HALF BAND WIDTH      = ',I5,5X,
    $ 'ELEMENT NO      = ',I5/)
    RETURN
    END
C
C*****
C
    SUBROUTINE ASSEMB(X,NELMAT,NELND,NP,D,SL,XL,RL,S,T,ID,
    $MEL,CL,NFCON,NFRAD,NNCON,NNRAD,HC,IFACE,HCL,SQRL,SHCL

```

```

$,CAP,ANG,F,IRFACE,Q)
IMPLICIT REAL*4 (A-H,O-Z)
COMMON/BLK1/NUMNP,NUMEL,NDM,MNEL,NUMAT,NEQ,NTP,MBAND,NPROP
$,NBEL,NNEF,IELMT
COMMON/BLK2/MA,IELB,IELG,NST
COMMON/BLK3/III
COMMON/BLK4/QR
COMMON/BLK5/IPHR,NSYR,NSMO,NSDAY,NCYR,NCMO,
$NCDAY,ND,NHOUR,ICDAY,IPDAY,IPC,IDAY
COMMON/BLK6/TINF(24),DT,EMS,EMA
DIMENSION X(NDM,1),NELMAT(1),NELND(1),NP(MNEL,1),
$D(NPROP,1),SL(1),XL(NDM,1),ID(1),LM(54),S(NUMNP,1),RL(1),
$R(1),MEL(1),CL(1),T(1),NFCN(1),NFRAD(1),HCL(1),
$NNCON(MNEL,6,1),NNRAD(MNEL,6,1),HC(1),IFACE(6,1),SQRL(1)
$,SHCL(1),CAP(NUMNP,1),ANG(6,1),F(1),QR(24,500),IRFACE(6,1)
$,Q(1)
DO 10 I = 1,NUMNP
DO 11 J = 1, MBAND
CAP(I,J) = 0.0
11 S(I,J) = 0.0
10 F(I) = 0.0
DO 20 L = 1,NUMEL
MA = NELMAT(L)
IELB = MEL(MA)
IELG = L
NEL = NELND(L)
DO 70 I = 1,NDM
DO 70 J = 1,NEL
NG = NP(J,L)
70 XL(I,J) = X(I,NG)
DO 90 I = 1,NST
RL(I) = 0.0
SQRL(I) = 0.0
90 SHCL(I) = 0.0
CALL ELMLIB(D(1,MA),NEL,XL,SL,RL,CL,HCL,SQRL,SHCL,
$NFCN,NFRAD,NNCON,NNRAD,HC,NFACE,2,IELB,Q)
IF(NFCN(IELG).EQ.0)GO TO 200
II = NFCN(IELG)
DO 205 III = 1,II
NFACE = IFACE(III,IELG)
CALL ELMLIB(D(1,MA),NEL,XL,SL,RL,CL,HCL,SQRL,SHCL,
$NFCN,NFRAD,NNCON,NNRAD,HC,NFACE,3,IELB,Q)
205 CONTINUE
200 CONTINUE
IF(NFRAD(IELG).EQ.0)GO TO 201
II = NFRAD(IELG)
DO 206 III = 1,II
NFACE = IRFACE(III,IELG)
ANGLE = ANG(III,IELG)
CALL RADN(NNRAD,NFRAD,IELG,NEL,NNEF,ANGLE,NP,QR,T)
CALL ELMLIB(D(1,MA),NEL,XL,SL,RL,CL,HCL,SQRL,SHCL,
$NFCN,NFRAD,NNCON,NNRAD,HC,NFACE,4,IELB,Q)
206 CONTINUE
C
C FORM LOCATION MATRIX
C
201 DO 30 J = 1,NST
N = NP(J,L)
LM(J) = N
30 CONTINUE
C
C ASSEMBLE
C
DO 50 I = 1,NST
IF(LM(I).EQ.0)GO TO 50
IJ = LM(I)
F(IJ) = F(IJ)+RL(I)-SQRL(I)+SHCL(I)
DO 60 J = 1,NST
JJ = LM(J)-IJ+1
IF(JJ.LE.0)GO TO 60
K = NST*(J-1)+I
S(IJ,JJ) = S(IJ,JJ)+SL(K)+HCL(K)
CAP(IJ,JJ) = CAP(IJ,JJ) + CL(K)
60 CONTINUE
50 CONTINUE
20 CONTINUE

```

```

      THETA = 0.6667
      DO 400 I = 1, NUMNP
      DO 401 J = 1, MBAND
      TEMP = CAP(I,J)*(1./DT)+THETA*S(I,J)
      S(I,J) = CAP(I,J)*(1./DT)-(1-THETA)*S(I,J)
401  CAP(I,J) = TEMP
400  F(I) = THETA*F(I) + (1-THETA)*F(I)
      RETURN
      END
C
C*****
C
      SUBROUTINE ELMLIB(DL,NEL,XL,SL,RL,CL,HCL,SQRL,SHCL,
      $NFCN,NFRAD,NNCON,NNRAD,HC,NFACE,ICN,IELB,Q)
C
C THIS SUBROUTINE CALLS THE APPROPRIATE ELEMENT SUBROUTINES
C
      IMPLICIT REAL*4(A-H,O-Z)
      DIMENSION DL(1),XL(1),SL(1),RL(1),CL(1),NFCN(1),
      $NFRAD(1),NNCON(NEL,6,1),NNRAD(NEL,6,1),HC(1),IFACE(6,1)
      $,HCL(1),SHCL(1),SQRL(1),Q(1)
      GO TO (1,2),IELB
1     CALL ELM1(DL,NEL,XL,SL,RL,CL,HCL,SQRL,SHCL,
      $NFCN,NFRAD,NNCON,NNRAD,HC,NFACE,ICN,Q)
      GO TO 10
2     CALL ELM2(DL,NEL,XL,SL,RL,CL,HCL,SQRL,SHCL,
      $NFCN,NFRAD,NNCON,NNRAD,HC,NFACE,ICN,Q)
10    RETURN
      END
C
C*****
C
      SUBROUTINE ELM1(DL,NEL,XL,SL,RL,CL,HCL,SQRL,SHCL,
      $NFCN,NFRAD,NNCON,NNRAD,HC,NFACE,ICN,Q)
C
C THREE DIMENSIONAL LINEAR AND QUADRATIC ELEMENT
C
      IMPLICIT REAL*4(A-H,O-Z)
      COMMON/BLK1/NUMNP,NUMEL,NDM,MNEL,NUMAT,NEQ,NTP,MBAND,NPROP
      $,NBEL,NNEF,IELMT
      COMMON/BLK2/MA,IELB,IELG,NST
      COMMON/BLK3/III
      COMMON/BLK4/QR
      COMMON/BLK5/IPHR,NSYR,NSMO,NSDAY,NCYR,NCMO,
      $NCDAY,ND,NHOUR,IHOUR,ICDAY,IPDAY,IPC,IDAY
      COMMON/BLK6/TINF(24),DT,EMS,EMA
      DIMENSION XL(NDM,1),SL(NST,1),DL(6),RG(27),SG(27),
      $TG(27),WG(27),SHP(4,27),XS(3,3),RL(1),CL(NST,1),DB(20,20),
      $NFCN(1),NFRAD(1),NNCON(NEL,6,1),NNRAD(NEL,6,1),HC(1)
      $,HCNTN(20,20),IFACE(6,1),SSH(5,20),RRG(9),SSG(9),TTG(9),
      $WWG(9),XXS(2,2),HCL(NST,1),SQRL(1),SHCL(1),QR(24,500),Q(1)
      $,TINF(24)
      GO TO (1,2,3,4),ICN
C
C READ AND WRITE MATERIAL PROPERTIES
C
1     READ(03,10)AKX,AKY,AKZ,RHO,CP,L
10    FORMAT(5E10.5,I5)
      WRITE(6,11)AKX,AKY,AKZ,RHO,CP,L
11    FORMAT(' THERMAL CONDUCTIVITY IN X DIRECTION = ',E13.7/
      $ ' THERMAL CONDUCTIVITY IN Y DIRECTION = ',E13.7/
      $ ' THERMAL CONDUCTIVITY IN Z DIRECTION = ',E13.7/
      $ ' DENSITY = ',E13.7/
      $ ' SPECIFIC HEAT = ',E13.7/
      $ ' NO OF GAUSS POINTS IN EACH PLANE = ',I5)
      DL(1) = AKX
      DL(2) = AKY
      DL(3) = AKZ
      DL(4) = RHO
      DL(5) = CP
      DL(6) = L
      RETURN
2     DO 20 I = 1,NST
      DO 21 J = 1,NST
      HCL(I,J) = 0.0
      CL(I,J) = 0.0

```



```

21 SL(I,J) = 0.0
20 SHCL(I) = 0.0
  IF(IELG.EQ.1) LINT=0
  L = DL(6)
  IF(L*L*L.NE.LINT)CALL PGAUSS(L,LINT,RG,SG,TG,WG)
  DO 30 K = 1,LINT
  CALL SHAPE(RG(K),SG(K),TG(K),XL,SHP,XS,XSJ,NEL,IELMT)
  DV = XSJ*WG(K)
  DO 430 KK = 1,3
  DO 430 I = 1,NEL
430 DB(KK,I) = DL(KK)*SHP(KK,I)*DV
  DO 431 I = 1,NEL
  DO 432 J = 1,I
  DO 433 KK = 1,3
433 SL(I,J) = SL(I,J) + SHP(KK,I)*DB(KK,J)
432 CL(I,J) = CL(I,J) + SHP(4,I)*SHP(4,J)*DL(4)*DL(5)*DV
431 RL(I) = RL(I) + SHP(4,I)*Q(IELG)*DV
C
C COMPUTE UPPER TRIANGULAR MATRIX BY SYMMETRY
C
  J = 1
  DO 70 JJ = 1,NST
  I = 1
  DO 80 II = 1,JJ
  SL(I,J) = SL(J,I)
  CL(I,J) = CL(J,I)
80 I = I + 1
70 J = J + 1
30 CONTINUE
  RETURN
3 CALL QUAD(L,LLINT,RRG,SSG,TTG,WWG,NFACE)
  TINFT(IHOUR)=TINF(IHOUR)
  IF(NFACE.EQ.1)GO TO 34
  GO TO 35
34 IF(TINFT(IHOUR).GT.TINF(IHOUR))GO TO 35
  TINFT(IHOUR)=TINF(IHOUR)+5.0
35 CONTINUE
  DO 40 K = 1,LLINT
  CALL SURF(RRG(K),SSG(K),TTG(K),XL,SSHP,XXS,
$XXSJ,NEL,NFACE)
  IF(NFACE.EQ.1)GO TO 31
  GO TO 32
31 DV1 = 1.0*WWG(K)*XXSJ
  GO TO 33
32 DV1 = HC(IHOUR)*WWG(K)*XXSJ
33 DO 90 I = 1,NEL
90 SSHP(5,I) = 0.0
  DO 91 I = 1,NEL
  IF(I.GT.NNEF)GO TO 92
  LL = NNCON(I,III,IELG)
  SSHP(5,LL) = SSHP(4,I)
92 CONTINUE
91 CONTINUE
  DO 94 I = 1,NEL
  DO 93 J = 1,NEL
93 HCL(I,J) = HCL(I,J) + SSHP(5,I)*SSHP(5,J)*DV1
  SHCL(I) = SHCL(I)+SSHP(5,I)*DV1*TINFT(IHOUR)
94 CONTINUE
  J = 1
  DO 71 JJ = 1,NST
  I = 1
  DO 81 II = 1,JJ
  HCL(I,J) = HCL(J,I)
81 I = I + 1
71 J = J + 1
40 CONTINUE
  RETURN
4 CALL QUAD(L,LLINT,RRG,SSG,TTG,WWG,NFACE)
  DO 701 K = 1,LLINT
  CALL SURF(RRG(K),SSG(K),TTG(K),XL,SSHP,XXS,XXSJ,NEL,NFACE)
  DV1 = WWG(K)*XXSJ*QR(IHOUR,IELG)
  DO 702 I = 1,NEL
702 SSHP(5,I) = 0.0
  DO 703 I = 1,NEL
  IF(I.GT.NNEF)GO TO 704
  LL = NNRAD(I,III,IELG)

```

```

      SSHP(5,LL) = SSHP(4,I)
704 CONTINUE
703 CONTINUE
      DO 705 I = 1,NEL
      SQRL(I) = SQRL(I)+SSHP(5,I)*DV1
705 CONTINUE
701 CONTINUE
      RETURN
      END
C
C*****
C
      SUBROUTINE SHAPE(RR,SS,TT,X,SHP,XS,XSJ,NEL,IELMT)
      IMPLICIT REAL*4 (A-H,O-Z)
      DIMENSION SHP(4,1),X(3,1),R(20),S(20),T(20),XS(3,3),
      $SX(3,3)
      DATA R/-1.0E00,1.0E00,1.0E00,-1.0E00,-1.0E00,1.0E00
      $,1.0E00,-1.0E00,0.0E00,1.0E00,0.0E00,-1.0E00,-1.0E00
      $,1.0E00,1.0E00,-1.0E00,0.0E00,1.0E00,0.0E00,-1.0E00/
      DATA T/-1.0E00,-1.0E00,-1.0E00,-1.0E00,-1.0E00,1.0E00,1.0E00,
      $1.0E00,1.0E00,-1.0E00,-1.0E00,-1.0E00,-1.0E00,0.0E00,
      $0.0E00,0.0E00,0.0E00,1.0E00,1.0E00,1.0E00,1.0E00/
      DATA S/-1.0E00,-1.0E00,1.0E00,1.0E00,-1.0E00,-1.0E00,
      $1.0E00,1.0E00,-1.0E00,0.0E00,1.0E00,0.0E00,-1.0E00,
      $-1.0E00,1.0E00,1.0E00,-1.0E00,0.0E00,1.0E00,0.0E00/
      IF(IELMT.EQ.1)GO TO 20
      GO TO 40
20  DO 100 I = 1,20
      SHP(4,I) = (1.+R(I)*RR)*(1.+S(I)*SS)*(1.+T(I)*TT)/8.
      SHP(1,I) = R(I)*(1.+S(I)*SS)*(1.+T(I)*TT)/8.
      SHP(2,I) = S(I)*(1.+R(I)*RR)*(1.+T(I)*TT)/8.
100 SHP(3,I) = T(I)*(1.+R(I)*RR)*(1.+S(I)*SS)/8.
      GO TO 30
40  DO 39 I = 1,8
      SHP(4,I)=(1.+R(I)*RR)*(1.+S(I)*SS)*(1.+T(I)*TT)*
      $(R(I)*RR+S(I)*SS+T(I)*TT-2.)/8.
      SHP(1,I)=R(I)*(1.+S(I)*SS)*(1.+T(I)*TT)*(2*R(I)*RR+
      $S(I)*SS+T(I)*TT-1.)/8.
      SHP(2,I)=S(I)*(1.+R(I)*RR)*(1.+T(I)*TT)*(R(I)*RR+
      $2.*S(I)*SS+T(I)*TT-1.)/8.
39  SHP(3,I)=T(I)*(1+R(I)*RR)*(1.+S(I)*SS)*(R(I)*RR+S(I)*
      $SS+2.*T(I)*TT-1.)/8.
      DO 41 I = 13,16
      SHP(4,I)=(1.-TT**2)*(1.+R(I)*RR)*(1.+S(I)*SS)/4.
      SHP(1,I)=R(I)*(1.-TT**2)*(1.+S(I)*SS)/4.
      SHP(2,I)=S(I)*(1.-TT**2)*(1.+R(I)*RR)/4.
41  SHP(3,I)=-TT*(1.+R(I)*RR)*(1.+S(I)*SS)/2.
      I = 9
42  SHP(4,I)=(1.-RR**2)*(1.+S(I)*SS)*(1.+T(I)*TT)/4.
      SHP(1,I)=-RR*(1.+S(I)*SS)*(1.+T(I)*TT)/2.
      SHP(2,I)=S(I)*(1.-RR**2)*(1.+T(I)*TT)/4.
      SHP(3,I)=T(I)*(1.-RR**2)*(1.+S(I)*SS)/4.
      I = I+2
      IF(I.GT.11)GO TO 45
      GO TO 42
45  IF(I.EQ.19)GO TO 42
      IF(I.GT.19)GO TO 43
      I = 17
      GO TO 42
43  I = 10
44  SHP(4,I)=(1.-SS**2)*(1.+R(I)*RR)*(1.+T(I)*TT)/4.
      SHP(1,I)=R(I)*(1.-SS**2)*(1.+T(I)*TT)/4.
      SHP(2,I)=-SS*(1.+R(I)*RR)*(1.+T(I)*TT)/2.
      SHP(3,I)=T(I)*(1.-SS**2)*(1.+R(I)*RR)/4.
      I = I+2
      IF(I.GT.12)GO TO 46
      GO TO 44
46  IF(I.EQ.20)GO TO 44
      IF(I.GT.20)GO TO 30
      I = 18
      GO TO 44
C
C CONSTRUCT JACOBIAN AND ITS INVERSE
C
30  DO 130 I = 1,3
      DO 130 J = 1,3

```

```

      XS(I,J) = 0.0
      DO 130 K = 1,NEL
130  XS(I,J) = XS(I,J)+SHP(I,K)*X(J,K)
      A1 = XS(2,2)*XS(3,3)-XS(2,3)*XS(3,2)
      A2 = -(XS(2,1)*XS(3,3)-XS(2,3)*XS(3,1))
      A3 = XS(2,1)*XS(3,2)-XS(2,2)*XS(3,1)
      B1 = -(XS(1,2)*XS(3,3)-XS(1,3)*XS(3,2))
      B2 = XS(1,1)*XS(3,3)-XS(1,3)*XS(3,1)
      B3 = -(XS(1,1)*XS(3,2)-XS(1,2)*XS(3,1))
      C1 = XS(1,2)*XS(2,3)-XS(2,2)*XS(1,3)
      C2 = -(XS(1,1)*XS(2,3)-XS(1,3)*XS(2,1))
      C3 = XS(1,1)*XS(2,2)-XS(1,2)*XS(2,1)
      XSJ = XS(1,1)*A1+XS(1,2)*A2+XS(1,3)*A3
      SX(1,1) = A1/XSJ
      SX(1,2) = B1/XSJ
      SX(1,3) = C1/XSJ
      SX(2,1) = A2/XSJ
      SX(2,2) = B2/XSJ
      SX(2,3) = C2/XSJ
      SX(3,1) = A3/XSJ
      SX(3,2) = B3/XSJ
      SX(3,3) = C3/XSJ
      DO 140 I = 1,NEL
      TEMP1=SHP(1,I)*SX(1,1)+SHP(2,I)*SX(2,1)+SHP(3,I)*SX(3,1)
      TEMP2=SHP(1,I)*SX(1,2)+SHP(2,I)*SX(2,2)+SHP(3,I)*SX(3,2)
      SHP(3,I)=SHP(1,I)*SX(1,3)+SHP(2,I)*SX(2,3)+SHP(3,I)
      $*SX(3,3)
      SHP(2,I) = TEMP2
140  SHP(1,I) = TEMP1
      RETURN
      END

```

C

C\*\*\*\*\*

C

```

      SUBROUTINE SURF(RR,SS,TT,X,SSHP,XS,XSJ,NEL,NFACE)
      IMPLICIT REAL*4 (A-H,O-Z)
      COMMON/BLK1/NUMNP,NUMEL,NDM,MNEL,NUMAT,NEQ,NTP,MBAND,NPROP
      $,NBEL,NNEF,IELMT
      DIMENSION SSHP(5,1),X(3,1),R(9),S1(9),S2(9),
      $T(9),XS(2,2),SX(2,2)
      DATA R/-1.0E0,1.0E0,-1.0E0,0.0E0,1.0E0,0.0E0,-1.0E0,0.0E0/,
      $T/-1.0E0,-1.0E0,1.0E0,1.0E0,-1.0E0,0.0E0,1.0E0,0.0E0,0.0E0/,
      $$S1/-1.0E0,-1.0E0,1.0E0,1.0E0,-1.0E0,0.0E0,1.0E0,0.0E0,0.0E0/,
      $$S2/-1.0E0,1.0E0,1.0E0,-1.0E0,0.0E0,1.0E0,0.0E0,-1.0E0,0.0E0/
      IF(NFACE.EQ. 1 .OR. NFACE.EQ. 2)GO TO 200
      IF(NFACE.EQ. 4 .OR. NFACE.EQ. 6)GO TO 210
      IF(NFACE.EQ. 3 .OR. NFACE.EQ. 5)GO TO 220
200  IF(IELMT.EQ.2)GO TO 300
      DO 100 I = 1,NNEF
      SSHP(4,I) = (1.0+R(I)*RR)*(1.0+S1(I)*SS)/4.0
      SSHP(1,I) = R(I)*(1.0+S1(I)*SS)/4.0
100  SSHP(2,I) = S1(I)*(1.0+R(I)*RR)/4.0
      GO TO 230
300  DO 311 I = 1,4
      SSHP(4,I)=(1.+R(I)*RR)*(1.+S1(I)*SS)*(R(I)*RR+S1(I)
      $*SS-1.)/4.
      SSHP(1,I)=R(I)*(1.+S1(I)*SS)*(2.*R(I)*RR+S1(I)*SS)/4.
311  SSHP(2,I)=S1(I)*(1.+R(I)*RR)*(R(I)*RR+2.*S1(I)*SS)/4.
      I = 5
313  SSHP(4,I)=(1.-RR**2)*(1.+S1(I)*SS)/2.
      SSHP(1,I)=-RR*(1.+S1(I)*SS)
      SSHP(2,I)=S1(I)*(1.-RR**2)/2.
      I = I+2
      IF(I.GT.7)GO TO 312
      GO TO 313
312  I = 6
314  SSHP(4,I)=(1.+R(I)*RR)*(1.-SS**2)/2.
      SSHP(1,I)=R(I)*(1.-SS**2)/2.
      SSHP(2,I)=-SS*(1.+R(I)*RR)
      I = I+2
      IF(I.GT.8)GO TO 230
      GO TO 314
210  IF(IELMT.EQ.2)GO TO 320
      DO 110 I = 1,NNEF
      SSHP(4,I) = (1.0+T(I)*TT)*(1.0+S2(I)*SS)/4.0
      SSHP(1,I) = S2(I)*(1.0+T(I)*TT)/4.0

```

```

110 SSHP(2,I) = T(I)*(1.0+S2(I)*SS)/4.0
    GO TO 230
320 DO 321 I = 1,4
    SSHP(4,I)=(1.+S2(I)*SS)*(1.+T(I)*TT)*(S2(I)*SS+T(I)
    $*TT-1.)/4.
    SSHP(1,I)=S2(I)*(1.+T(I)*TT)*(2.*S2(I)*SS+T(I)*TT)/4.
321 SSHP(2,I)=T(I)*(1.+S2(I)*SS)*(S2(I)*SS+2.*T(I)*TT)/4.
    I = 5
323 SSHP(4,I)=(1.-SS**2)*(1.+T(I)*TT)/2.
    SSHP(1,I)=-SS*(1.+T(I)*TT)
    SSHP(2,I)=T(I)*(1.-SS**2)/2.
    I = I+2
    IF(I.GT.7)GO TO 324
    GO TO 323
324 I = 6
325 SSHP(4,I)=(1.+S2(I)*SS)*(1.-TT**2)/2.
    SSHP(1,I)=S2(I)*(1.-TT**2)/2.
    SSHP(2,I)=-TT*(1.+S2(I)*SS)
    I = I+2
    IF(I.GT.8)GO TO 230
    GO TO 325
220 IF(IELMT.EQ.2)GO TO 330
    DO 120 I = 1,NNEF
    SSHP(4,I) = (1.0+R(I)*RR)*(1.+T(I)*TT)/4.0
    SSHP(1,I) = R(I)*(1.0+R(I)*RR)/4.0
120 SSHP(2,I) = T(I)*(1.0+R(I)*RR)/4.0
    GO TO 230
330 DO 331 I = 1,4
    SSHP(4,I)=(1.+R(I)*RR)*(1.+T(I)*TT)*(R(I)*RR+T(I)
    $*TT-1.)/4.
    SSHP(1,I)=R(I)*(1.+T(I)*TT)*(2.*R(I)*RR+T(I)*TT)/4.
331 SSHP(2,I)=T(I)*(1.+R(I)*RR)*(R(I)*RR+2.*T(I)*TT)/4.
    I = 5
333 SSHP(4,I)=(1.-RR**2)*(1.+T(I)*TT)/2.
    SSHP(1,I)=-RR*(1.+T(I)*TT)
    SSHP(2,I)=T(I)*(1.-RR**2)/2.
    I = I+2
    IF(I.GT.7)GO TO 334
    GO TO 333
334 I = 6
335 SSHP(4,I)=(1.+R(I)*RR)*(1.-TT**2)/2.
    SSHP(1,I)=R(I)*(1.-TT**2)/2.
    SSHP(2,I)=-TT*(1.+R(I)*SS)
    I = I+2
    IF(I.GT.8)GO TO 230
    GO TO 335
230 DO 130 I = 1,2
    DO 130 J = 1,2
    XS(I,J) = 0.0
    DO 130 K = 1,NNEF
130 XS(I,J) = XS(I,J)+SSHP(I,K)*SSHP(J,K)
    XSJ = XS(1,1)*XS(2,2)-XS(1,2)*XS(2,1)
    RETURN
    END
C
C*****
C
C      SUBROUTINE PGAUSS(L,LINT,R,S,T,W)
C      IMPLICIT REAL*4 (A-H,O-Z)
C      DIMENSION LR(27),LS(27),LT(27),LW(27),R(1),S(1),T(1),W(1)
C      DATA LR/-1,1,1,-1,-1,1,1,-1,0,1,0,-1,-1,1,1,-1,0,1,0,-1,
C      $0,0,0,0,-1,1,0/,LS/-1,-1,1,1,-1,-1,1,1,-1,0,1,0,-1,-1,
C      $1,1,-1,0,1,0,0,0,0,0,0,0,0,0,0,0,0,0,0,0,0,0,0,0,0,0,0,0,
C      $-1,-1,0,0,0,0,1,1,1,1,-1,1,0,0,0,0,0,0,0,0,0,0,0,0,0,0,0,
C      DATA LW/8*25,12*40,7*0/
C      LINT = L*L*L
C      GO TO(1,2,3),L
C
C      1*1*1 INTEGRATION
C
C      1   R(1) = 0.0
C          S(1) = 0.0
C          T(1) = 0.0
C          W(1) = 8.0
C      RETURN
C

```

C 2\*2\*2 INTEGRATION

```
C
2  G = 1.0E00/SQRT(3.0E00)
   DO 21 I = 1,8
   R(I) = G*LR(I)
   S(I) = G*LS(I)
   T(I) = G*LT(I)
   W(I) = 1.0E00
21  CONTINUE
   RETURN
```

C 3\*3\*3 INTEGRATION

```
C
3  G = SQRT(0.6E00)
   H = 1.0E00/145.8
   DO 22 I = 1,27
   R(I) = G*LR(I)
   S(I) = G*LS(I)
   T(I) = G*LT(I)
   W(I) = H*LW(I)
22  CONTINUE
   RETURN
   END
```

```
C
C*****
C
SUBROUTINE QUAD(L,LLINT,R,S,T,W,NFACE)
IMPLICIT REAL*4 (A-H,O-Z)
DIMENSION LR(9),LS1(9),LW(9),R(1),S(1),T(1),W(1),
$LT(9),LS2(9)
DATA LR/-1,1,1,-1,0,1,0,-1,0/,LT/-1,-1,1,1,-1,0,1,0,0/
DATA LS1/-1,-1,1,1,-1,0,1,0,0/,LS2/-1,1,1,-1,0,1,0,-1,0/
DATA LW/4*25,4*40,64/
LLINT = L*L
GO TO(1,2,3),L
```

C 1\*1 INTEGRATION

```
C
1  R(1) = 0.0
   S(1) = 0.0
   T(1) = 0.0
   W(1) = 4.0
   RETURN
```

C 2\*2 INTEGRATION

```
C
2  G = 1.0D00/SQRT(3.0E00)
   DO 11 I = 1,4
   IF(NFACE .EQ. 1 .OR. NFACE .EQ. 2)GO TO 10
   IF(NFACE .EQ. 4 .OR. NFACE .EQ. 6)GO TO 20
   IF(NFACE .EQ. 3 .OR. NFACE .EQ. 5)GO TO 30
10  T(I) = 0.0
   R(I) = G*LR(I)
   S(I) = G*LS1(I)
   W(I) = 1.0E00
   GO TO 12
20  R(I) = 0.0
   S(I) = G*LS2(I)
   T(I) = G*LT(I)
   W(I) = 1.0E00
   GO TO 12
30  S(I) = 0.0
   R(I) = G*LR(I)
   T(I) = G*LT(I)
   W(I) = 1.0E00
12  CONTINUE
11  CONTINUE
   RETURN
```

C 3\*3 INTEGRATION

```
C
3  G = SQRT(0.60E00)
   H = 1.0E00/81.0E00
   DO 31 I = 1,9
   IF(NFACE .EQ. 1 .OR. NFACE .EQ. 2)GO TO 40
   IF(NFACE .EQ. 4 .OR. NFACE .EQ. 6)GO TO 50
```

```

40  IF(NFACE .EQ. 3 .OR. NFACE .EQ. 5)GO TO 60
    T(I) = 0.0
    S(I) = G*LS1(I)
    R(I) = G*LR(I)
    W(I) = H*LW(I)
    GO TO 22
50  R(I) = 0.0
    S(I) = G*LS2(I)
    T(I) = G*LT(I)
    W(I) = H*LW(I)
    GO TO 22
60  S(I) = 0.0
    R(I) = G*LR(I)
    T(I) = G*LT(I)
    W(I) = H*LW(I)
22  CONTINUE
31  CONTINUE
    RETURN
    END
C
C *****
C
SUBROUTINE RADN(NNRAD,NFRAD,IELG,NEL,NNEF,ANGLE,NP,QR,T)
IMPLICIT REAL*4 (A-H,O-Z)
REAL*4 ANGLE,QR,T,TINF,DT,GR,EMS,EMA
CHARACTER F*1
DIMENSION AMH(24),F(24),MS(24),HD(24),HB(24),
$HV(24),R(24),QSN(24),QQ(24),NP(NEL,1),T(1),
$NNRAD(NEL,6,1),NFRAD(1),QR(24,500),NDAY(12),APMH(24)
COMMON/BLK3/III
COMMON/BLK5/IPHR,NSYR,NSMO,NSDAY,NCYR,NCMO,
$NCDAY,ND,NHOUR,IHOUR,ICDAY,IPDAY,IPC,IDAY
COMMON/BLK6/TINF(24),DT,EMS,EMA
DATA NDAY/31,28,31,30,31,30,31,30,31,30,31,31/
IF(IDAY.EQ.0)GO TO 75
GO TO 76
75  DO 77 I = 1,24
77  APMH(I)=0.0
76  TT = 0.0
    HM = 0.0
    IF(ICDAY.EQ.1.AND.IHOUR.EQ.1)GO TO 49
    GO TO 222
49  IF(IELG.EQ.1.AND.III.EQ.1)GO TO 50
    GO TO 222
50  READ(14,102)MSTNID,MYR,MO,MDAY,MELM,(MS(I),AMH(I),
$F(I),I=1,24)
    WRITE(6,103)MSTNID,MYR,MO,MDAY
102  FORMAT(17,13,12,12,13,24(I1,F5.0,A1))
103  FORMAT(2X,17,5X,13,5X,12,5X,12)
    DO 21 I = 1,24
    IF(AMH(I).NE.99999.)APMH(I)=AMH(I)
    IF(AMH(I).EQ.99999.)AMH(I)=APMH(I)
    AMH(I)=AMH(I)*0.277778
    HM = HM+AMH(I)
21  CONTINUE
    ND = ND+1
    IF(ND.GT.365)ND=ND-365
    PI = 3.141593
    ALAT = 49.9*2.*PI/360.
    AA = ALAT-PI/2.
    DECL = 23.45*SIN(2*PI*((284.+ND)/365.))
    DECL = (2*PI*DECL)/360.0
    SC = 1353
    A1 = TAN(ALAT)
    A2 = TAN(DECL)
    A3 = -A1*A2
    WS = ARCOS(A3)
    A = (2.*PI*ND/365.)
    RR = 1 + 0.033*COS(A)
    HO = (24./PI)*SC*(RR*(COS(ALAT)*COS(DECL)*SIN(WS))+
$(WS*SIN(ALAT)*SIN(DECL)))
    B = HM/HO
    C = 0.8710458 + 1.12281*B-(7.962557*(B**2.5))
    $+(6.55845*(B**3.5))
222  DO 111 J = 1,24
    IJK = 13

```

```

      I1J = IJK-J
      W = (I1J*15.0)*2.0*PI/360.0
      IF(F(J).EQ.'W'.OR.F(J).EQ.'Z')GO TO 51
      GR=0.2
      GO TO 53
51  GR=0.7
53  GAMA = (ANGLE*2*PI)/360.0
      THETAZ = SIN(ALAT)*SIN(DECL) + COS(DECL)*COS(ALAT)*
$COS(W)
      THETAT = COS(DECL)*COS(GAMA)*COS(W)*SIN(ALAT)
$+COS(DECL)*SIN(GAMA)*SIN(W)-SIN(DECL)*COS(GAMA)
$*COS(ALAT)
      RB = THETAT/THETAZ
      IF(RB.GT.5.0.OR.RB.LT.-5.0)RB=0.0
      HD(J) = AMH(J) * C
      HB(J) = AMH(J)-HD(J)
      HV(J) = (2.*RB*AMH(J)+2.*RB*HB(J)+HD(J)+GR*AMH(J))/4.0
      STEF = 5.6697E-08
      QSN(J) = HV(J) * EMS
      QQ(J) = QSN(J)
111 CONTINUE
      K = 1
      IN = IABS(24/NHOUR)
      DO 70 I1 = 1,IN
      TEMP = 0.0
      KK = K+NHOUR-1
      DO 80 I = K,KK
80  TEMP = TEMP+QQ(I)
      QR(I1,IELG) = TEMP/NHOUR
      QE = 0.5*STEF*EMA*(TINF(I1)**4)
      QS = 0.5*STEF*EMA*(210**4)
      QR(I1,IELG) = QR(I1,IELG)+QE+QS
70  K = K+NHOUR
60  CONTINUE
      DO 20 I = 1,NNEF
      DO 30 J = 1,NEL
30  IF(J.EQ.NNRAD(I,I1,IELG))NNG=NP(J,IELG)
20  TT = TT+T(NNG)
      TT = TT/NNEF
      QO = STEF*EMA*(TT**4)
      QR(IHOUR,IELG)=QR(IHOUR,IELG)-QO
      RETURN
      END
C
C*****
C
      SUBROUTINE DECOMP (GSM,NP,NBW)
      IMPLICIT REAL*4 (A-H,O-Z)
      DIMENSION GSM(NP,NBW)
      DATA EPS/1.E-20/
      DO 12 I=1,NP
      M=NP-I+1
      IF (NBW-M) 1,2,2
1  M=NBW
2  DO 12 J=1,M
      N=NBW-J
      IF (I-1-N) 3,4,4
3  N=I-1
4  SUM=GSM(I,J)
      IF (N) 7,7,5
5  DO 6 K=1,N
      IK=I-K
      JK=J+K
      KK=K
6  SUM=SUM-GSM(IK,K+1)*GSM(IK,JK)
7  IF (J-1) 8,9,8
8  GSM(I,J)=SUM*TEMP
      GO TO 12
9  IF (SUM-EPS*GSM(I,1)) 10,10,11
10 WRITE (04,13) I
      STOP
11 TEMP=1./SQRT(SUM)
      GSM(I,J)=TEMP
12 CONTINUE
      RETURN
13 FORMAT (/////10X,32HDECOMPOSITION TERMINATED ON ROW ,I3,30HPOSSIBL

```

```

1E ERROR IN ELEMENT DATA)
END
C
C*****
C
SUBROUTINE BANSOL (GSM,GF,X,NP,NBW)
IMPLICIT REAL*4 (A-H,O-Z)
DIMENSION GSM(NP,NBW),GF(NP),X(NP)
C
C REDUCE LOAD VECTOR
C
DO 5 I=1,NP
  J=I-NBW+1
  IF (I+1-NBW) 1,1,2
1  J=1
2  SUM=GF(I)
  IF (I-1) 5,5,3
3  IT=I-1
  DO 4 K=J,IT
    IKK=I-K+1
4    SUM=SUM-GSM(K,IKK)*X(K)
5  X(I)=SUM*GSM(I,1)
C
C BACKWARD SUBSTITUTION
C
DO 10 IT=1,NP
  I=NP-IT+1
  J=I+NBW-1
  IF (J-NP) 7,7,6
6  J=NP
7  SUM=X(I)
  IPL1=I+1
  IF (IPL1-J) 8,8,10
8  DO 9 K=IPL1,J
    KII=K-I+1
9  SUM=SUM-GSM(I,KII)*X(K)
10 X(I)=SUM*GSM(I,1)
  RETURN
END
C
C*****
C
SUBROUTINE TRANS (GCM,GHM,TR,F,RF,NP,NBW,NPP,FT,ID)
IMPLICIT REAL*4 (A-H,O-Z)
COMMON/BLK1/NUMNP,NUMEL,NDM,MNEL,NUMAT,NEQ,NTP,MBAND,NPROP
$,NBEL,NNEF,IELMT
COMMON/BLK5/IPHR,NSYR,NSMO,NSDAY,NCYR,NCMO,
$,NCDAY,ND,NHOUR,IHOUR,ICDAY,IPDAY,IPC,IDAY
COMMON/BLK6/TINF(24),DT,EMS,EMA
DIMENSION GCM(NP,NBW),GHM(NP,NBW),TR(NP),F(NP),RF(NP)
$,NPP(MNEL,1),FT(1),ID(1),AVETMP(100),TEMP1(900,300)
DO 31 I = 1,NUMNP
DO 32 J = 1,NBW
32 TEMP1(I,J)=GCM(I,J)
31 FT(I) = TR(I)
SDT=DT
NIT = NHOUR*3600/DT
DO 510 KK=1,NIT
CALL MULTBD (GHM,TR,RF,NP,NBW)
DO 507 I=1,NP
507 RF(I)=F(I)+RF(I)
DO 511 I = 1,NUMNP
IF(ID(I).NE.1)GO TO 511
DO 10 J = 2,NBW
I1 = I-J+1
I2 = I+J-1
IF(I1.GE.1)RF(I1)=RF(I1)-TEMP1(I1,J)*FT(I)
10 IF(I2.LE.NP)RF(I2)=RF(I2)-TEMP1(I,J)*FT(I)
RF(I)=FT(I)
IF(KK.EQ.1)GO TO 97
GO TO 511
97 DO 20 J = 1,NBW
I1 = I-J+1
IF(I1.GE.1)GCM(I1,J)=0.0
20 GCM(I,J)=0.0
GCM(I,1)=1.0

```



```

511 CONTINUE
    IF(KK.EQ.1)CALL DECOMP(GCM,NP,NBW)
    CALL BANSOL(GCM,RF,TR,NP,NBW)
    DO 53 I = 1,NUMNP
    IF(ID(I).NE.1)GO TO 53
    TR(I) = FT(I)
53 CONTINUE
510 CONTINUE
    IPC = IPC+NHOUR
    IF(IPC.GE.IPHR)GO TO 61
    GO TO 62
61 IPDAY = IPDAY+IABS(IPHR/24)
    IPC = 0
    WRITE(6,63)IPDAY
    WRITE(6,64)
    WRITE(6,60)(I,TR(I),I=1,NUMNP)
60 FORMAT(3(3X,I4,3X,E12.6))
64 FORMAT(3X,' NODE',4X,'TEMPERATURE',3X,'NODE',4X,
$'TEMPERATURE',3X,'NODE',4X,'TEMPERATURE'//)
63 FORMAT(' DAYS ELAPSED = ',I5//)
62 RETURN
    END

C
C*****
C
    SUBROUTINE MULTBD (GSM,GF,RF,NP,NBW)
    IMPLICIT REAL*4 (A-H,O-Z)
    DIMENSION GSM(NP,NBW),GF(NP),RF(NP)
    DO 503 I=1,NP
    SUM=0.0
    K=I-1
    DO 502 J=2,NBW
    M=J+I-1
    IF (M.GT.NP) GO TO 501
    SUM=SUM+GSM(I,J)*GF(M)
501 IF (K.LE.0) GO TO 502
    SUM=SUM+GSM(K,J)*GF(K)
    K=K-1
502 CONTINUE
503 RF(I)=SUM+GSM(I,1)*GF(I)
    RETURN
    END

C
C*****
C
    SUBROUTINE ELM2(DL,NEL,XL,SL,RL,CL,HCL,SQRL,SHCL,
$NFCN,NFRAD,NNCON,NNRAD,HC,NFACE,ICN)
    RETURN
    END

```

## Appendix D

### FE3DHT - 3D finite element heat transfer program

#### Main Program

This program reads and writes control informations. It assigns location for each of the matrices and vectors in a large one dimensional array A. It calls the subroutine DAYCAL, READ, INITEM, BOUNDT, ASSEMB, and TRANS. Organizes the flow of the whole program.

NHOUR is the number of hours after which the boundary conditions are read and the element matrices are calculated again. Subroutines BOUNDT, ASSEMB, and TRANS are called 24/NHOUR times each day and the Do loop extends for the total number of days simulation is required.

#### Subroutine DAYCAL

Calculates the total number of days the simulation is to be run. Total number of days are calculated based on the starting day, month, and year and the closing day, month, and year.

#### Subroutine READ

Reads and writes the following information:

- (i) Node data: Node number and the X, Y, and Z coordinates of each node.
- (ii) Element data: Element number, material set number, number of nodes in the element, global node number of each node in the element and the internal heat generation in the element.
- (iii) Boundary condition codes: Node number and its boundary condition code. (set equal to 1 for the bottom nodes).

- (iv) Convection and radiation boundary conditions: Element number, number of faces in the convection boundary and the number of faces in the radiation boundary. Then the number of each boundary face in the convection boundary and the angle between the normal to face and the south for each radiation boundary.
- (v) Material data: Material set number and the element type number are read. For each material set it calls the subroutine ELMLIB, which directs the control to the first part of the appropriate element subroutine. In the element subroutine the material data are read and written in the output file.

Subroutine READ also calls the subroutine CONRAD for each of the convection and radiation boundary faces of every boundary element, and the subroutine BANDW once. Also it calls the subroutine BOUNDT with the control information directed to the first part of the BOUNDT.

#### Subroutine CONRAD

It assigns the local node number for all the nodes in each of the convection and radiation faces of every boundary element.

#### Subroutine BOUNDT

This subroutine has three parts. The value of IC passed on by the calling argument activates the corresponding part of the subroutine.

- IC - 1: Called by the subroutine READ. Reads the thermal properties of the soil, concrete, bin wall material, air, diameter of the bin. This part of the subroutine is called only once.
- IC - 2 : Calculates the soil temperature using the model of Singh et al. (1977). Based on the predicted soil temperature of the

day, the bottom temperature of the grain bulk is calculated using the finite difference method. Finally the calculated soil temperature is assigned to those nodes for which the boundary condition code ID is 1. After every 24 hours of simulation the control is passed on to this part of the subroutine by the main program.

IC = 3: Reads the hourly values of the ambient air temperature and the local wind velocity averages these values over the time interval NHOURL. Calculates the convection coefficient HC using Fennigan and Longstaff (1982) model. Called by the main program once in every 24 hours of simulation.

#### Subroutine INITEM

Reads and writes the initial temperature of each node and stores these values in the vector T.

#### Subroutine BANDW

Calculates the half band width by scanning through the global node numbers of each node in all the elements in the domain.

#### Subroutine ASSEMB

Matrices CAP, S, F, RL, and SQRL are initialized in this subroutine. For each element, ASSEMB calls the element subroutine ELM1 thrice (once for calculating the volume integrals, once for surface integrals involving the convection boundary faces and the third time for evaluating the surface integrals over the radiation boundary faces). After the element matrices are calculated and passed from the element subroutine they are assembled in the global matrices and vectors.

Before return, the capacitance matrix will be divided by the time increment DT and added with the stiffness matrix S, after multiplying the stiffness matrix by a factor THETA. Depending on the value of THETA the finite difference scheme used for the time domain can be changed.

When THETA = 0    Forward difference scheme  
                   = 0.5 Crank Nicholson method  
                   = 0.667 Galerkin method  
                   = 1.0 Backward difference scheme

Similarly the stiffness matrix will be multiplied by the factor (1-THETA) and added with the capacitance matrix CAP after dividing the CAP by the time increment DT, before the return.

#### Subroutine EIMLIB

This directs the control to the appropriate element subroutine depending on the value of IELB, passed on by the calling argument. IELB is an input data, read in the subroutine READ. The operator has the control over the value of IELB. The program can be easily extended for one and two dimensional heat transfer problems by adding separate subroutines which can be called by assigning different values for IELB. Presently, for the three dimensional subroutine the value of IELB is 1.

#### Subroutine EIM1

This handles the linear and quadratic three dimensional quadrilateral elements. It is comprised of four parts. Depending on the value of ICN, passed on by the calling argument, the control is directed to the different parts of the subroutine.

ICN = 1: Called by the subroutine READ. It reads and writes the thermal conductivity of grain in X, Y, and Z coordinates,

density and specific heat of the grain, and the number of Gauss points in each plane. It stores these values in the array DL.

ICN = 2: Invoked by the subroutine ASSEMB. Initializes HCL, CL, SL and SHCL. Calls the subroutine PGAUSS once, to get the Gauss points and calls the subroutine SHAPE once for each of the Gauss points. It evaluates the matrices SL, CL and the vector RL, at each Gauss point and adds over all the Gauss points.

ICN = 3: Called by the subroutine ASSEMB. It calls the subroutine QUAD to get the Gauss points in the plane of the convection face and calls the subroutine SURF for each of the Gauss points. Matrix HCL and the vector SHCL are calculated at each Gauss point and added over all the Gauss points.

ICN = 4: Does the same operation as in the case of the third part but the vector SQRL is calculated by this part of the subroutine.

#### Subroutine SHAPE

For each of the Gauss points, shape functions  $N_i$  are stored in SHP(4,I),  $\partial N_i / \partial r$  are stored in SHP(1,I),  $\partial N_i / \partial s$  are stored in SHP(2,I) and  $\partial N_i / \partial t$  are stored in SHP(3,I). It also calculates the Jacobian, its inverse and the determinant of the Jacobian. On return  $\partial N_i / \partial x$  are stored in SHP(1,I),  $\partial N_i / \partial y$  are stored in SHP(2,I) and  $\partial N_i / \partial z$  are stored in SHP(3,I).

This subroutine is capable of handling both linear and quadratic elements. Depending on the value of IELMT (-1 for the linear element and -2 for the quadratic element), it calculates the shape functions for the corresponding element.

#### Subroutine SURF

Calculates the shape functions for the face in the convection or radiation boundary. The control is directed to three different parts of the subroutine depending on the value of NFACE, passed on by the calling argument. Each part can handle both linear and quadratic elements. SHP(4,I) stores the shape functions ( $N_i$ ).  $\partial N_i / \partial r$  (for r-s or r-t plane or  $\partial N_i / \partial s$  (for s-t plane) are stored in SHP(1,I).  $\partial N_i / \partial s$  (for r-s plane) or  $\partial N_i / \partial t$  (for s-t plane or r-t plane) are stored in SHP(2,I). It also calculates the Jacobian and the determinant of the Jacobian.

#### Subroutine PGAUSS

The Gauss points and the weights are calculated and transferred to the calling program. The value of L directs to either of the three parts of the subroutine.

IF L = 1, 1 X 1 X 1 integration

L = 2, 2 X 2 X 2 integration

L = 3, 3 X 3 X 3 integration.

#### Subroutine QUAD

Gauss points and weights for each plane in question are calculated and transferred to the calling program. Can handle 1 X 1, 2 X 2 and 3 X 3 integration.

#### Subroutine RADN

Reads the radiation on the horizontal surface of the location and the ground cover. Calculates the radiation on the strip of the bin wall where the element is located, following the procedures described under the chapter "Model development". On return, QR will be the radiation coefficient for the time of the day on the bin wall segment where the element is located.

**Subroutine DECOMP**

Decomposes the combination of capacitance and conductance matrices passed in by the main program using Choleski's decomposition method.

**Subroutine BANSOL**

Solves the equation  $\{CAP\} \{TR\}_{t+1} = \{RF\}$  for TR at time  $t+\Delta$ , by reducing the load vector RF and using backward substitution.

**Subroutine TRANS**

This subroutine modifies the capacitance matrix and the load vector to take care of the prescribed nodal temperatures. The method given in Rao (1980) is used. The subroutines MULTBD and BANSOL are called by TRANS. After calling MULTBD and BANSOL once, the values on the load vector TR of the nodes for which the temperature is prescribed are replaced by the prescribed temperature values, before calling them again.

Finally when the number of hours after which the information to be printed (IPHR) is reached, it prints the node numbers and the corresponding temperature values in the output file.

**Subroutine MULTBD**

Multiplies the conductance matrix and the load vector.



## Appendix E

### Variables used in the program

AO, AN and BN	- Constants in the soil temperature model
AIRK	- Thermal conductivity of air ( $\text{W m}^{-1} \text{K}^{-1}$ )
AIRRO	- Density of air ( $\text{kg m}^{-3}$ )
AIRVIS	- Viscosity of air ( $\text{N s m}^{-2}$ )
AKX	- Thermal conductivity of grain in x-plane ( $\text{W m}^{-1} \text{K}^{-1}$ )
AKY	- Thermal conductivity of grain in y-plane ( $\text{W m}^{-1} \text{K}^{-1}$ )
AKZ	- Thermal conductivity of grain in z-plane ( $\text{W m}^{-1} \text{K}^{-1}$ )
CCP	- Specific heat of concrete ( $\text{J kg}^{-1} \text{K}^{-1}$ )
CK	- Thermal conductivity of concrete ( $\text{W m}^{-1} \text{K}^{-1}$ )
CROW	- Density of concrete ( $\text{kg m}^{-3}$ )
CP	- Specific heat of grain ( $\text{J kg}^{-1} \text{K}^{-1}$ )
DIA	- Diameter of the bin (m)
DT	- Time step (h)
EMA	- Absorptivity of the bin wall material
EMS	- Emissivity of the bin wall material
GK	- Thermal conductivity of grain in y-plane ( $\text{W m}^{-1} \text{K}^{-1}$ )
GR	- Ground reflectance
IELB	- Element type number in the library (1 for three dimensional subroutine)
IELG	- Current element number
IELMT	- Element type number (linear or quadratic)
IHOUR	- Time of the day (h)
IPDAY	- Number of days elapsed after the start
IPHR	- Number of hours after which output to be printed
L	- Number of Gauss points in each plane

MA	- Material characteristic set number
MBAND	- Half band width
MNEL	- Maximum number of nodes connected to an element
NBEL	- Number of boundary elements
NCDAY	- Closing day
NCMO	- Closing month
NCYR	- Closing year
NDM	- Number of dimensions
NEL	- Number of nodes connected to the current element
NHOUR	- Number of hours before recalculation
NNIEL	- Number of nodes in each layer.
NPROP	- Maximum number of material characteristic sets associated with the element type
NSDAY	- Starting day
NSMO	- Starting month
NSYR	- Starting year
NST	- Total number of degrees of freedom in an element
NTP	- Number of nodes for which temperature is specified
NUMEL	- Number of elements in the grid
NUMNP	- Number of node points in the grid
NUMAT	- Number of material characteristic sets
RHO	- Density of grain ( $\text{kg m}^{-3}$ )
SCP	- Specific heat of soil ( $\text{J kg}^{-1} \text{K}^{-1}$ )
SK	- Thermal conductivity of soil ( $\text{W m}^{-1} \text{K}^{-1}$ )
SROW	- Density of soil ( $\text{kg m}^{-3}$ )

## Arrays in the program

ANG(6,NUMEL)	-	Angle that the normal of the outer face of an element bears with the south (+ towards east and - towards west)
CL(MNEL,MNEL)	-	Local array of capacitance matrix
D(NPROP,NUMAT)	-	Material data for each material set
DL(NPROP)	-	Local array of material data
F(24)	-	Stores the information regarding whether the soil surface is covered with snow or not (read from the data file R7477)
FT(NUMNP)	-	Temporary array of final temperature values
HCL(MNEL,MNEL)	-	Local array of surface integrals involving the convection terms
ID(NUMNP)	-	Boundary condition code for each node in the grid
ID	-	1, nodes at the bottom of the bulk (temperature is calculated using the soil temperature model) ID can be set to other values if any other values are to be prescribed for nodes lying in the boundary.
IFACE(6,NUMEL)	-	Face number in the convection boundary (Refer Fig.E1) (top = 1, bottom = 2, front = 3, right = 4, rear = 5, left = 6)
IRFACE(6,NUMEL)	-	Face number in the radiation boundary Refer Fig.E1) (top = 1, bottom = 2, front = 3, right = 4, rear = 5, left = 6)
AMH(24)	-	Radiation on a horizontal surface for the given location and day (read from the data file R7477)
MEL(NUMAT)	-	Element type number corresponding to each element
NELMAT(NUMEL)	-	Material set number of each element
NFCON(NUMEL)	-	Number of faces of an element in the convection boundary (all six faces of a quadrilateral element can be in the convection boundary)
NFRAD(NUMEL)	-	Number of faces of an element in the radiation

boundary (all six faces of an element can be in the radiation boundary)

NNCON(MNEL,6,NUMEL)	-	Local node numbers in a given convection face
NNRAD(MNEL,6,NUMEL)	-	Local node numbers in a given radiation face
NP(MNEL,MNEL)	-	Element nodal connectivity array. It stores the global node numbers corresponding to local node numbers of each element)
QR(24,NUMEL)	-	Radiation coefficient of the given element at any time of the day
RF(NUMNP)	-	Temporary vector storing the nodal temperatures
RL(MNEL)	-	Local array of integrals involving the heat generation term
S(NUMNP,MBAND)	-	Global array of summation of matrices SL and HCL (global stiffness matrix)
SHCL(MNEL)	-	Local array of surface integrals involving convection terms, both along the circumference and the top of the grain bulk)
SL(MNEL,MNEL)	-	Local array of element conductance matrix
SQRL(MNEL)	-	Local array of surface integrals involving radiation term
T(NUMNP)	-	Vector that stores the current temperature of each node. At time $t = 0$ , T stores the initial temperatures
TR(NUMNP)	-	Array of temperatures that are printed in the output file
TD(24)	-	Hourly ambient temperature for the given day and location (read from the weather data set file WIN7477)
WIND(24)	-	Hourly wind velocity for the given day and location (read from the data set file WINN7477.CMBND)
X(NDM,NUMNP)	-	Coordinate array
XL(NDM,MNEL)	-	Local array of global coordinates of element nodes
IC	-	switch used to direct the control to the appropriate part of the subroutine BOUNDT

ICN                                -    Switch used to direct the control to the appropriate part of the element subroutine

**Location of matrices and vectors in a large  
one dimensional array A**

A(N1)	=	X(NDM, NUMNP)
A(N2)	=	NELMAT(NUMEL)
A(N3)	=	NELND(NUMEL)
A(N4)	=	NP(MNEL, NUMEL)
A(N5)	=	D(NPROP, NUMAT)
A(N6)	=	ID(NUMNP)
A(N7)	=	MEL(NUMAT)
A(N8)	=	SL(MNEL, MENL)
A(N9)	=	CL(MNEL, MNEL)
A(N10)	=	XL(NDM, MNEL)
A(N12)	=	RL(MNEL)
A(N13)	=	NFCON(NUMEL)
A(N14)	=	S(NUMNP, MBAND)
A(N15)	=	CAP(NUMNP, MBAND)
A(N16)	=	NFRAD(NUMEL)
A(N18)	=	NNCON(MNEL, 6, NUMEL)
A(N19)	=	NNRAD(MNEL, 6, NUMEL)
A(N20)	=	HC(6, NUMEL)
A(N21)	=	IFACE(6, NUMEL)
A(N22)	=	HCL(MNEL, MNEL)
A(N23)	=	SQRL(MNEL)
A(N24)	=	SHCL(MNEL)

A(N25)	- ANG(6, NUMEL)
A(N26)	- F(NUMNP)
A(N27)	- IRFACE(6, NUMEL)
A(N28)	- RF(NUMNP)
A(N29)	- FT(NUMNP)
A(N31)	- Q(NUMEL)
A(N32)	- T(NUMNP)

Note:  $N_i$ s are the location number in the array A.

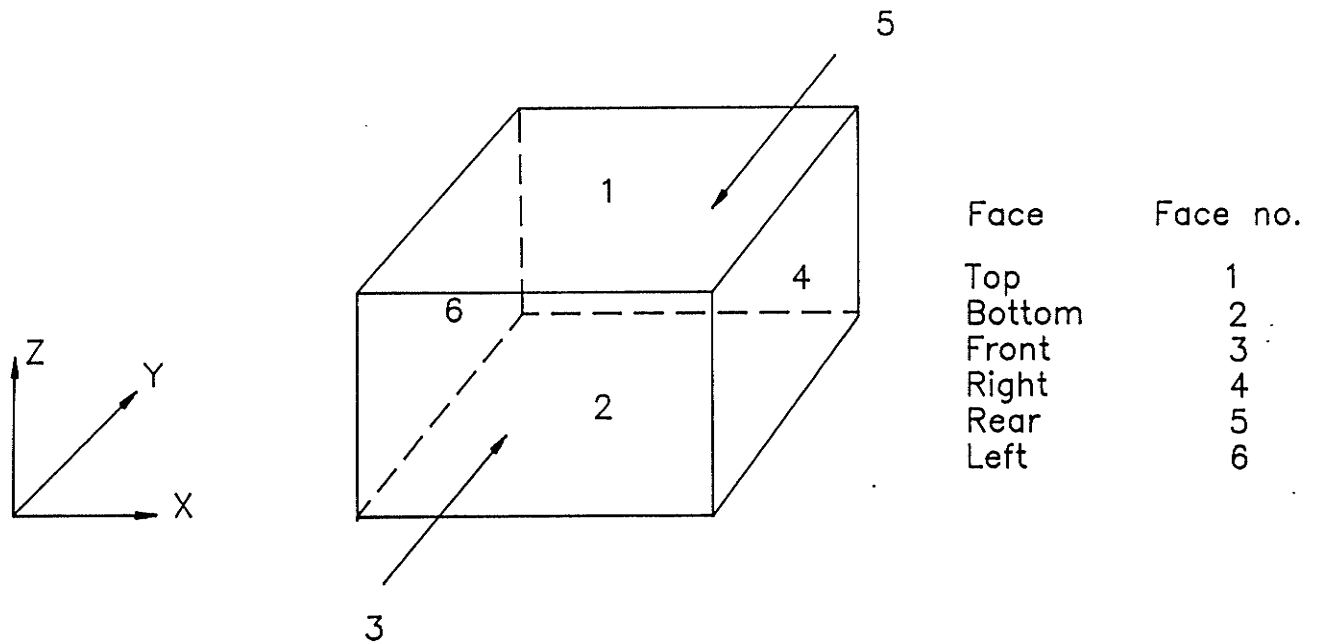


Fig E.1: Face numbers for convection and radiation boundaries in an element.

## APPENDIX F

### INPUT DATA FOR FE3DHT LISTED IN ORDER OF LINES

<u>Columns</u>	<u>Format</u>	<u>Variable</u>	<u>Description</u>
<u>Heading</u>			
1-60	15A4	HEAD	Title to be printed (in one line)
<u>Control information (in one line)</u>			
1-5	I5	NUMNP	Number of nodes in the grid
6-10	I5	NUMEL	Number of elements in the grid
11-15	I5	NDM	Number of dimensions
16-20	I5	MNEL	Maximum number of nodes per element
21-25	I5	NUMAT	Number of material sets
26-30	I5	NTP	Number of nodes for which temperature is prescribed
31-35	I5	NPROP	Number of material data
36-40	I5	NBEL	Number of boundary elements
41-45	I5	NNEF	Number of nodes in each face
46-50	I5	IELMT	Element type number (= 1 for linear element and = 2 for quadratic element)
<u>Information regarding the time (in one line)</u>			
1-5	I5	NSYR	Starting year
6-10	I5	NSMO	Starting month
11-15	I5	NSDAY	Starting day
16-20	I5	NCYR	Closing year
21-25	I5	NCMO	Closing month
26-30	I5	NCDAY	Closing day
31-35	I5	NHOUR	Number of hours before recalculation
36-40	I5	IPHR	Number of hours after which the information to be printed
41-50	F10.5	DT	Time step (hrs)
<u>Coordinate information (one line for each node)</u>			
1-5	I5	M	Node number
11-20	F10.5	X(1,M)	X-coordinate of the node M
21-30	F10.5	X(2,M)	Y-coordinate of the node M
31-40	F10.5	X(3,M)	Z-coordinate of the node M
<u>Element data (one line for each element)</u>			
1. If linear element :			
1-5	I5	M	Element number
11-15	I5	NELMAT(M)	Material set number of element M
16-20	I5	NEL	Number of nodes in element M



21-60	8I5	NP(I,M)	Global node number of each node in the element
61-70	F10.5	Q(M)	Internal heat generation in the element M (= 0 if no internal heat generation)

2. If quadratic element :

1-5	I5	M	Element number
11-15	F10.5	NELMAT(M)	Material set number of element M
16-20	I5	NEL	Number of nodes in the element M
21-60	8I5	NP(I,M)	I = 1 to 8. Global node number of the first 8 nodes of the element (next line)
1-60	12I5	NP(I,M)	I = 9 to 20. Global node number of the next 12 nodes of the element
61-70	F10.5	Q(M)	Internal heat generation in the element M (= 0 if no internal heat generation)

Boundary condition codes (one line for each boundary node)

1-5	I5	N	Node number for which the temperature is prescribed
6-10	I5	ID(N)	ID = 1 for bottom nodes

(if NTP = 0 above informations should not be given)

Convection and radiation boundary conditions

1-5	I5	M	Element number
6-10	I5	NFCON(M)	Number of faces in the convection boundary
11-15	I5	NFRAD(M)	Number of faces in the radiation boundary

(above three data are entered in one line)

1-30	6I5	IFACE(I,M)	Faces in the convection boundary (= 1 for top face, = 2 for bottom face = 3 for front face, = 4 for left face = 5 for rear face, and = 6 for right face)
------	-----	------------	---

(above informations are given in one line. If NFCON(M) = 0, this information should not be given)

1-5	I5	IFACE	Face in the radiation side
31-40	F10.5	ANG(I,M)	Angle that the face makes with the south (+ towards east and - towards west)

(above data are entered in one line per NFRAD. IF NFRAD(M) = 0, the above line can be omitted in the input file)

Convection and radiation boundary conditions should be entered in the

order given above for each of the boundary nodes.

Material characteristic data

1-5	I5	MA	Material set number
6-10	I5	IELB	Element type number

Each material set card must be followed immediately by the material property data.

1-10	F10.5	AKX	Thermal conductivity in X-direction
11-20	F10.5	AKY	Thermal conductivity in Y-direction
21-30	F10.5	AKZ	Thermal conductivity in Z-direction
31-40	F10.5	RHO	Grain density
41-50	F10.5	CP	Specific heat of grain
51-55	I5	L	Number of Gauss points in each plane
			If L = 2, Volume integral = 2 X 2 X 2
			Surface integral = 2 X 2

Other data required (in three lines)

1-10	F10.5	DIA	Diameter of the bin
11-20	F10.5	AIRK	Thermal conductivity of air
21-30	F10.5	AIRRO	Density of air
31-40	F10.5	AIRVIS	Viscosity of air
41-50	F10.5	SK	Thermal conductivity of soil
1-10	F10.5	SROW	Density of soil
11-20	F10.5	SCP	Specific heat of soil
21-30	F10.5	GK	Thermal conductivity of grain
31-40	F10.5	CK	Thermal conductivity of concrete
41-50	F10.5	CROW	Density of concrete
1-10	F10.5	CCP	Specific heat of concrete
11-20	F10.5	EMS	Emissivity of bin wall material
21-30	F10.5	EMA	Absorptivity of bin wall material
31-35	I5	NNIEL	Number of nodes in each layer.

Initial nodal temperatures

1-60	6F10.5	T(I)	Initial temperature of node I. 6 values are typed in one line. Should be given for all the nodes.
------	--------	------	---

## APPENDIX G

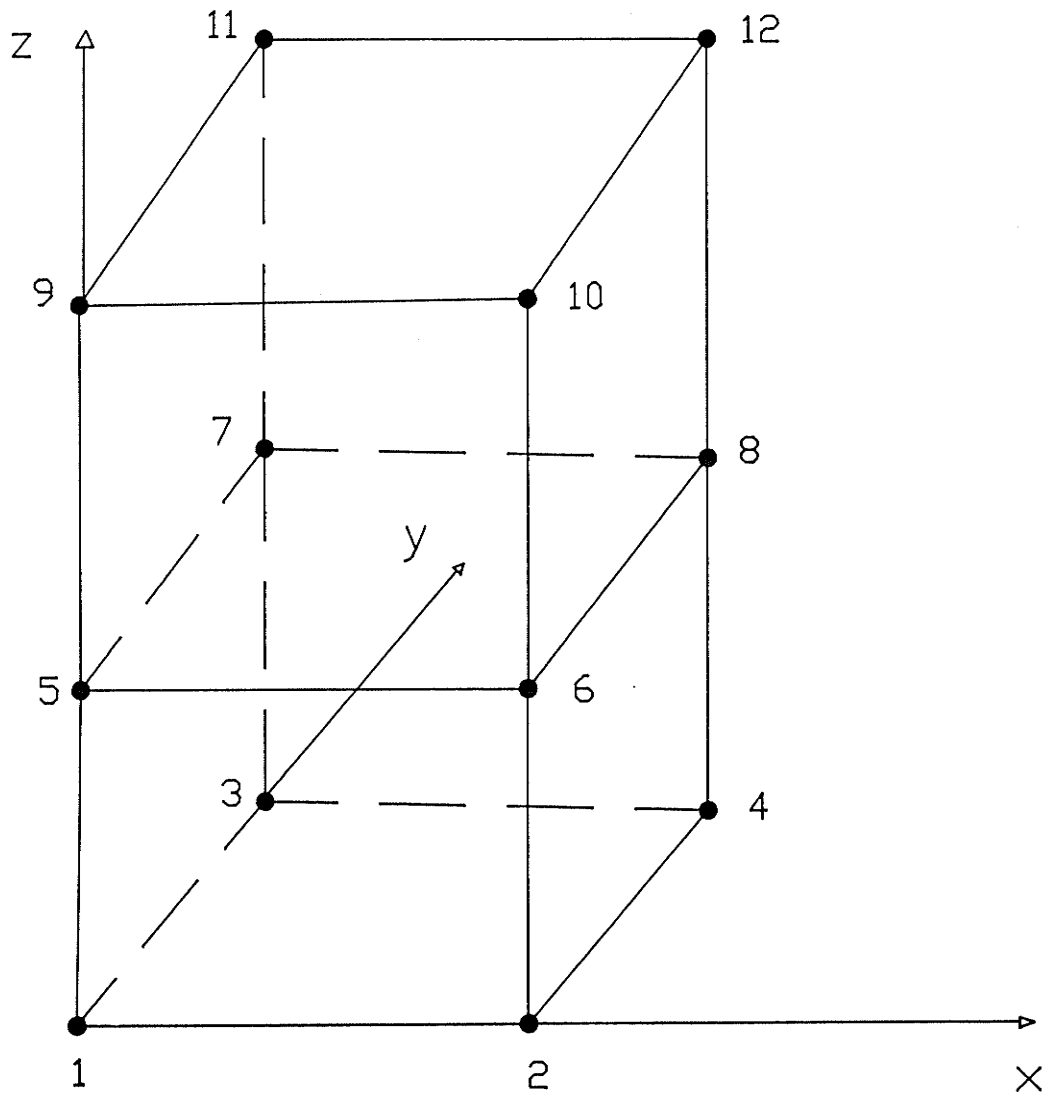


Fig G1: A rectangular domain discretized into two linear elements. (not to scale)



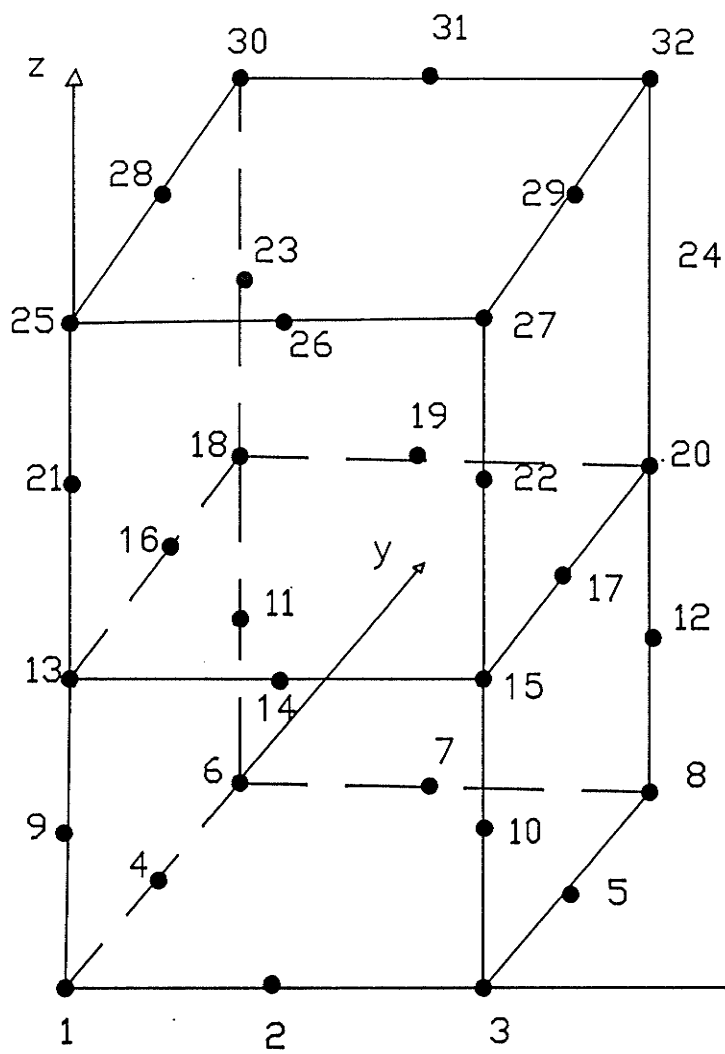


Fig G2: A rectangular domain discretized into two quadratic elements. (not to scale)

[illegible]

/\*

NOTE :

1. ALL THE FACES IN BOTH THE ELEMENTS OTHER THAN THE ONE JOINING THE TWO ELEMENTS ARE ASSUMED TO BE IN THE CONVECTION BOUNDARY CONVECTION BOUNDARY
2. FACES 3 AND 4 OF BOTH THE ELEMENTS ARE ASSUMED TO BE IN THE RADIATION BOUNDARY. THE FACES ARE ASSUMED TO BEAR THE MENTIONED ANGLES WITH THE LOCAL MERIDIAN
3. INTERNAL HEAT GENERATION IN BOTH THE ELEMENTS IS ASSUMED TO BE 0
4. TEMPERATURES IN THE BOTTOM LAYER OF THE GRID ARE PRESCRIBED BY THE TEMPERATURE CALCULATED BY THE SOIL TEMPERATURE MODEL

# APPENDIX - H

Table H1 : Measured and predicted temperatures (K) in a 5.56 m diameter bin containing rapeseed to a depth of 3.2 m, located near Winnipeg.

Radius													
Centre					1.0 m			2.0 m			Wall		
DATE	H	Mes	PLE	PQE	Mes	PLE	PQE	Mes	PLE	PQE	Mes	PLE	PQE
Aug13/74	0	286.0	287.2	288.6	286.8	287.2	288.4	289.6	288.0	288.3	291.6	295.9	291.5
	1	287.0	287.7	288.2	289.5	288.6	290.5	294.4	291.4	295.0	297.7	295.9	298.0
	2	296.0	291.5	293.3	296.4	292.2	295.6	297.3	293.7	297.3	298.0	296.1	298.0
	3	295.0	296.5	297.2	295.8	296.6	296.6	295.9	297.5	297.3	298.0	296.4	297.3
Sep17/74	0	288.0	286.9	288.6	287.3	287.6	288.8	287.3	287.5	288.1	287.3	288.4	288.6
	1	292.0	289.3	290.1	292.5	290.3	292.5	292.3	290.1	295.2	289.4	288.6	290.0
	2	295.0	291.4	295.3	294.9	292.1	297.2	293.5	291.3	297.5	290.3	288.9	289.8
	3	290.0	289.8	288.6	291.1	290.3	288.6	290.1	289.7	288.2	289.8	282.1	288.9
Oct21/74	0	285.0	286.1	286.1	284.8	285.8	286.6	282.5	284.4	284.7	284.8	281.8	282.2
	1	291.0	289.6	290.0	290.6	289.6	291.2	286.9	286.6	286.8	280.1	281.9	284.2
	2	291.0	289.8	291.8	290.5	289.8	292.8	286.8	287.0	287.8	280.6	282.1	284.1
	3	281.0	284.7	282.7	282.3	284.7	282.8	281.0	283.4	282.6	279.6	281.9	282.8
Nov20/74	0	284.0	283.2	283.8	283.0	282.5	283.7	279.2	280.9	281.6	276.9	272.5	276.2
	1	290.0	287.3	291.4	288.8	286.9	290.5	283.4	283.7	283.5	271.2	272.6	276.9
	2	288.5	286.9	292.3	287.8	286.6	289.3	283.0	283.8	284.5	271.5	272.6	275.3
	3	273.5	279.3	275.4	275.7	279.2	274.9	273.9	278.2	276.4	269.9	271.8	276.6
Dec11/74	0	282.0	280.9	281.7	280.0	280.4	281.5	275.9	278.3	279.2	274.8	271.2	263.0
	1	288.0	285.7	288.7	286.1	285.6	288.0	278.6	278.9	276.3	270.5	271.3	267.2
	2	285.0	283.6	286.6	284.3	283.5	284.3	277.9	277.9	275.4	270.9	271.4	266.6
	3	272.0	275.6	265.5	272.4	275.7	266.7	270.7	273.6	264.3	270.6	270.9	265.3
Jan03/75	0	279.0	278.9	279.7	278.1	278.4	279.5	273.9	275.6	276.2	273.6	268.9	268.0
	1	285.0	283.9	286.6	282.9	282.5	285.8	275.0	276.0	279.5	268.9	269.1	268.1
	2	282.0	281.2	284.4	280.1	279.9	281.9	273.1	274.7	278.7	267.7	269.1	268.8
	3	268.0	272.3	267.4	268.7	272.3	267.4	267.6	270.2	267.4	268.1	269.7	266.7
Jan16/75	0	278.0	277.7	278.4	276.6	276.9	278.1	272.7	274.2	275.1	266.4	268.9	260.2
	1	283.0	281.6	283.9	280.8	280.1	282.9	272.9	274.4	277.9	255.7	254.6	257.0
	2	280.0	279.6	281.9	278.4	278.2	279.4	271.9	273.9	277.2	255.9	254.2	258.6
	3	261.0	266.7	256.8	263.5	266.4	257.0	259.9	264.8	256.8	253.0	253.9	256.1
Feb03/75		277.0	275.8	276.8	276.0	275.2	276.3	272.2	272.1	273.1	266.7	260.8	272.0
	1	281.0	279.1	277.2	279.0	278.3	277.3	270.7	268.8	272.4	262.5	260.5	267.7
	2	278.0	275.2	274.7	276.4	274.6	273.3	269.2	267.1	271.3	262.2	260.9	269.8
	3	262.0	263.9	267.4	261.9	264.3	267.0	260.1	260.8	267.9	263.2	262.8	267.0
Feb18/75	0	276.0	274.5	275.4	274.3	274.0	274.8	270.9	270.3	271.3	266.7	259.8	264.3
	1	279.0	277.7	282.8	276.8	276.6	278.9	267.4	265.2	268.4	258.9	259.7	264.5
	2	275.0	272.3	277.5	273.3	271.4	272.5	265.0	262.5	266.4	259.0	259.3	265.4
	3	260.0	264.5	262.9	261.9	264.4	263.0	259.7	261.4	262.5	259.0	260.4	262.5
Mar04/75	0	274.0	273.7	274.6	273.8	273.1	274.0	271.5	269.1	270.2	268.1	260.1	267.7
	1	277.0	276.6	278.2	274.5	273.3	276.1	268.2	265.6	268.2	266.1	260.1	267.7
	2	273.0	272.4	275.4	271.2	269.5	272.4	266.4	263.9	267.2	265.9	259.8	268.1
	3	265.0	267.1	266.6	265.1	266.1	267.1	264.2	264.8	265.7	267.1	265.9	266.5
Mar18/75	0	273.0	272.9	273.8	273.0	272.2	273.1	270.9	268.7	270.6	275.0	273.6	278.6
	1	275.0	273.1	275.4	272.5	271.8	272.7	268.2	262.6	265.9	274.5	273.6	280.2
	2	271.0	268.9	273.5	269.2	267.8	270.0	265.1	260.8	265.9	275.8	273.7	280.6
	3	275.0	270.3	278.6	271.0	270.2	278.6	270.9	267.8	278.2	280.0	274.7	278.6
Apr04/75	0	273.0	272.1	273.7	273.0	271.2	272.9	270.9	269.2	271.2	272.6	262.3	278.7
	1	273.0	270.4	269.4	271.7	269.5	270.1	268.6	264.6	268.5	268.5	262.6	275.8
	2	271.0	268.8	271.8	269.6	267.7	271.0	267.5	264.6	271.1	270.6	263.2	277.4
	3	268.0	266.8	275.0	267.2	271.8	274.6	267.0	265.6	275.8	271.4	266.4	275.1

Table H1 Continued .....

Apr17/75	0	271.0	271.8	273.1	270.5	271.1	272.5	270.0	269.2	270.9	271.2	273.3	273.1
	1	270.0	270.0	270.7	268.7	269.5	269.9	267.4	263.8	267.3	275.3	273.2	275.9
	2	268.0	267.8	272.1	268.1	267.3	270.4	267.1	262.5	269.0	275.6	273.5	275.4
	3	276.0	270.8	274.1	275.0	271.8	274.1	270.5	272.2	274.3	277.5	275.1	274.7
May15/75	0	273.0	271.9	272.4	273.1	271.7	273.0	276.4	272.2	272.8	287.9	287.8	288.4
	1	272.0	268.4	275.4	271.6	267.3	272.6	275.1	270.6	274.6	284.3	287.6	285.4
	2	274.0	270.6	282.7	273.9	269.9	278.7	277.1	272.3	279.9	285.6	287.9	285.4
	3	284.0	284.0	283.0	283.3	283.7	284.2	283.9	285.1	281.2	287.6	289.0	281.7
May29/75	0	274.0	272.8	274.1	274.9	272.9	274.9	279.3	275.1	276.5	295.6	291.3	284.4
	1	272.0	268.2	268.4	272.6	268.2	271.0	278.4	274.6	274.6	290.0	291.4	286.7
	2	277.0	272.6	278.4	276.9	272.6	279.2	281.6	277.5	280.8	291.4	291.6	286.4
	3	289.0	285.5	285.8	287.9	288.4	286.7	289.0	287.6	285.2	291.5	291.9	284.5
Jun12/75	0	276.0	274.4	275.4	276.9	274.9	276.6	281.0	277.8	278.7	298.5	290.0	294.7
	1	273.0	269.1	277.7	273.8	270.6	276.9	280.3	276.7	275.1	296.8	290.0	294.3
	2	279.0	273.9	287.4	279.5	275.2	285.3	283.5	279.5	282.8	298.3	290.6	292.5
	3	296.0	286.5	291.0	290.8	287.0	292.4	291.6	288.6	290.5	304.0	298.4	290.8
Jul103/75	0	279.0	277.1	278.0	280.5	277.7	279.6	285.9	280.7	280.7	304.9	296.4	295.6
	1	275.0	272.2	271.2	276.8	273.4	276.3	284.5	283.3	281.3	298.0	296.2	299.7
	2	283.0	277.7	282.4	283.1	278.6	285.3	288.6	284.5	285.2	300.6	296.9	298.9
	3	297.0	292.0	297.0	296.5	292.3	296.9	297.1	294.4	297.6	303.5	298.6	297.3
Aug01/75	0	283.0	280.3	280.8	285.0	281.1	282.6	290.1	284.4	284.2	297.7	294.4	303.7
	1	280.0	276.7	280.1	282.0	278.2	281.6	290.5	284.7	288.2	298.4	294.2	308.1
	2	289.0	282.8	290.7	289.1	284.0	290.0	294.5	290.2	293.4	299.6	293.9	307.1
	3	298.0	294.8	305.7	298.9	294.9	306.2	299.8	297.8	305.8	298.6	293.9	306.5
Aug12/75	0	285.0	281.2	282.6	286.0	281.9	284.1	289.6	285.7	286.0	295.7	294.1	290.8
	1	282.0	277.6	282.0	284.0	279.7	284.9	291.6	287.7	290.3	297.6	294.2	292.5
	2	290.0	283.7	293.5	290.5	285.4	293.9	295.3	291.0	295.4	298.7	295.6	292.7
	3	296.0	293.2	293.6	296.9	293.8	293.4	297.6	295.8	292.4	299.6	295.6	290.0
Aug28/75	0	286.0	282.5	284.4	286.8	283.8	285.4	288.5	286.1	287.4	290.8	290.2	295.4
	1	285.0	280.0	285.7	286.9	282.5	286.8	292.1	288.4	295.8	291.0	290.2	293.3
	2	291.0	285.3	293.0	291.6	287.2	291.5	294.8	291.2	297.6	292.4	290.3	293.3
	3	290.0	285.3	290.1	290.8	291.8	289.6	291.1	293.3	290.9	292.9	290.3	292.3
Sep04/75	0	287.0	283.2	285.1	287.3	283.8	285.9	288.8	286.1	287.7			
	1	286.0	281.6	283.5	287.8	283.5	286.7	292.4	288.7	290.4			
	2	291.0	286.2	291.7	291.8	287.8	291.8	294.4	291.2	293.9			
	3	290.0	290.6	286.7	289.1	291.1	287.1	290.8	293.3	286.6			
Sep18/75	0	287.0	283.6	285.3	286.8	284.2	286.1	287.1	285.9	286.9			
	1	287.0	282.7	284.8	289.1	285.1	287.9	291.0	287.7	289.5			
	2	290.0	286.4	291.6	291.0	288.2	292.4	292.3	289.2	292.6			
	3	290.0	288.4	291.6	290.5	289.1	291.7	290.8	289.2	291.8			
Oct03/75	0	287.0	283.9	285.1	286.5	284.2	285.8	285.9	284.9	285.9			
	1	289.0	284.8	287.0	289.6	285.7	289.7	289.9	287.8	291.2			
	2	290.0	287.5	293.0	290.8	288.1	292.8	290.5	289.3	293.2			
	3	286.0	287.7	284.7	287.3	287.8	284.8	287.0	288.5	285.0			
Oct15/75	0	286.0	283.7	284.7	286.0	283.8	285.3	285.0	284.1	285.0			
	1	289.0	285.5	285.8	289.6	285.7	288.9	289.5	287.5	288.4			
	2	290.0	287.9	291.1	290.1	288.9	291.4	289.6	289.1	291.2			
	3	280.0	287.1	283.3	282.6	287.1	283.8	281.8	287.4	283.3			
Oct30/75	0	285.0	283.1	284.1	285.3	283.0	284.5	282.1	283.1	284.0			
	1	289.0	285.5	289.7	289.0	285.9	289.9	286.8	286.6	292.1			
	2	289.0	287.4	292.4	289.0	287.8	290.1	286.9	287.9	291.4			
	3	279.0	282.4	275.4	280.8	282.0	275.1	278.9	282.7	276.0			
Nov13/75	0	285.0	282.2	283.2	283.9	282.1	283.4	282.1	281.6	282.4			
	1	289.0	286.0	287.8	288.6	285.4	288.8	285.4	285.6	287.4			
	2	288.0	287.2	289.4	287.9	286.7	287.9	285.3	286.4	287.4			
	3	270.0	273.3	270.3	272.7	274.4	270.9	272.6	282.0	270.6			
Nov28/75	0	283.0	281.2	281.8	281.5	280.8	282.1	277.3	280.3	281.0			
	1	287.0	284.7	283.6	286.8	284.9	285.8	281.8	283.3	285.4			
	2	285.0	285.5	285.7	285.4	285.7	285.5	281.3	284.1	286.2			
	3	269.0	274.0	270.6	269.6	274.5	270.5	268.1	273.3	271.2			



Table H1 Continued .....

Dec17/75	0	281.0	279.6	280.6	279.8	279.6	280.6	275.1	277.8	278.3
	1	287.0	284.6	282.4	285.6	284.4	284.3	276.5	278.8	279.8
	2	284.0	282.9	281.0	283.3	282.6	280.5	275.9	278.1	278.5
	3	252.0	252.9	255.1	258.1	253.1	255.3	255.5	252.8	255.4
Jan15/76	0	278.0	277.6	277.5	276.9	276.9	277.2	272.7	273.1	273.4
	1	283.0	281.8	281.9	280.6	280.3	283.0	270.2	270.5	272.5
	2	287.0	277.2	287.6	277.3	275.9	276.4	268.0	268.5	269.9
	3	256.0	265.3	252.5	259.6	264.7	252.8	256.7	262.5	251.6
Feb12/76	0	276.0	274.8	274.7	274.9	273.9	274.2	272.0	269.7	270.6
	1	279.0	277.9	281.1	276.4	275.6	276.9	267.9	265.9	268.1
	2	274.0	272.6	275.0	272.1	270.7	269.5	264.9	263.4	265.8
	3	263.0	269.3	264.1	263.5	268.4	263.8	262.9	266.9	264.1
Mar17/76	0	274.0	271.7	273.1	273.9	271.1	272.4	271.4	269.1	270.9
	1	274.0	271.3	274.7	272.9	270.6	274.9	268.0	264.3	270.8
	2	271.0	268.7	275.3	269.6	268.2	273.6	266.4	263.3	270.8
	3	265.0	266.2	260.8	265.2	266.4	260.7	264.2	264.5	259.9
Apr21/76	0	274.0	271.3	272.2	274.0	270.7	272.0	274.0	269.8	271.4
	1	273.0	269.7	276.3	272.0	266.7	272.5	273.6	268.9	280.4
	2	273.0	270.9	272.2	272.7	268.5	277.2	274.9	270.4	274.7
	3	279.0	279.4	281.4	278.0	278.3	281.1	278.0	280.0	280.7
May11/76	0	275.0	271.4	271.9	274.9	271.4	272.7	277.5	273.0	273.4
	1	273.0	267.7	272.3	272.9	268.4	272.1	276.6	271.2	278.3
	2	275.0	270.6	279.9	275.1	271.2	278.5	278.3	273.2	273.3
	3	284.0	281.6	279.4	283.3	281.9	279.0	284.0	282.8	275.3
Jun16/76	0	279.0	275.6	276.2	280.6	275.8	277.5	284.9	279.1	279.8
	1	275.0	270.8	273.4	276.0	271.1	275.6	284.5	281.3	283.6
	2	283.0	277.3	285.1	282.8	277.5	285.0	288.8	285.2	289.9
	3	289.0	288.8	282.3	288.3	288.5	283.2	289.0	292.1	291.6
Jul12/76	0	282.0	278.5	279.8	283.6	279.5	281.3	288.3	282.8	282.9
	1	279.0	274.6	277.8	280.9	276.2	280.6	289.1	284.2	290.2
	2	287.0	280.6	290.3	287.5	281.8	290.3	292.9	287.6	296.7
	3	294.0	292.1	294.8	294.4	292.4	294.4	295.4	294.7	293.7
Aug13/76	0	285.0	281.9	282.9	286.6	282.7	284.4	289.8	287.8	285.7
	1	284.0	278.9	281.5	286.0	281.1	284.1	292.6	293.3	290.1
	2	291.0	284.3	290.9	291.3	286.0	290.8	295.8	295.1	294.2
	3	295.0	293.3	295.6	294.1	293.9	295.8	295.0	296.9	295.6
Sep08/76	0	287.0	283.8	284.8	288.1	284.2	285.9	290.3	289.5	287.3
	1	287.0	282.2	285.1	289.1	284.5	287.3	294.4	297.5	285.5
	2	293.0	286.7	292.2	293.1	288.6	292.2	296.3	298.3	288.2
	3	294.0	293.6	297.4	293.9	294.2	292.9	293.9	297.3	296.2
Sep13/76	0	285.0	283.9	285.1	286.1	284.3	286.1	287.9	286.4	287.2
	1	286.0	283.3	282.3	287.3	284.9	286.6	292.4	289.9	291.9
	2	291.0	287.9	291.0	292.1	289.2	292.4	294.4	292.5	295.2
	3	287.0	292.1	295.3	291.3	292.2	295.5	291.8	293.9	286.2
Oct12/76	0	284.0	283.8	284.9	284.4	284.1	285.7	283.6	285.1	286.0
	1	287.0	285.2	285.8	288.6	286.9	290.1	288.4	287.9	293.2
	2	288.0	288.1	291.9	289.9	289.4	293.0	289.1	289.5	295.8
	3	282.0	286.1	281.4	282.4	286.9	281.5	282.5	286.2	281.7
Dec14/76	0	278.0	280.1	280.0	277.0	279.8	280.1	272.1	277.4	276.8
	1	284.0	284.5	287.8	282.8	284.8	285.9	273.3	276.6	276.1
	2	281.0	281.7	283.0	280.3	281.8	279.4	272.1	275.2	272.9
	3	266.0	265.1	271.4	264.5	265.2	271.3	262.7	262.6	271.5
Jan18/77	0	274.0	277.0	277.1	272.4	276.1	276.6	266.4	267.7	272.7
	1	279.0	280.3	280.2	275.6	278.6	278.6	264.1	267.7	267.5
	2	274.0	274.7	275.2	272.2	273.3	272.3	262.1	264.9	263.6
	3	258.0	258.1	259.6	254.5	258.0	258.7	252.6	254.6	245.2

Table H1 Continued.....

Feb17/77	0	273.0	273.8	274.3	272.0	272.6	273.2	269.5	268.1	269.4
	1	275.0	275.4	274.3	272.2	271.8	273.0	264.9	264.2	273.0
	2	271.0	270.6	272.4	268.7	267.7	270.0	262.7	262.2	272.9
	3	263.0	267.6	274.4	263.1	266.7	273.8	262.0	265.1	276.0
Mar10/77	0	271.0	271.7	272.6	271.4	270.7	271.9	270.4	268.0	269.8
	1	272.0	270.8	271.9	270.0	269.5	269.4	265.9	262.9	265.8
	2	268.0	267.6	270.3	266.6	266.6	267.5	264.5	261.7	265.4
	3	275.0	271.0	278.7	272.0	271.0	278.7	272.2	269.2	278.8
Apr13/77	0	273.0	270.3	271.0	272.0	270.0	271.2	272.9	269.9	271.2
	1	271.0	267.9	270.2	270.4	267.5	269.6	271.2	266.9	270.6
	2	271.0	268.2	275.0	270.6	267.9	272.9	271.6	267.5	273.9
	3	287.0	278.2	286.1	280.0	278.2	284.0	280.3	278.4	283.2
May10/77	0	273.0	273.6	272.0	273.6	271.1	272.7	277.4	273.4	274.1
	1	272.0	267.5	265.7	272.0	267.6	269.2	277.5	273.3	277.3
	2	276.0	271.6	276.6	275.6	271.8	277.9	279.9	275.8	283.9
	3	297.0	283.6	295.3	290.9	287.1	295.4	291.4	284.9	296.8
Jun20/77	0	279.0	275.7	277.4	280.1	276.8	278.6	283.1	280.8	281.7
	1	276.0	271.6	276.0	277.1	274.0	278.2	284.9	281.9	279.3
	2	283.0	278.2	288.5	283.5	280.0	288.1	288.3	285.5	286.7
	3	302.0	288.8	292.1	293.6	289.4	290.4	293.4	291.4	287.6
Jul13/77	0	281.0	283.1	280.5	282.1	282.7	281.9	286.0	282.6	283.9
	1	278.0	279.9	280.8	280.1	279.9	284.8	287.6	289.7	289.3
	2	286.0	290.6	292.4	286.0	291.1	293.8	291.1	291.0	296.1
	3	291.0	292.1	289.4	292.5	292.2	290.2	293.1	292.4	287.6
Aug16/77	0	284.0	287.6	283.6	284.5	287.4	284.9	286.8	287.4	286.1
	1	283.0	288.3	279.2	285.1	288.9	284.5	291.3	290.3	286.4
	2	290.0	291.1	287.9	290.3	291.6	290.6	293.6	292.2	289.9
	3	292.0	292.1	291.3	288.5	292.3	291.3	288.9	292.3	290.7
Sep13/77	0	285.0	287.8	285.8	285.1	287.5	286.3	285.7	286.8	287.3
	1	286.0	289.1	285.0	287.5	289.3	288.1	290.0	289.4	287.0
	2	290.0	290.8	291.2	290.3	291.1	291.5	291.0	290.5	289.4
	3	287.0	290.9	285.9	286.9	291.0	286.6	287.1	290.8	286.1
Oct21/77	0	283.0	285.5	284.3	282.6	285.1	284.7	282.0	284.2	284.4
	1	287.0	288.4	286.7	287.0	288.9	288.5	285.1	286.9	283.7
	2	287.0	288.9	289.6	287.0	289.3	288.9	285.0	287.2	284.1
	3	277.0	276.7	278.3	278.3	286.9	279.5	278.3	286.1	278.2
Nov17/77	0	283.0	283.3	282.6	282.0	282.7	282.9	279.5	281.8	282.0
	1	287.0	287.0	285.6	286.5	287.0	287.2	283.8	285.3	284.3
	2	286.0	287.8	288.4	285.8	287.7	287.6	283.1	286.1	285.9
	3	274.0	281.2	275.4	274.8	274.9	275.9	274.0	272.3	274.8
Dec15/77	0	279.0	280.5	280.4	277.5	280.4	280.5	273.4	278.1	278.3
	1	284.0	285.4	284.2	283.4	286.5	284.2	274.4	276.3	276.4
	2	281.0	282.2	279.3	280.6	283.0	277.4	273.0	274.6	271.9
	3	265.0	267.0	263.5	265.6	267.7	263.2	264.4	263.8	264.5

Note : Mes - Measured temperatures

PLE - Temperatures predicted by linear element

PQE - Temperatures predicted by quadratic element

H - Height from the floor: 0 - Near the floor

1 - 1.0 m from the floor

2 - 2.0 m from the floor

3 - 2.7 m from the floor

Table H2 : Measured and predicted temperatures (K) in a 5.56 m diameter bin containing barley to a depth of 3.2 m, located near Winnipeg.

Radius													
Centre				1.0 m			2.0 m			Wall			
DATE	H	Mes	PLE	PQE	Mes	PLE	PQE	Mes	PLE	PQE	Mes	PLE	PQE
Aug13/74	0	285.0	285.0	285.0	286.0	286.0	286.0	288.6	288.6	288.6	291.3	291.3	291.3
	1	289.0	289.0	289.0	290.6	290.6	290.6	293.9	293.9	293.9	296.4	296.4	296.4
	2	293.0	293.0	293.0	294.4	294.4	294.4	295.9	295.9	295.9	295.9	295.9	295.9
	3	295.0	295.0	295.0	295.6	295.6	295.6	297.0	297.0	297.0	295.9	295.9	295.9
	4	295.0	295.0	295.0	297.3	297.3	297.3	296.8	296.8	296.8	298.8	298.8	298.8
Sep17/74	0	287.0	288.1	290.7	286.9	288.0	289.1	286.9	287.5	288.6	287.3	290.4	289.1
	1	291.0	290.6	292.9	291.3	291.2	292.4	290.4	289.5	290.3	291.1	290.7	293.3
	2	293.0	293.0	294.6	293.8	293.4	294.1	292.1	290.9	290.9	290.6	291.0	292.4
	3	294.0	292.3	292.8	293.3	292.6	292.0	291.5	289.9	289.0	290.4	291.9	293.1
	4	291.0	291.5	290.3	292.0	291.8	290.9	290.6	290.2	289.8	290.8	292.3	291.5
Oct22/74	0	284.0	286.1	287.6	283.1	285.5	286.4	281.8	283.2	285.0	279.0	282.3	281.9
	1	288.0	289.7	295.5	286.5	288.8	292.9	283.4	285.4	284.1	278.3	282.3	280.5
	2	290.0	290.8	294.5	288.8	289.9	292.4	285.2	285.9	284.9	278.9	282.4	278.8
	3	289.0	288.5	292.3	288.4	287.8	289.9	285.0	284.4	282.6	279.6	282.5	280.1
	4	283.0	285.5	282.6	279.1	285.2	277.5	279.0	283.6	276.3	277.9	282.8	277.5
Nov20/74	0	283.0	283.2	283.6	282.1	282.4	282.6	278.9	280.8	281.1	273.5	275.8	278.1
	1	286.0	286.4	286.4	284.5	286.3	285.6	279.5	282.3	283.6	270.7	276.0	276.0
	2	288.0	287.5	286.9	286.1	287.1	286.1	281.6	283.1	283.3	271.0	276.1	276.5
	3	286.0	284.6	282.7	284.9	284.6	282.0	280.1	279.9	282.0	271.2	276.2	276.9
	4	277.0	279.8	276.5	272.2	279.9	276.6	271.6	277.7	276.2	269.9	276.5	275.3
Dec11/74	0	280.0	280.7	280.9	278.3	280.1	279.9	274.9	277.8	277.8	271.2	269.4	265.0
	1	282.0	284.4	287.8	279.8	283.8	284.7	273.3	277.7	278.1	269.4	269.7	265.4
	2	284.0	285.2	286.3	281.6	284.1	283.8	275.5	277.7	277.6	269.7	270.1	265.3
	3	282.0	280.7	280.8	280.5	280.2	278.4	274.4	273.9	274.8	269.7	272.0	265.4
	4	275.0	274.9	276.9	271.2	274.8	273.2	270.9	271.6	273.3	269.5	273.0	273.7
Jan03/75	0	278.0	278.2	278.7	276.8	277.4	277.5	273.9	274.6	275.2	270.2	267.7	276.9
	1	279.0	281.7	280.7	276.4	280.1	278.7	270.7	273.6	276.8	267.9	268.1	273.3
	2	280.0	281.3	279.4	278.0	279.5	277.7	272.4	273.0	274.8	268.5	268.5	274.3
	3	279.0	276.9	274.5	276.9	275.8	273.2	270.9	270.8	274.4	269.7	269.5	274.6
	4	275.0	272.7	273.2	271.5	272.2	273.1	270.5	269.8	273.1	271.7	270.2	272.1
Jan16/75	0	275.0	277.0	277.8	275.1	276.1	276.1	273.0	273.4	274.1	267.7	272.5	264.5
	1	276.0	279.8	279.6	274.4	278.0	277.6	268.6	273.1	276.7	255.4	255.3	257.6
	2	277.0	279.2	277.8	275.3	277.2	276.1	270.5	272.9	274.3	255.9	255.2	259.0
	3	275.0	275.2	272.5	273.6	274.5	271.1	268.6	269.5	272.3	256.6	255.5	258.4
	4	264.0	266.8	256.7	257.4	266.4	256.9	256.6	264.7	256.8	254.1	256.1	256.5
Feb03/75	0	276.0	274.9	275.2	274.9	274.3	273.8	272.1	271.2	271.7	268.1	266.9	266.9
	1	275.0	277.6	282.0	272.9	275.8	276.6	265.1	268.3	267.5	261.2	256.9	256.9
	2	275.0	276.6	278.1	273.1	274.5	274.1	266.6	267.7	265.8	261.0	256.7	256.7
	3	273.0	271.5	271.9	271.4	270.5	267.5	264.2	263.7	262.7	260.0	255.4	255.4
	4	264.0	262.2	267.3	263.7	261.4	263.6	263.0	259.2	261.4	264.0	255.1	255.1
Feb18/75	0	275.0	273.4	274.1	273.8	272.8	272.4	271.6	269.3	270.2	268.4	264.2	256.4
	1	273.0	275.1	279.2	270.4	273.7	274.2	262.7	263.0	263.3	261.4	264.1	260.6
	2	273.0	273.5	274.8	270.5	271.8	271.0	263.9	262.0	260.7	260.9	264.4	260.0
	3	271.0	267.5	268.6	268.9	266.5	264.7	262.1	259.0	257.9	259.9	266.7	261.1
	4	264.0	262.9	257.6	261.9	262.6	258.4	261.5	258.8	256.3	263.0	267.7	257.2
Mar04/75	0	275.0	272.4	273.2	273.8	271.5	271.5	271.9	268.1	269.4	269.2	258.0	263.9
	1	273.0	273.3	272.0	269.5	270.0	269.9	266.0	264.3	267.5	266.0	258.0	261.7
	2	272.0	270.8	269.5	269.2	267.7	267.4	266.0	262.9	265.4	265.5	257.8	262.4
	3	270.0	267.8	267.9	268.1	266.1	266.4	265.5	264.2	267.4	265.4	258.7	262.9
	4	265.0	264.9	263.0	266.6	264.1	261.4	266.4	263.7	260.9	267.4	258.7	260.1
Mar18/75	0	274.0	271.2	272.4	273.8	270.6	270.5	271.9	267.9	269.8	272.2	272.3	277.6
	1	271.0	270.2	273.0	270.0	268.9	268.7	267.7	261.9	265.1	275.1	272.0	278.8
	2	271.0	268.1	270.6	268.1	266.9	267.2	266.1	260.9	265.5	274.0	271.9	278.7
	3	269.0	266.4	269.7	267.5	265.1	266.3	266.1	264.9	265.5	273.9	272.3	279.6
	4	272.0	271.2	272.3	276.4	270.9	277.4	276.4	275.3	276.4	278.6	272.4	276.6

Table H2 Continued.....

Apr04/75	0	274.0	270.6	272.1	273.8	270.0	270.4	272.2	268.7	270.5	269.7	270.1	265.3
	1	271.0	268.0	274.9	269.6	266.8	268.9	269.1	265.2	270.6	269.5	269.9	262.9
	2	269.0	266.5	272.3	268.1	265.5	267.6	268.2	265.2	268.3	268.6	270.5	264.2
	3	268.0	266.3	274.4	267.7	266.4	268.9	267.7	266.4	271.2	268.7	272.2	266.0
	4	267.0	264.9	262.2	270.1	264.9	272.1	270.5	265.3	271.1	272.1	270.7	270.6
Apr17/75	0	273.0	270.2	271.9	272.1	270.1	270.4	271.9	268.9	270.8	273.9	279.9	282.9
	1	269.0	268.2	267.7	268.6	266.5	266.9	270.5	264.8	268.0	277.1	279.3	285.8
	2	268.0	266.5	268.0	267.6	265.2	267.1	269.4	264.2	267.8	277.1	279.4	285.2
	3	271.0	268.7	272.1	270.1	267.4	271.3	272.1	271.9	272.3	277.8	280.3	285.5
	4	278.0	276.0	283.8	277.8	275.6	283.9	277.6	277.2	283.9	278.0	280.1	284.4
May16/75	0	273.0	270.8	272.9	273.6	271.5	272.5	275.9	273.6	274.7	282.8	289.5	281.6
	1	270.0	267.2	265.9	270.9	267.5	267.5	278.6	273.4	278.1	288.3	289.3	292.3
	2	271.0	267.2	269.1	273.0	268.3	270.6	278.9	274.5	278.2	288.1	289.6	292.2
	3	280.0	273.8	279.2	278.6	274.2	279.8	282.4	282.4	285.6	288.4	290.2	292.2
	4	287.0	283.7	290.9	289.1	284.2	291.4	289.5	287.5	290.8	291.4	290.9	290.0
Jun12/75	0	276.0	274.3	276.0	276.9	275.4	276.2	280.1	278.7	279.8	287.8	290.3	290.3
	1	273.0	270.0	271.7	275.1	272.2	273.9	282.8	282.3	276.3	297.9	294.8	300.4
	2	278.0	271.8	277.3	280.3	274.3	279.6	284.6	284.1	287.9	296.3	295.1	298.8
	3	285.0	278.4	283.9	284.1	279.8	285.7	287.0	287.7	289.8	295.4	295.3	298.5
	4	292.0	286.9	297.0	295.8	287.8	295.8	296.1	290.9	297.4	300.5	294.9	298.1
Jul10/75	0	281.0	278.5	281.1	282.1	279.4	281.1	287.0	284.7	283.4	292.8	296.5	287.0
	1	278.0	274.9	279.2	280.9	276.3	280.1	289.8	285.5	288.7	294.6	296.7	293.8
	2	285.0	277.0	283.2	287.0	278.7	284.1	292.4	287.9	290.8	296.6	296.7	292.2
	3	294.0	284.4	295.2	292.4	285.7	294.7	296.3	293.5	296.4	296.9	296.9	292.2
	4	294.0	290.6	291.5	295.6	291.2	293.8	296.1	294.9	296.4	297.4	297.3	299.1
Jul25/75	0	282.0	280.3	282.9	282.5	281.2	282.9	288.0	284.6	285.7	291.6	296.9	291.1
	1	282.0	277.0	282.9	285.5	279.4	282.1	291.8	286.9	291.7	294.5	297.0	295.1
	2	288.0	279.6	287.7	290.5	282.2	286.8	294.6	289.1	293.3	295.0	297.5	294.3
	3	295.0	286.2	296.7	294.4	288.0	294.4	297.1	293.9	297.7	295.8	298.8	295.3
	4	294.0	292.9	292.6	295.3	294.4	293.2	295.6	296.3	291.6	295.3	299.2	291.8
Aug08/75	0	284.0	281.8	284.4	285.6	282.6	284.5	289.1	285.8	287.3	292.3	295.1	289.6
	1	284.0	279.2	287.9	287.0	283.3	285.0	293.5	288.9	294.5	294.4	295.3	294.3
	2	290.0	282.0	291.1	292.4	286.0	289.4	295.6	291.2	295.6	295.0	295.7	293.3
	3	295.0	288.1	300.6	295.3	290.8	296.2	297.4	295.1	299.9	295.6	297.1	295.1
	4	296.0	292.9	298.5	295.8	293.9	292.3	296.0	296.0	290.2	295.0	297.7	289.5
Aug21/75	0	285.0	283.3	285.6	286.4	284.1	285.5	288.3	286.8	288.3	288.5	290.2	290.6
	1	287.0	281.7	288.3	288.9	285.9	286.4	292.9	289.3	295.0	289.8	290.3	290.9
	2	291.0	284.7	291.9	293.4	287.2	290.8	295.0	291.6	296.6	290.1	290.5	290.9
	3	292.0	288.9	297.5	294.3	290.7	294.1	295.9	292.9	298.6	290.4	290.8	290.7
	4	291.0	291.2	289.8	291.1	292.0	290.0	291.5	292.9	288.9	290.5	291.3	288.4
Sep04/75	0	286.0	284.3	286.6	287.0	284.9	286.1	288.1	286.7	288.5	288.0	287.4	290.0
	1	289.0	284.2	286.8	290.4	285.5	287.3	292.4	289.7	292.7	290.1	287.4	291.5
	2	292.0	286.8	290.6	293.4	288.1	290.8	294.0	291.3	294.0	289.9	287.3	291.4
	3	293.0	290.3	294.6	294.1	290.9	293.6	294.5	293.5	295.8	290.4	286.9	292.0
	4	290.0	291.5	289.0	290.1	290.9	289.3	290.1	293.5	288.8	290.0	287.2	289.6
Sep25/75	0	286.0	285.0	286.9	286.0	285.3	286.2	286.0	285.8	286.9	285.0	286.3	287.7
	1	290.0	286.0	288.5	290.4	287.1	288.3	289.3	287.7	289.3	286.1	286.5	290.1
	2	292.0	288.2	290.8	292.5	289.1	290.6	290.9	289.1	289.9	286.4	286.7	290.8
	3	291.0	289.2	291.7	291.8	289.8	290.6	290.4	288.9	290.2	286.6	286.9	291.1
	4	287.0	288.4	288.1	286.8	288.7	288.6	286.4	288.2	287.6	285.6	287.1	288.5
Oct09/75	0	286.0	284.9	286.3	285.8	284.7	285.6	286.0	284.6	285.7	287.6	290.9	286.1
	1	290.0	286.6	284.6	289.6	287.1	286.1	288.9	286.1	289.9	288.6	291.1	290.3
	2	291.0	285.7	287.7	291.3	288.7	288.6	289.8	287.2	290.1	289.3	292.2	289.3
	3	291.0	288.3	287.4	290.6	288.1	288.1	289.5	288.2	290.9	289.9	295.5	290.1
	4	290.0	291.0	287.9	289.1	291.4	288.4	288.8	290.3	287.3	287.8	286.4	288.3
Oct16/75	0	286.0	281.0	285.9	285.8	284.2	285.3	284.6	284.1	285.3	280.8	282.9	284.4
	1	290.0	286.2	286.1	289.5	286.7	287.0	287.9	286.8	290.5	279.5	283.2	281.8
	2	291.0	288.1	288.8	290.8	288.4	289.0	289.4	288.2	291.1	280.0	283.5	282.3
	3	290.0	287.9	287.8	290.1	288.7	289.0	288.5	286.8	290.7	280.4	284.3	282.1
	4	282.0	285.6	280.8	281.1	286.0	281.0	281.0	285.1	281.1	278.6	284.8	281.2

Table H2 Continued .....

Oct30/75	0	285.0	283.7	285.0	284.8	283.4	284.2	282.8	283.0	284.1	279.0	277.0	280.8
	1	289.0	286.2	286.8	288.5	286.5	286.9	285.3	285.7	287.7	278.6	277.3	279.1
	2	291.0	287.0	288.6	290.0	288.1	288.4	287.1	286.9	288.1	278.8	277.3	279.6
	3	288.0	286.9	286.5	288.5	287.4	286.1	285.8	284.4	287.1	278.1	277.4	280.0
	4	280.0	282.7	278.8	280.3	282.9	278.9	279.8	279.8	278.5	278.8	277.8	278.3
Nov13/75	0	284.0	282.7	283.9	283.0	282.2	282.9	280.5	281.3	282.3	273.6	271.7	275.4
	1	288.0	286.4	288.1	286.3	285.4	287.3	282.5	285.2	287.2	270.6	271.9	274.0
	2	289.0	287.6	288.8	287.5	288.6	287.8	284.3	285.8	287.4	271.1	271.7	274.1
	3	286.0	286.4	286.9	286.0	286.0	285.6	283.1	283.9	285.9	270.9	271.3	273.6
	4	274.0	280.8	270.7	272.9	280.4	271.1	275.5	278.6	271.3	269.5	271.3	272.2
Nov28/75	0	283.0	281.3	282.2	282.1	280.7	281.4	277.9	279.8	280.7	271.7	268.3	272.7
	1	287.0	284.3	284.1	285.0	284.8	284.1	278.4	280.9	282.8	268.2	268.7	269.0
	2	288.0	285.9	285.2	286.3	286.1	285.0	281.0	282.0	282.6	268.5	268.7	270.0
	3	285.0	282.2	279.2	284.4	283.0	279.0	279.3	276.4	278.9	267.5	268.9	270.0
	4	272.0	275.2	269.6	271.4	275.7	269.8	269.6	272.6	269.5	268.1	269.2	268.7

Note : Mes - Measured temperatures

PLE - Temperatures predicted by linear element

PQE - Temperatures predicted by quadratic element

H - Height from the floor : 0 - Near the floor

1 - 1.0 m from the floor

2 - 2.0 m from the floor

3 - 2.7 m from the floor

4 - 3.2 m from the floor